

PWG3 Summary:

Anisotropic collective flow and development of the corresponding measurement techniques for the MPD experiment

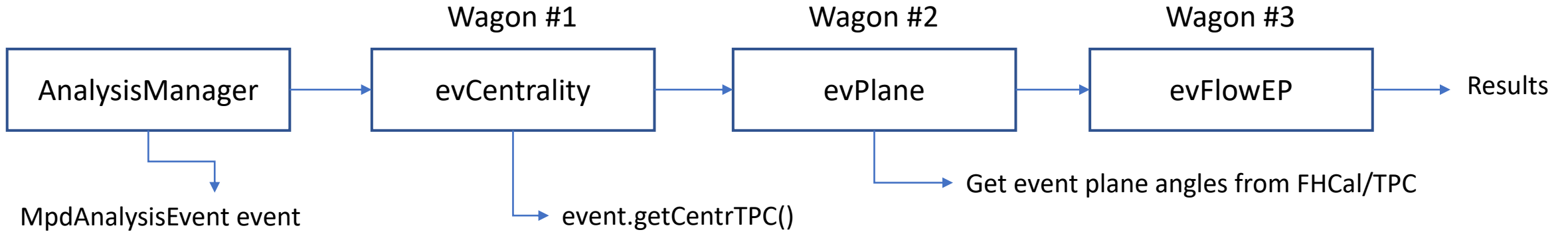
Arkadiy Taranenko^{1,2}

¹National Research Nuclear University MEPhI, Moscow

²VBLHEP JINR, Dubna

XIII MPD Collaboration Meeting, Dubna, Russia, 23-25 April 2024

evFlowEP wagon for flow measurements in MPD

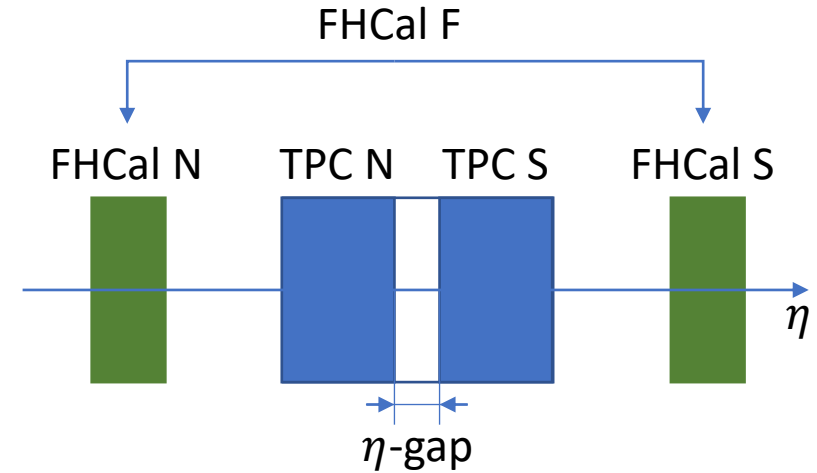
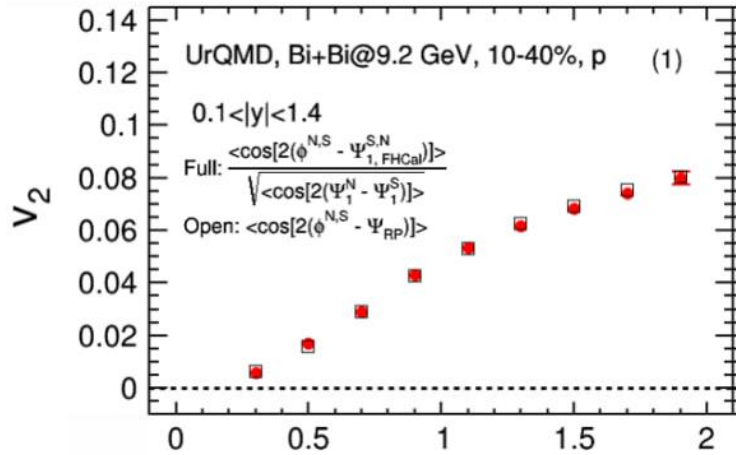
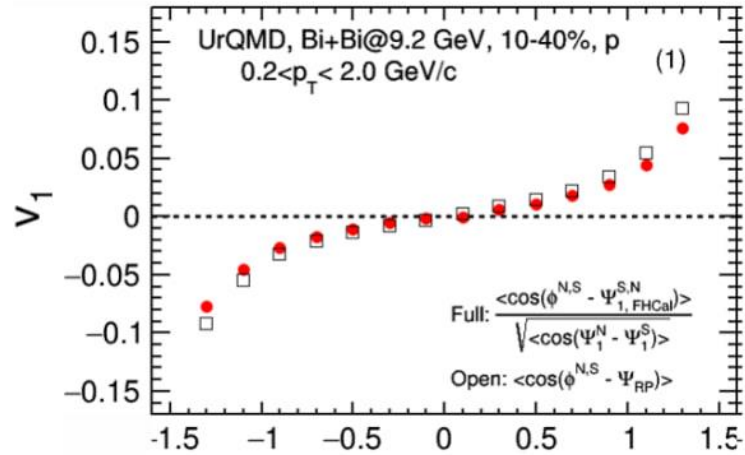


Directed flow:

$$v_1 = \frac{\langle \cos(\phi - \Psi_1^{EP}) \rangle}{Res(\Psi_1)}$$

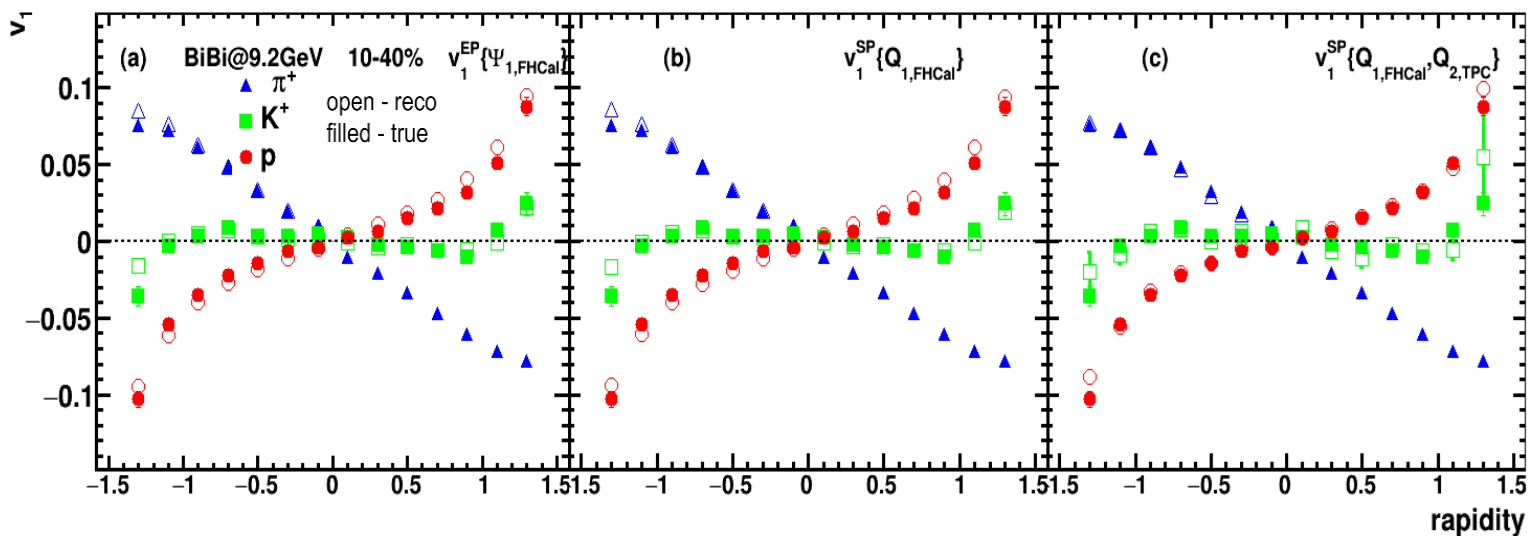
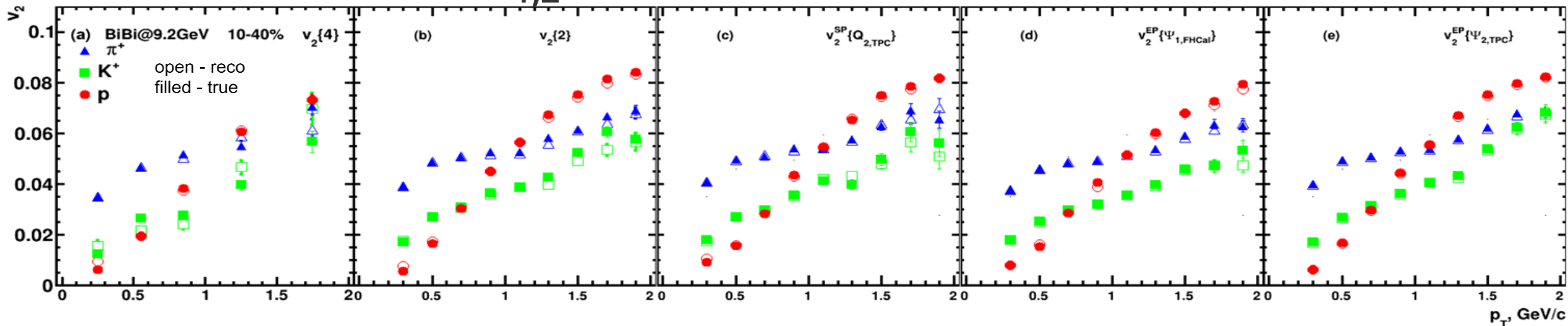
Elliptic flow:

$$v_2(\Psi_2) = \frac{\langle \cos[2(\phi - \Psi_2^{EP})] \rangle}{Res(\Psi_2)} \quad v_2(\Psi_1) = \frac{\langle \cos[2(\phi - \Psi_{1,FHCaI}^{EP})] \rangle}{Res(\Psi_1)}$$



See details in A.Demanov's talk on Cross-PWG 05.03.2024

Performance of $v_{1,2}$ of identified hadrons in MPD



Good performance for v_1 , v_2 using several methods for flow measurements (EP, SP, Q-Cumulants)

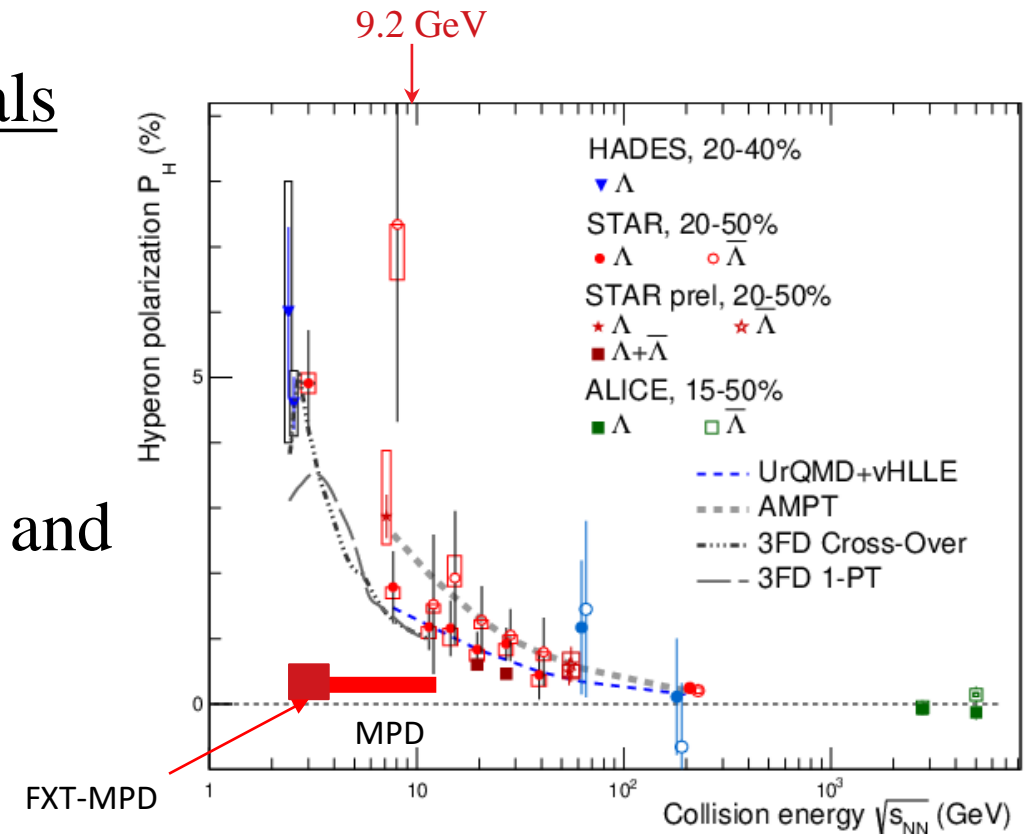
Good performance for flow measurements for all methods used (EP, SP, Q-cumulants)

Global Polarization at Nuclotron-NICA energies

- Predicted and observed global polarization signals rise as the collision energy is reduced:

NICA energy range will provide new insight

- $\Lambda(\bar{\Lambda})$ - splitting of global polarization
- Comparison of models, detailed study of energy and kinematical dependences, improving precision
- Probing the vortical structure using various observables

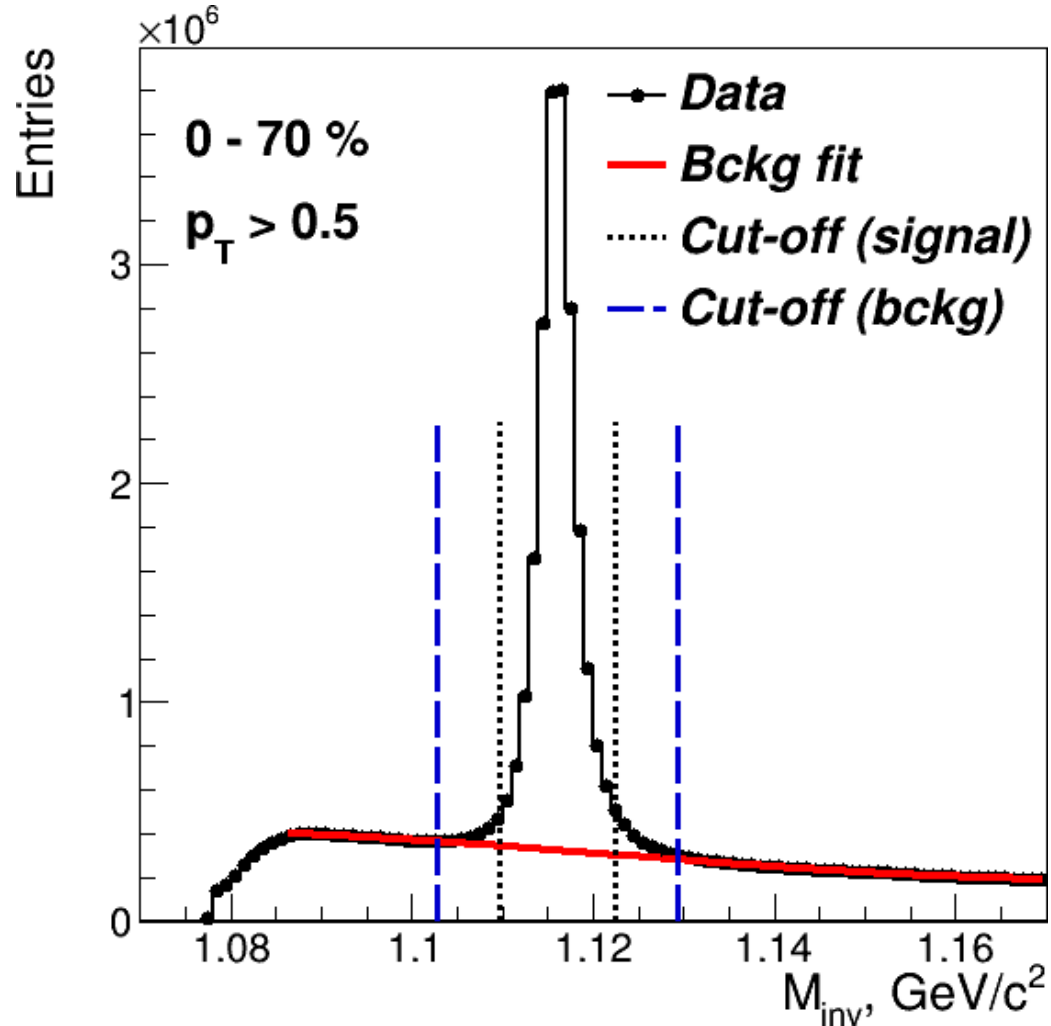


S. Singha, EPJ Web Conf. 276 (2023) 06012

J. Adam et al. (STAR Collaboration), Phys. Rev. C 98, 014910 (2018)

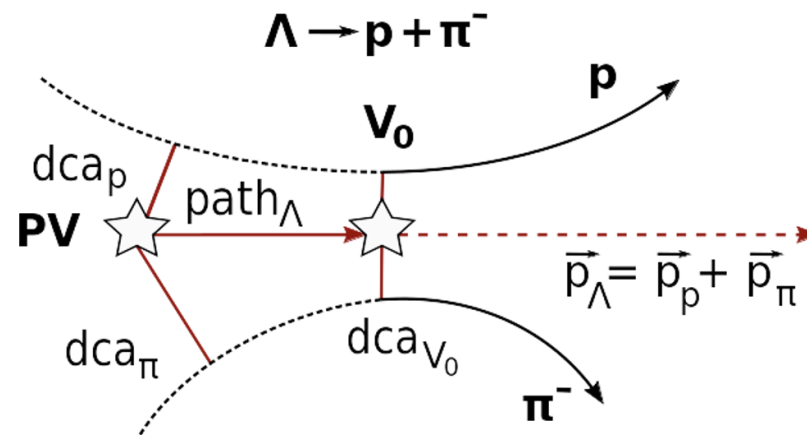
O. Teryaev and R. Usubov, Phys. Rev. C 92, 014906 (2015)

Λ selection: MpdRoot



Fitting procedure (sideband method):

- Global fit (Gauss + Legendre polynomials)
- Background fit in sidebands ($\pm 7\sigma$)
- Signal Cut-off: $\langle M \rangle \pm 3\sigma$
- Λ selection criteria:
 - $\langle \omega \rangle$ -selection (1 parameter)
 - $\langle \chi \rangle$ -selection (5 parameters)



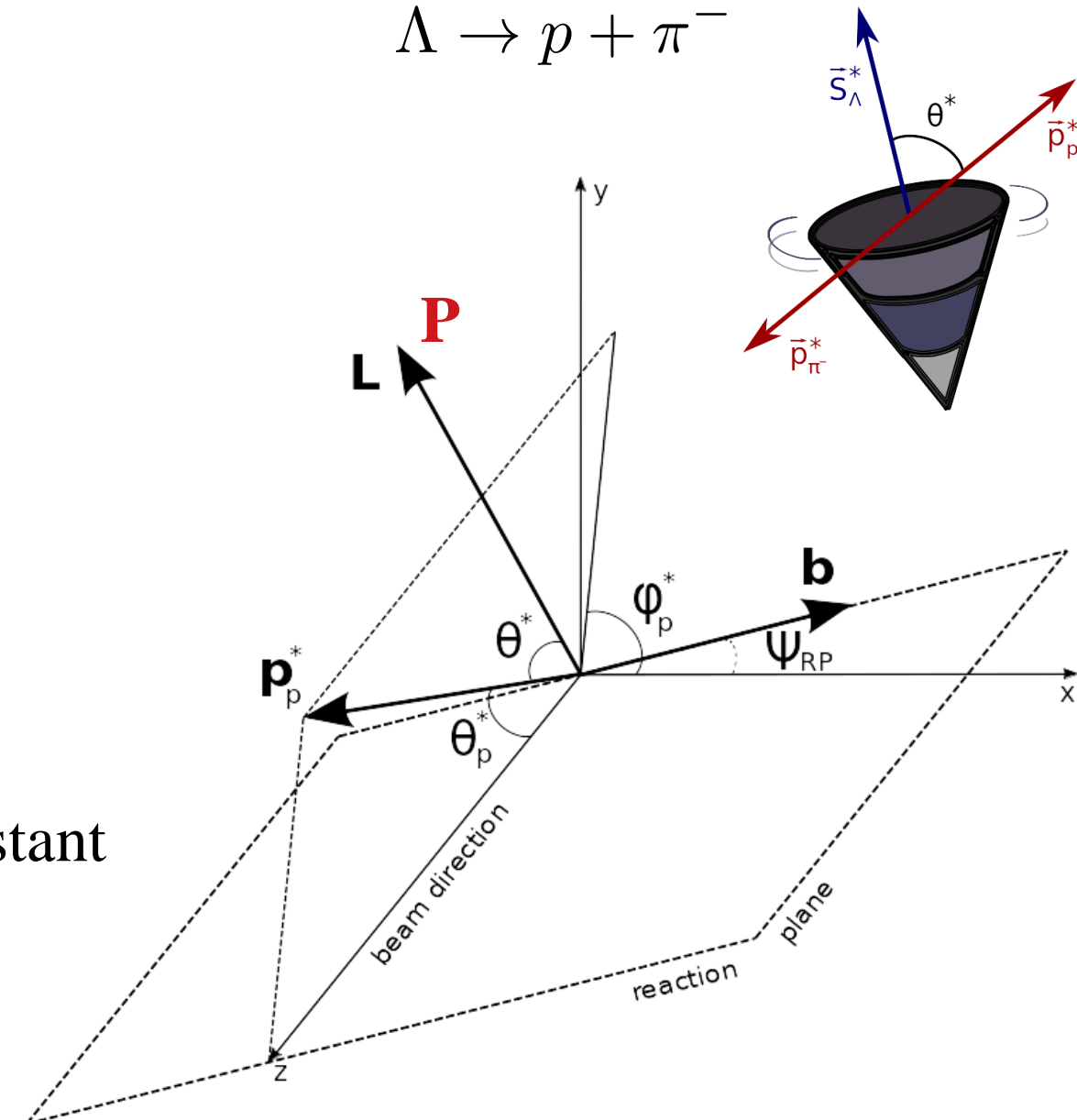
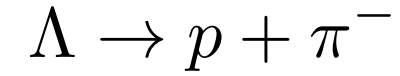
$$\omega_2 = \ln \frac{\sqrt{\chi_\pi^2 \chi_p^2}}{\chi_\Lambda^2 + \chi_{V_0}^2}$$

Global hyperon polarization

- w.r.t. reaction plane (RP)
- Emerges in HIC due to the system angular momentum
- Measured through the weak decay:

$$\frac{dN}{d \cos \theta^*} = \frac{1}{2} (1 + \alpha_H |\vec{P}_H| \cos \theta^*)$$

- * — denotes hyperon rest frame
- θ^* — angle between the decay particle (proton) and polarization direction
- $\alpha_\Lambda \simeq -\alpha_{\bar{\Lambda}} \simeq 0.732$ - hyperon decay constant



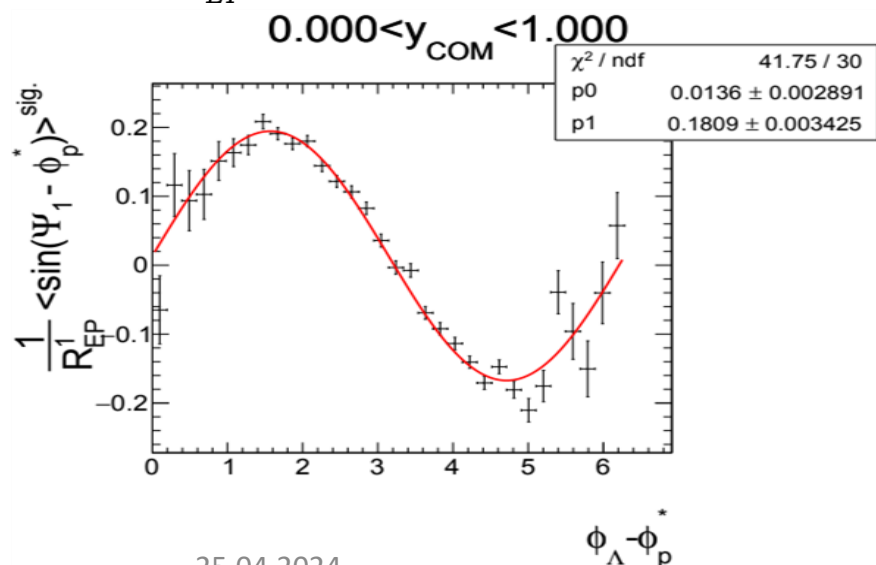
P_H measurements: inv. mass fit method

- Use invariant mass distribution
- Calculate Sig/All, Bg/All ratios
- Fit $\langle \sin(\Psi_{EP} - \phi_p^*) \rangle$ as a function of inv. mass:

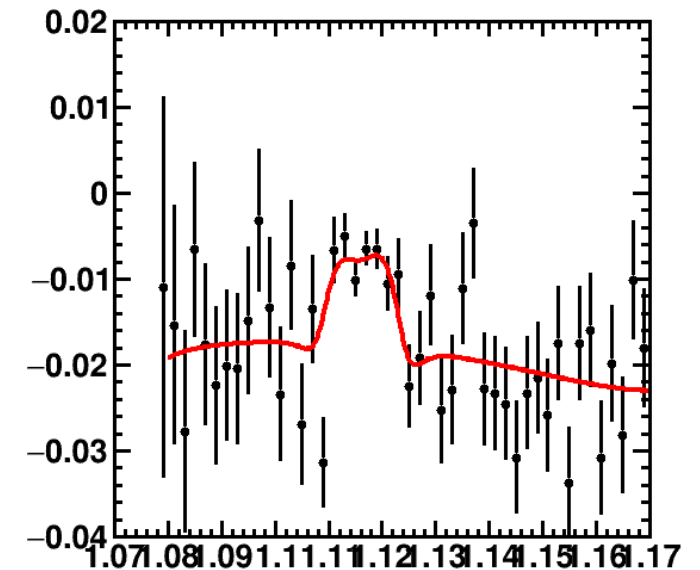
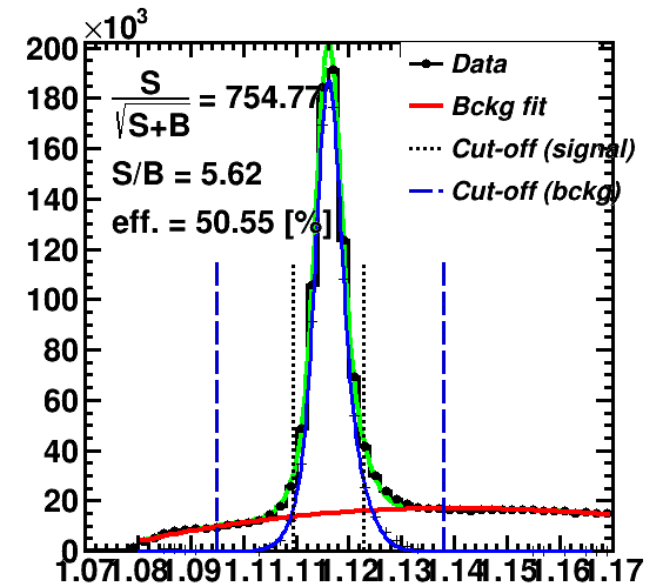
$$P^{SB}(m_{inv}, p_T) = P^S(p_T) \frac{N^S(m_{inv}, p_T)}{N^{SB}(m_{inv}, p_T)} + P^B(m_{inv}, p_T) \frac{N^B(m_{inv}, p_T)}{N^{SB}(m_{inv}, p_T)}$$

- Use $P^S(p_T) = \langle \sin(\Psi_{RP} - \phi_p^*) \rangle^{sig}$ to find P_H^{true} using fit:

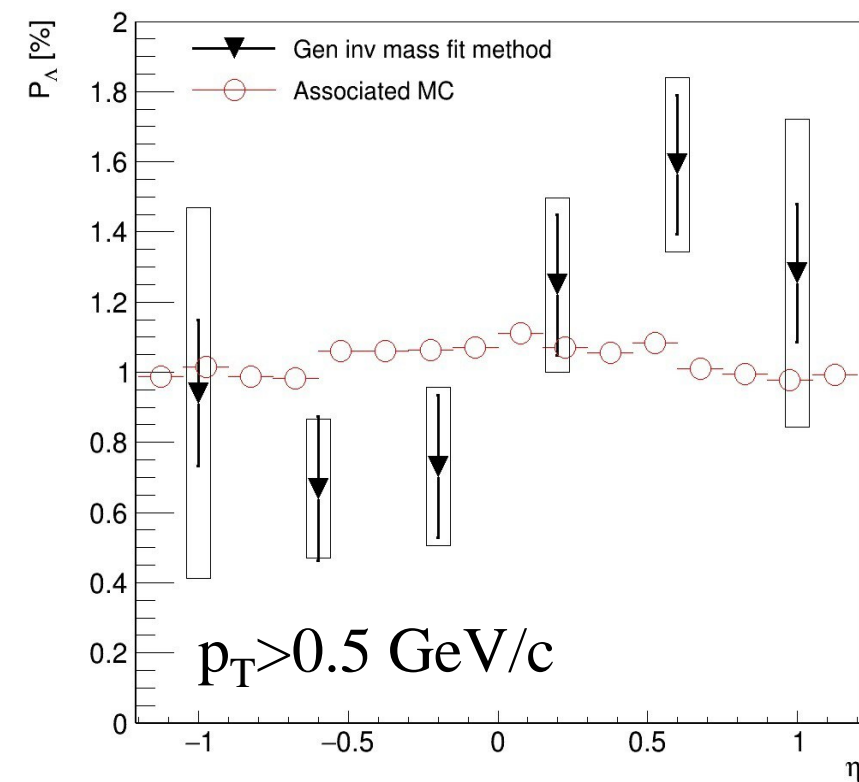
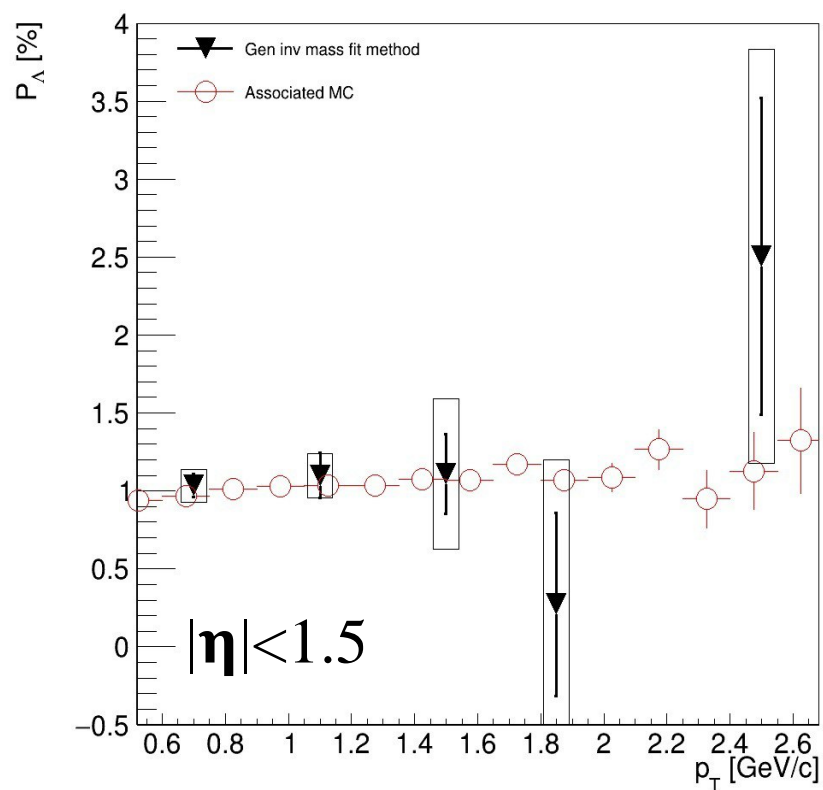
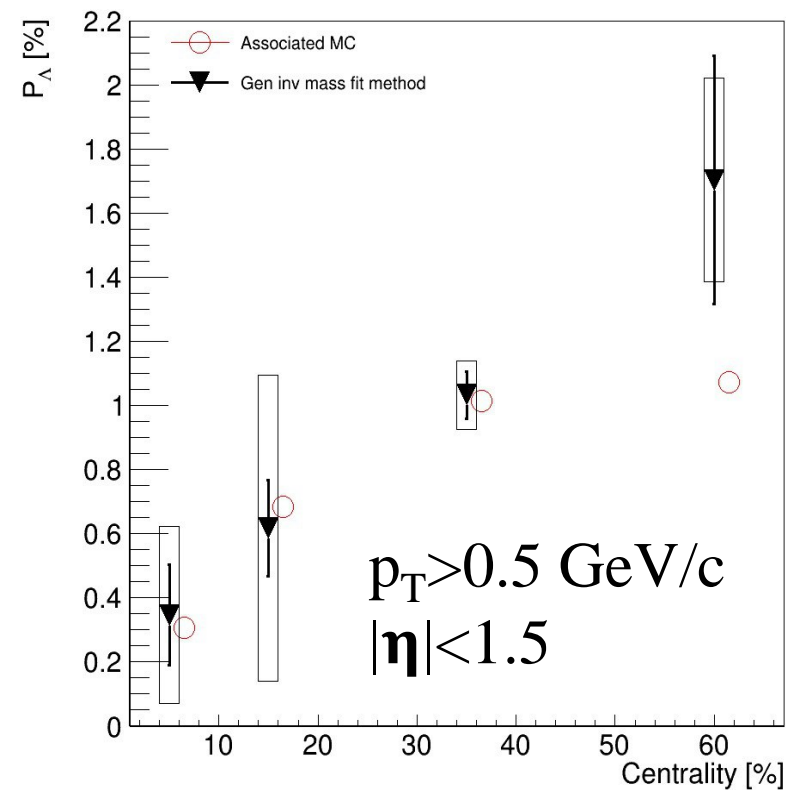
$$\frac{8}{\pi\alpha_\Lambda} \frac{1}{R_{EP}^{(1)}} \langle \sin(\Psi_1 - \phi_p^*) \rangle^{sig} = \overline{P}_\Lambda^{true} + cv_1 \sin(\phi_\Lambda - \phi_p^*)$$



Last fit corrects effects of directed flow and acceptance contributions to P_H



Centrality dependence of P_{Λ}



Good agreement with Associated MC

More statistics needed for differential (p_T, η) measurements

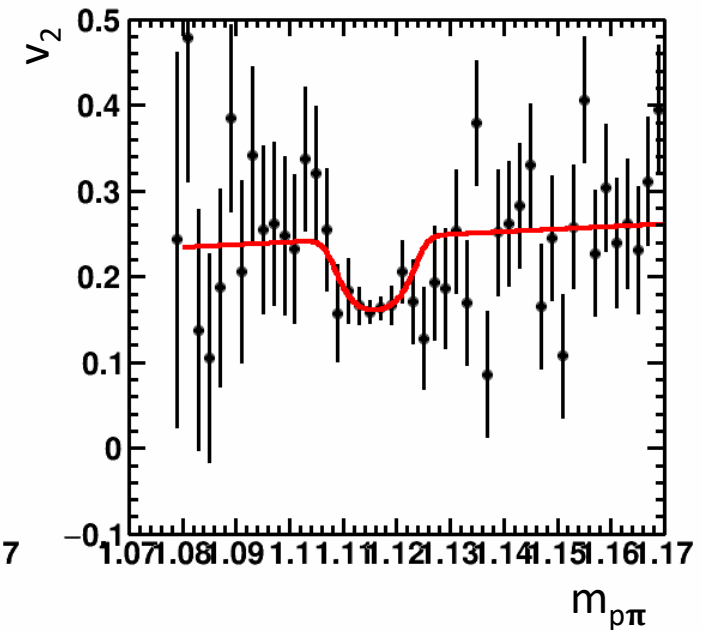
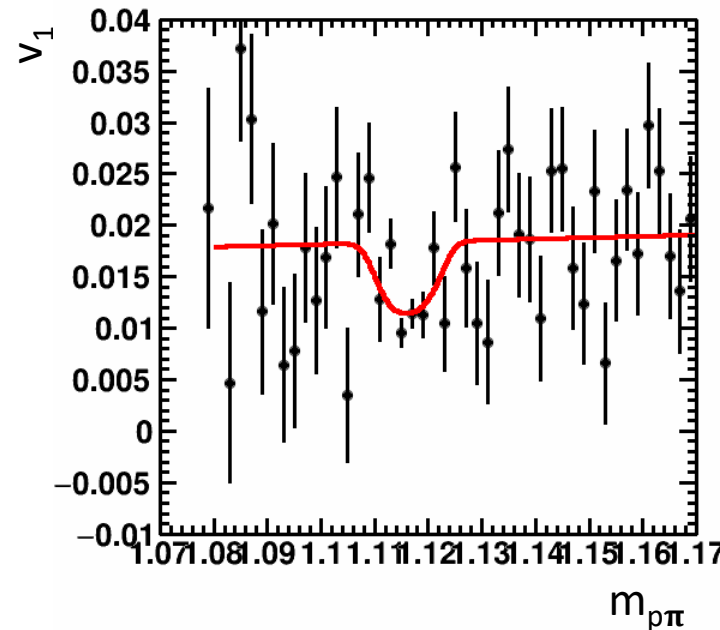
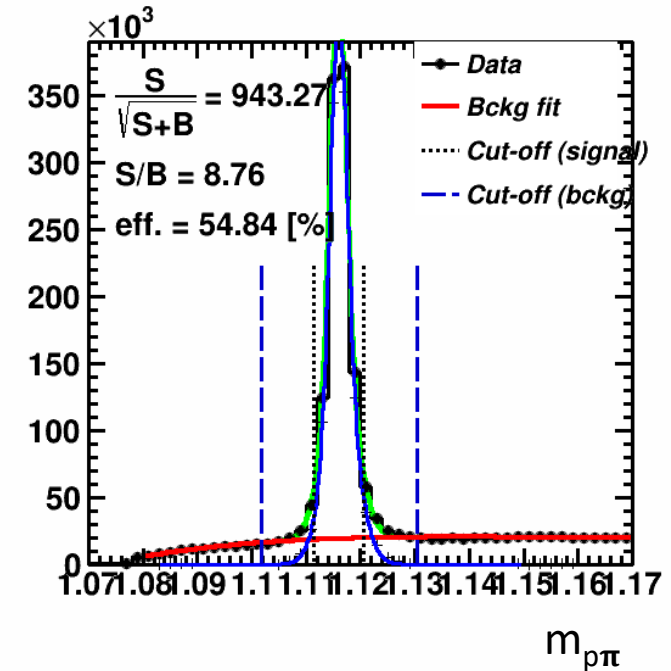
Anisotropic flow of V0 particles

Differential flow can be defined using the following fit:

$$v_n^{SB}(m_{inv}) = v_n^S \frac{N^S(m_{inv})}{N^{SB}(m_{inv})} + v_n^B(m_{inv}) \frac{N^B(m_{inv})}{N^{SB}(m_{inv})}$$

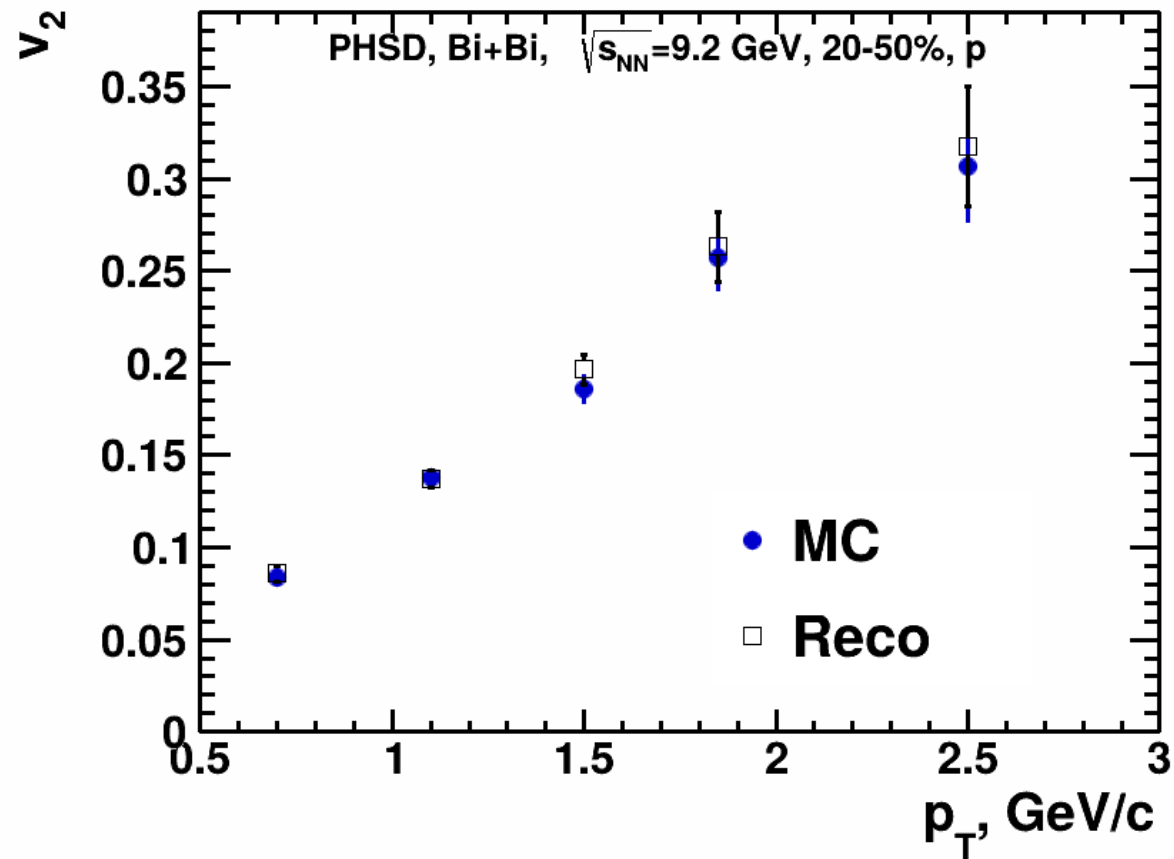
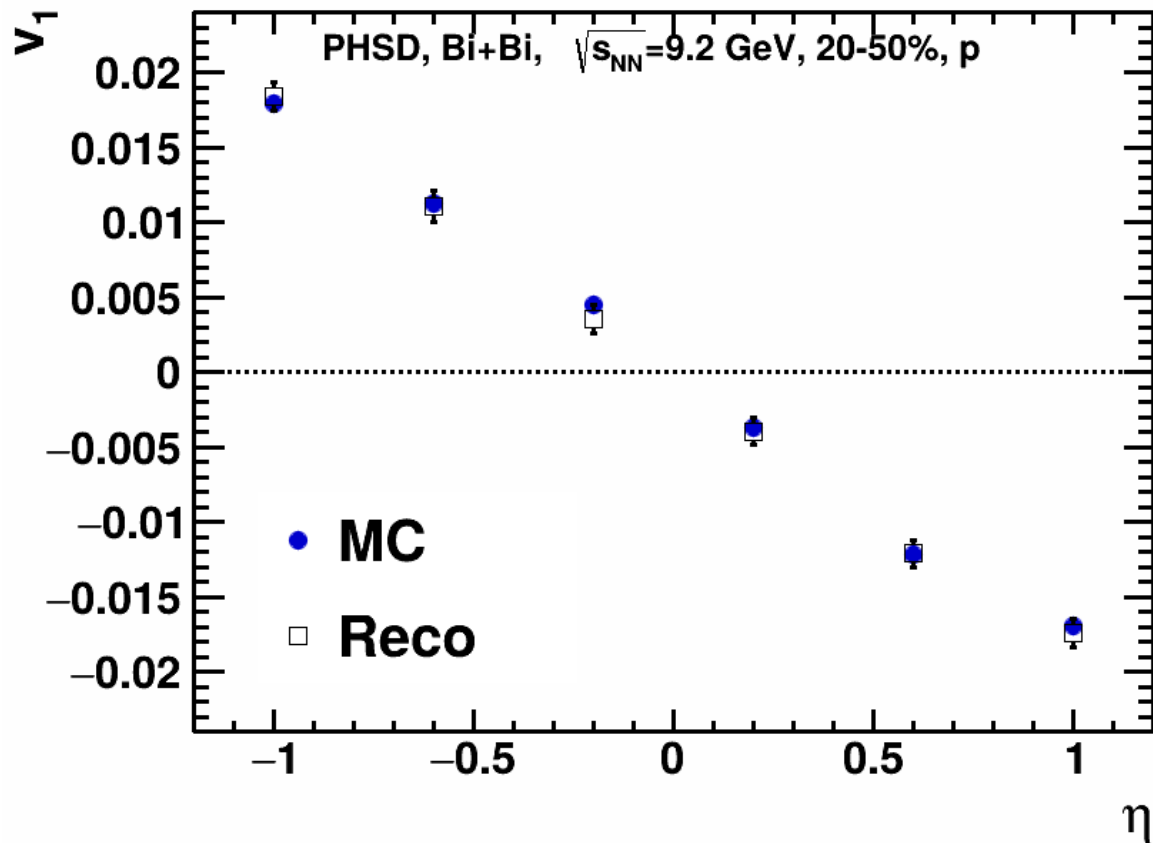
where:

- v_n^S - signal anisotropic flow (set as a parameter in the fit)
- $v_n^B(m_{inv})$ - background flow (set as polynomial function)
- $N^{SB}(m_{inv})$ - m_{inv} distribution (signal + background)
- $N^S(m_{inv})$ - m_{inv} signal distribution
- $N^B(m_{inv})$ - m_{inv} background distribution



Performance of $v_{1,2}$ of Λ hyperons in MPD

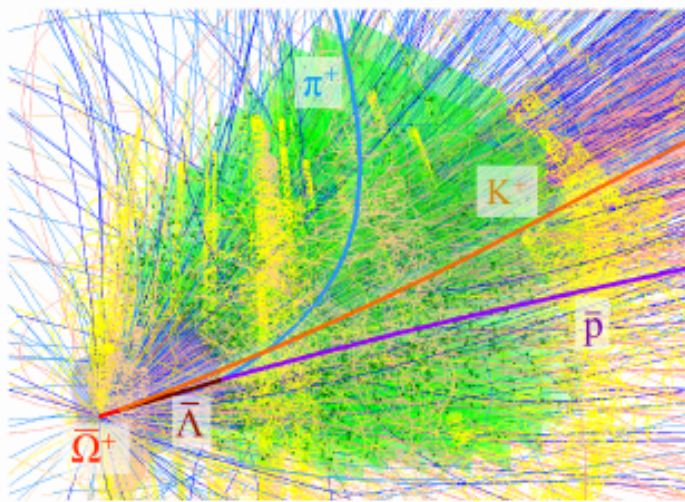
V. Troshin



Good performance for v_1 , v_2 using invariant mass fit and event plane methods

KFParticle formalism

Particles in heavy-ion collision:



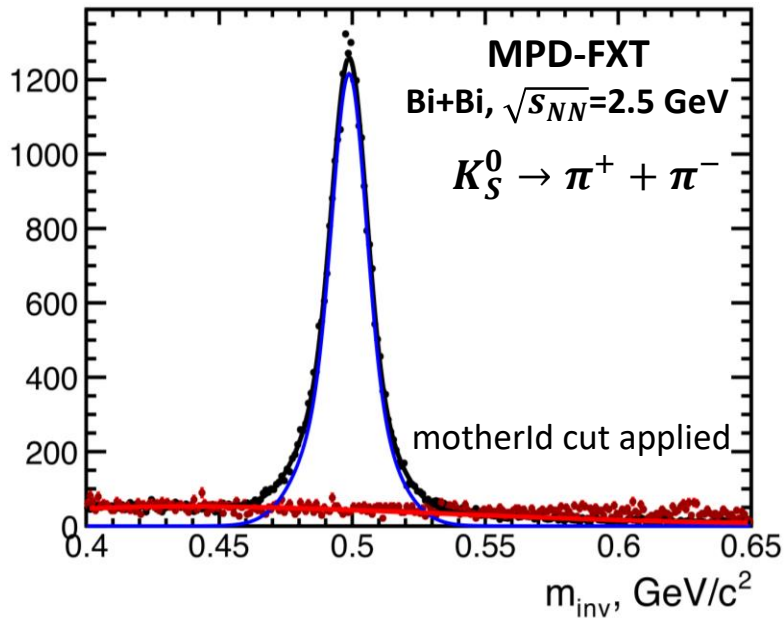
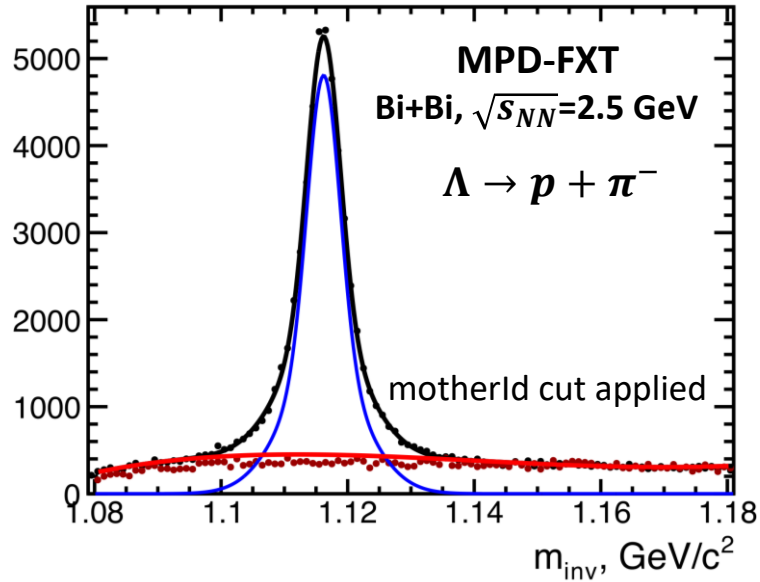
KFParticle:

- developed for complete reconstruction of short-lived particles with their P , E , m , $c\tau$, L , Y

Main benefits:

- based on the Kalman filter mathematics
- independent in sense of experimental setup (collider, fixed target)
- allows one reconstruction of decay chains (cascades)
- daughter and mother particles are described and considered the same way
- daughter particles are added to the mother particle independently

V0 selection: PFSimple



PFSimple: interface for the KFParticle package

KFParticle: package developed for complete reconstruction of short-lived particles

- Successfully used in many experiments
- Based on the Kalman filter mathematics
- Independent in the sense of experimental setup (collider, fixed target)

First tests for Λ , K_S^0 from the MPD-FXT production are ready:

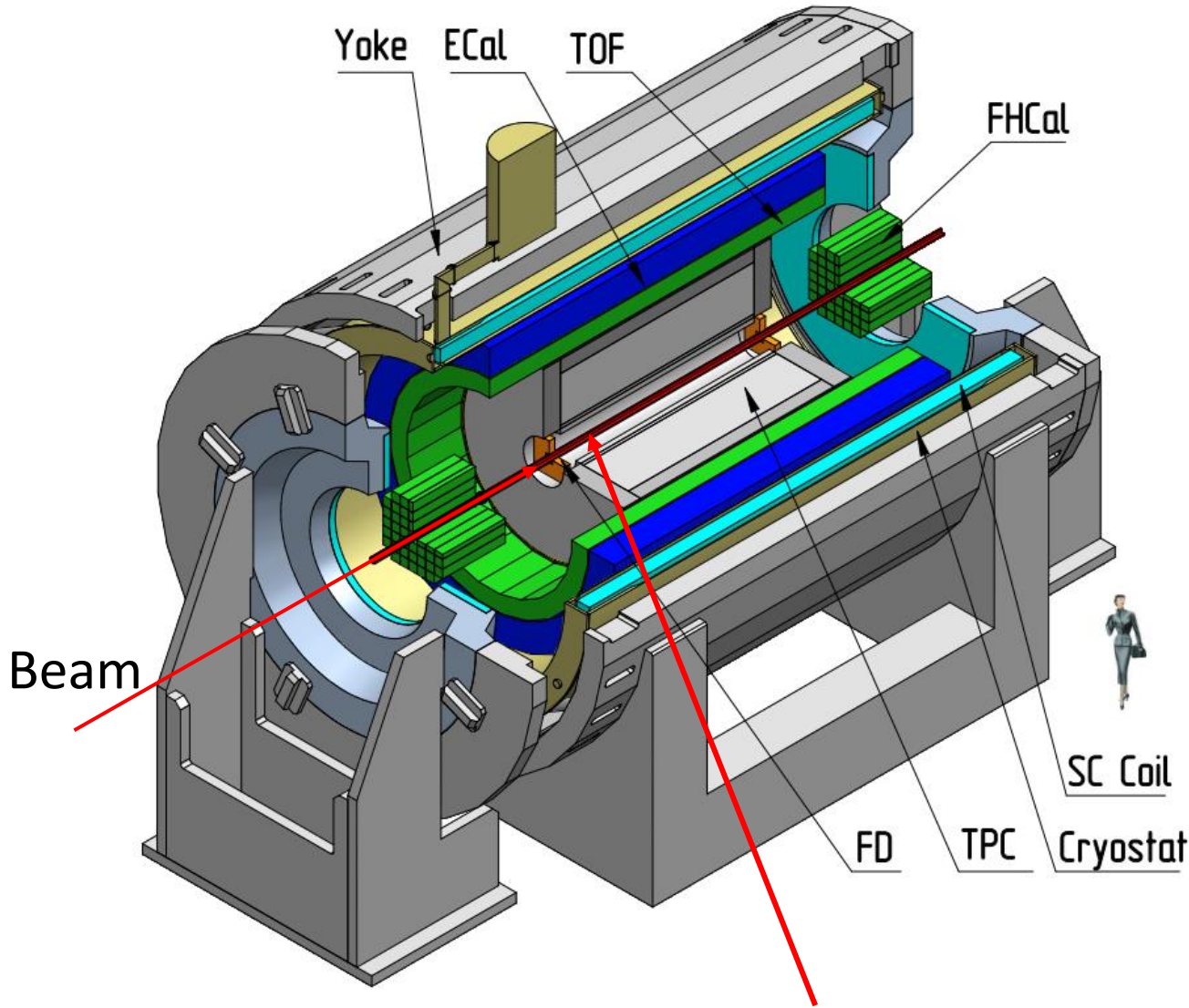
- Basic topological cuts:

$$\chi_{topo}^2 < 50, \chi_{geo}^2 < 50, L > 3 \text{ cm}, \frac{L}{dL} > 5 \text{ cm}$$

- Signal extraction: sideband fits, rotation background were tested

PFSimple is already available as a module in the cvmfs

MPD in Fixed-Target Mode (MPD-FXT)



Target (z=-115 cm)

- Model used: UrQMD mean-field
 - Bi+Bi, $E_{kin} = 1.45$ AGeV ($\sqrt{s_{NN}} = 2.5$ GeV)
 - Bi+Bi, $E_{kin} = 2.92$ AGeV ($\sqrt{s_{NN}} = 3.0$ GeV)
 - Bi+Bi, $E_{kin} = 4.65$ AGeV ($\sqrt{s_{NN}} = 3.5$ GeV)
- Point-like target
- GEANT4 transport
- Multiplicity-based centrality determination
- Particle species selection via dE/dx (TPC) and m^2 (TOF+TPC)
- Primary track selection: $|DCA| < 1$ cm
- Track quality selection:
 - $N_{hits} > 27$ (proton), $N_{hits} > 22$ (pion)

Flow vectors

From momentum of each measured particle define a u_n -vector in transverse plane:

$$u_n = e^{in\phi}$$

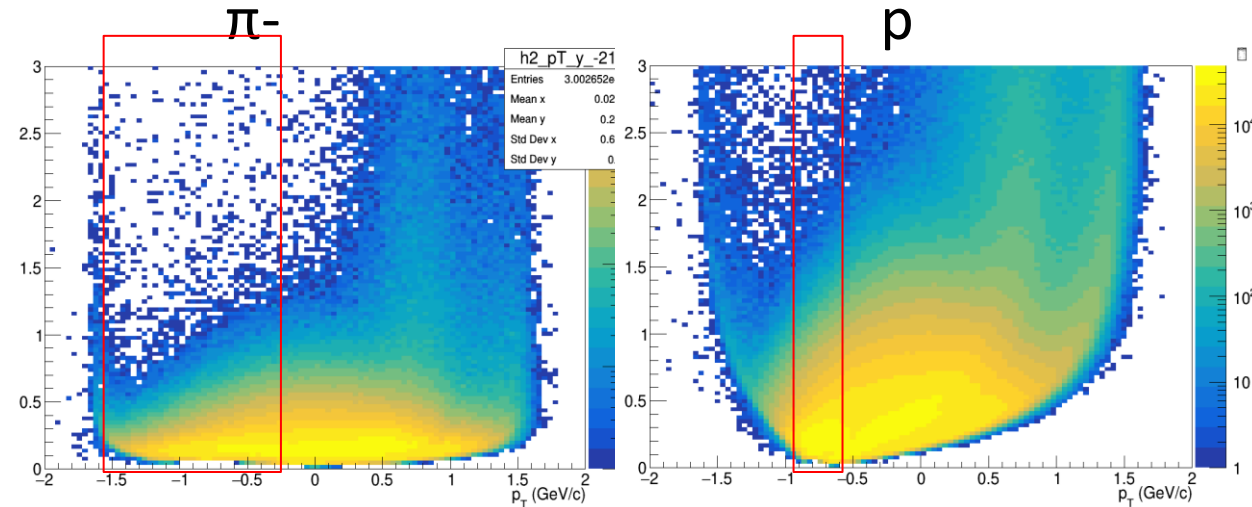
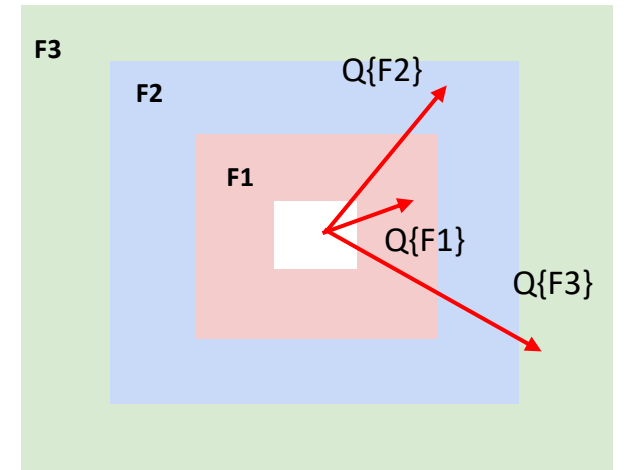
where ϕ is the azimuthal angle

Sum over a group of u_n -vectors in one event forms Q_n -vector:

$$Q_n = \frac{\sum_{k=1}^N w_n^k u_n^k}{\sum_{k=1}^N w_n^k} = |Q_n| e^{in\Psi_n^{EP}}$$

Ψ_n^{EP} is the event plane angle

Modules of FHCaI divided into 3 groups



Additional subevents from tracks not pointing at FHCaI:

Tp: p; $-1.0 < y < -0.6$;

Tπ: π-; $-1.5 < y < -0.2$;

Flow methods for v_n calculation

M Mamaev et al 2020 PPNuclei 53, 277–281

Tested in HADES: M Mamaev et al 2020 J. Phys.: Conf. Ser. 1690 012122

Scalar product (SP) method:

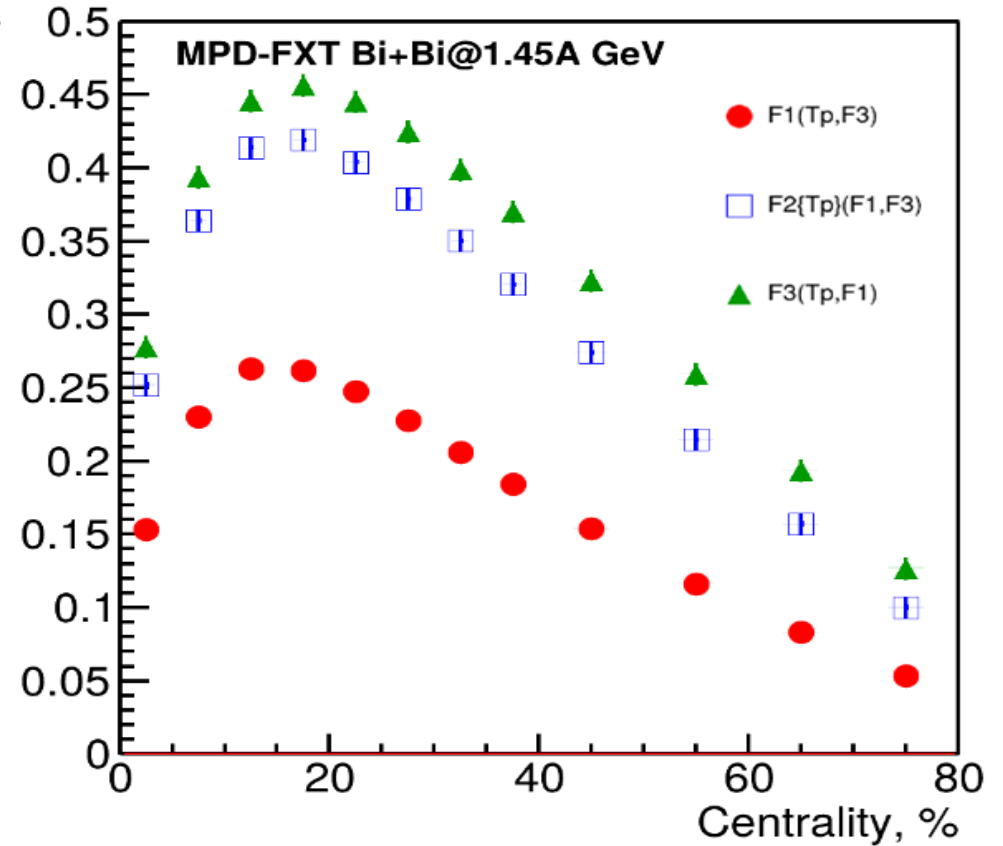
$$v_1 = \frac{\langle u_1 Q_1^{F1} \rangle}{R_1^{F1}} \quad v_2 = \frac{\langle u_2 Q_1^{F1} Q_1^{F3} \rangle}{R_1^{F1} R_1^{F3}}$$

Where R_1 is the resolution correction factor

$$R_1^{F1} = \langle \cos(\Psi_1^{F1} - \Psi_1^{RP}) \rangle$$

Symbol “F2(F1,F3)” means R_1 calculated via (3S resolution):

$$R_1^{F2(F1,F3)} = \frac{\sqrt{\langle Q_1^{F2} Q_1^{F1} \rangle \langle Q_1^{F2} Q_1^{F3} \rangle}}{\sqrt{\langle Q_1^{F1} Q_1^{F3} \rangle}}$$

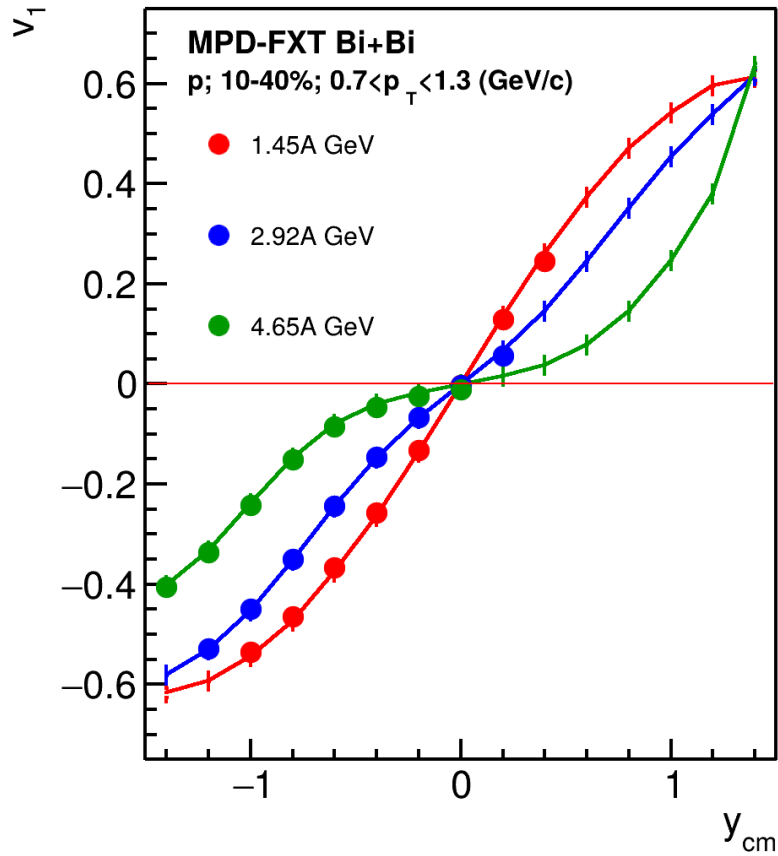


Symbol “F2{Tp}(F1,F3)” means R_1 calculated via (4S resolution):

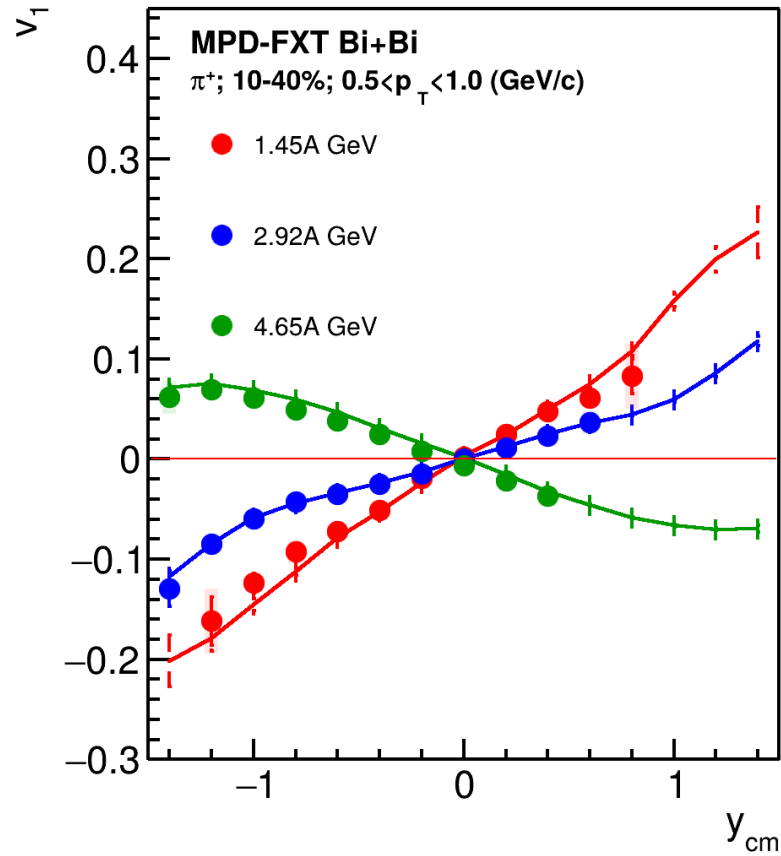
$$R_1^{F2\{Tp\}(F1,F3)} = \langle Q_1^{F2} Q_1^{Tp} \rangle \frac{\sqrt{\langle Q_1^{F1} Q_1^{F3} \rangle}}{\sqrt{\langle Q_1^{Tp} Q_1^{F1} \rangle \langle Q_1^{Tp} Q_1^{F3} \rangle}}$$

Results: $v_1(y)$

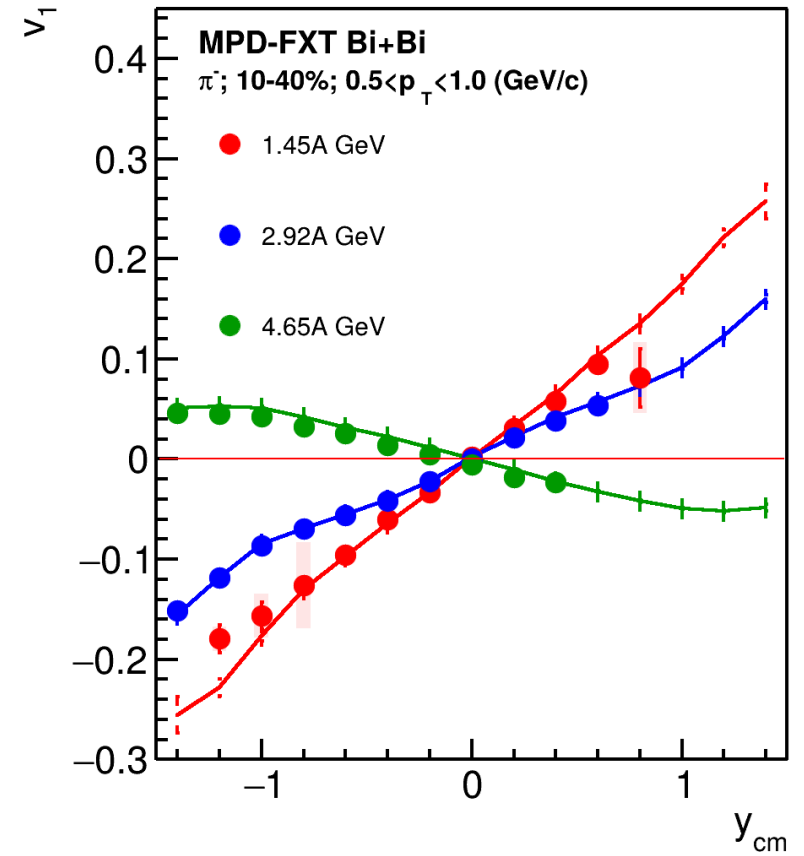
p



π^+



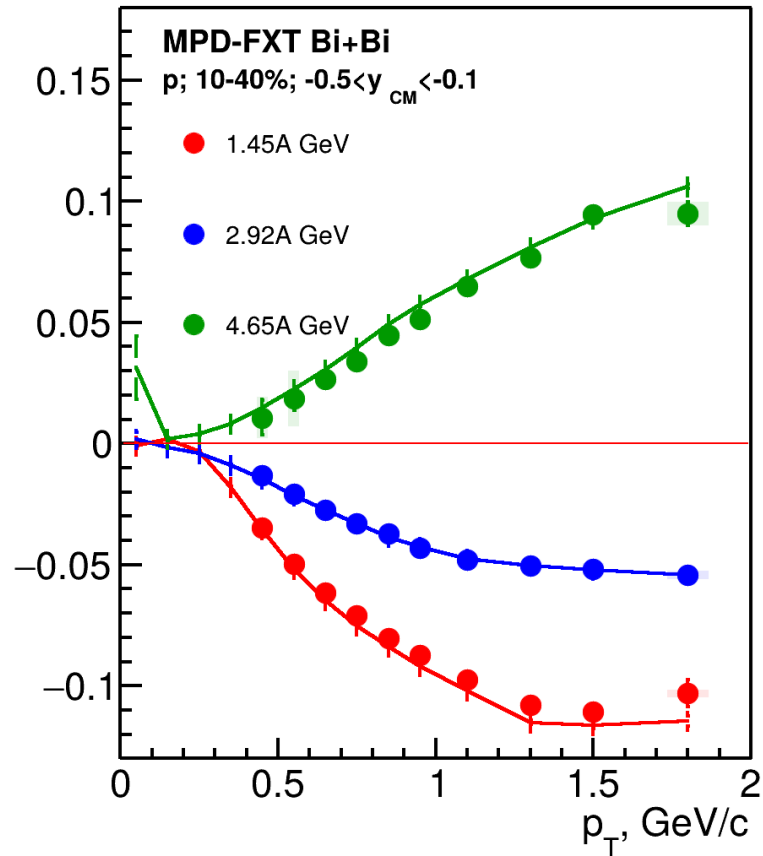
π^-



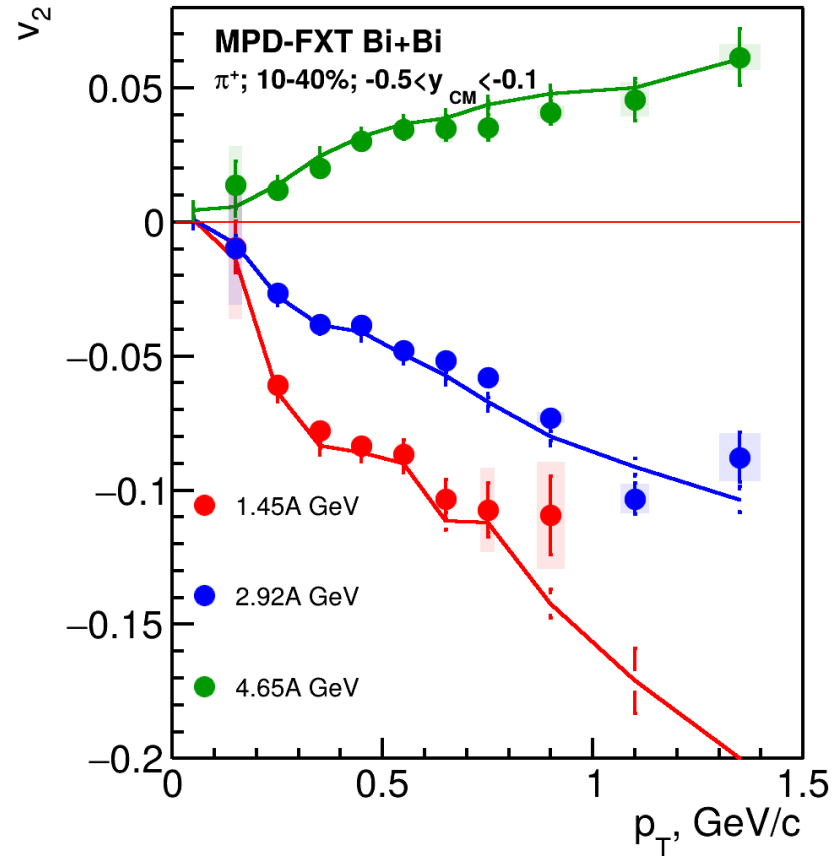
Good agreement with MC data

Results: $v_2(p_T)$

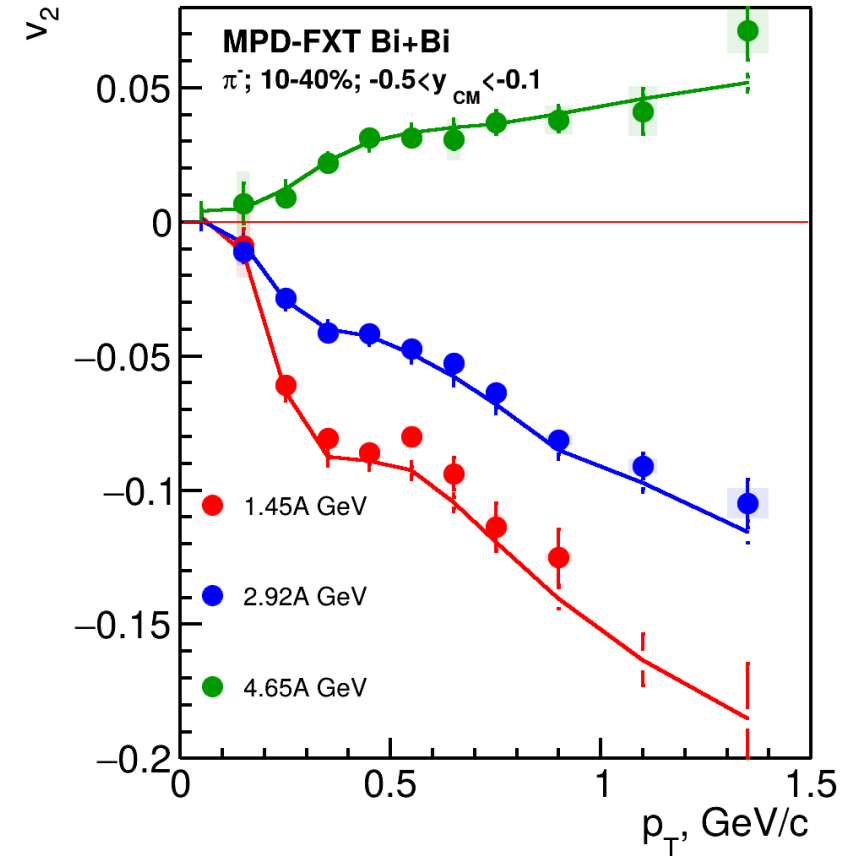
p



π^+

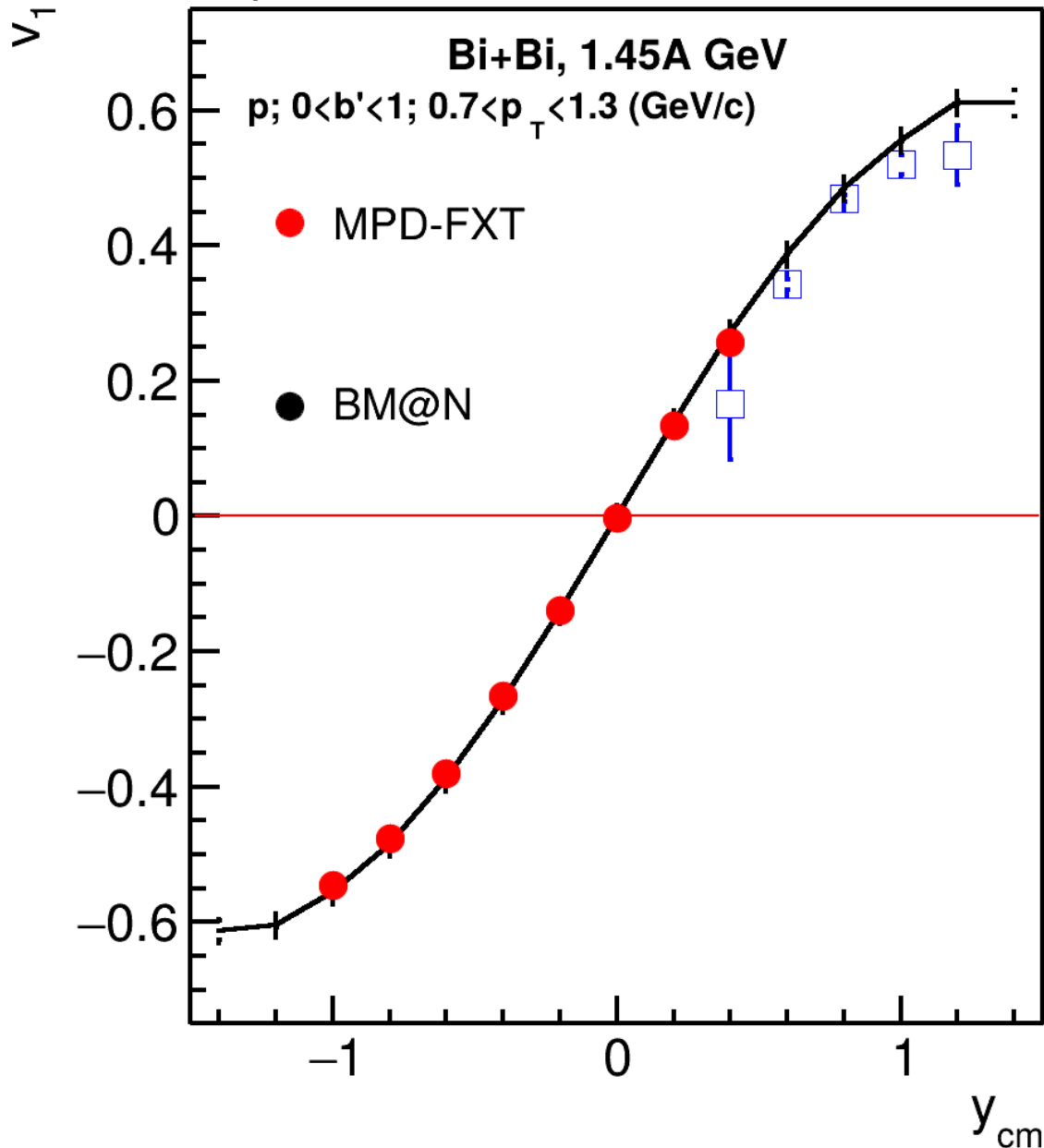


π^-



Good agreement with MC data

Comparison with BM@N performance



BM@N TOF system (TOF-400 and TOF-700) has poor midrapidity coverage at $\sqrt{s_{NN}} = 2.5$ GeV

- One needs to check higher energies ($\sqrt{s_{NN}} = 3, 3.5$ GeV)
- More statistics are required due to the effects of magnetic field in BM@N:
 - Only “yy” component of $\langle uQ \rangle$ and $\langle QQ \rangle$ correlation can be used

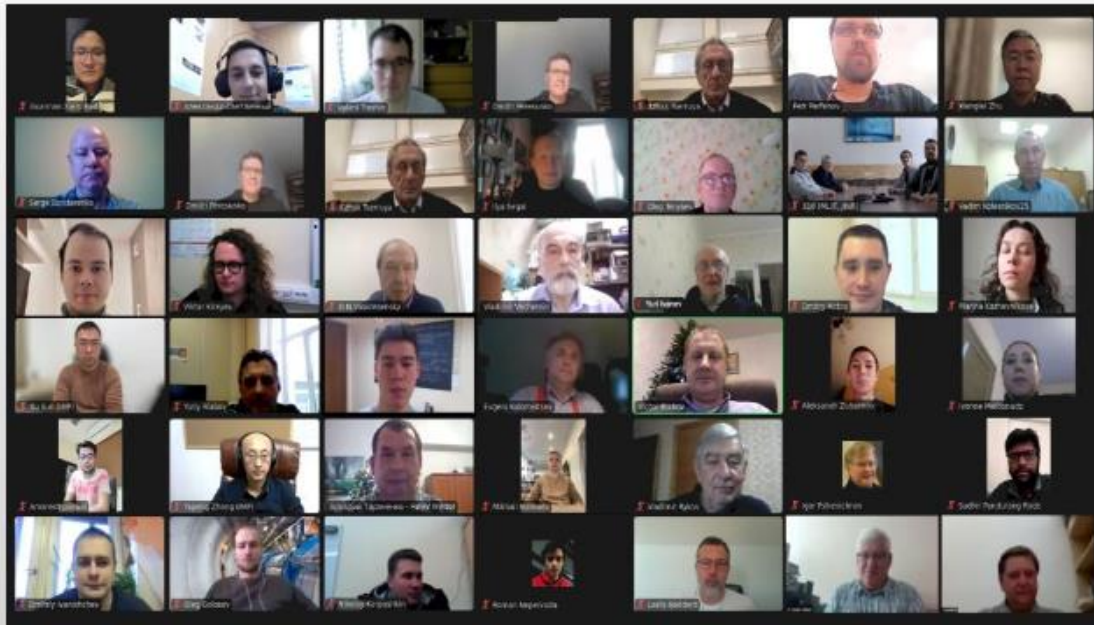
Despite the challenges, both MPD-FXT and BM@N can be used in v_n measurements:

- To widen rapidity coverage
- To perform a cross-check in the future

Conferences and workshops

❖ JINR-MEPHI organized International Workshop NICA-2023 (<http://indico.oris.mephi.ru/event/301/overview>):

- ✓ 100+ participants from different countries:
Belarus, Bulgaria, Israel, India, China, Kazakhstan, Mexico, Russia, Turkey, Serbia, USA and Uzbekistan
- ✓ active participation of the MPD Chinese group in the organizing committee and the work of the workshop
- ✓ 22 presentations in three days on experimental and theoretical topics
- ✓ joint platform for discussion of NICA physics at BM@N and MPD



Co-chairs

Arkadiy Taranenko (MEPhI, JINR)
Evgeni Kolomeitsev (JINR, UMB, Banska Bystrica)
Victor Riabov (PNPI, MEPHI)

Organizing committee

Zebo Tang (USTC, China)
Yi Wang (Tsinghua University, China)
Shusu Shi (CCNU, China)
Natalia Barbashina (MEPhI)
Ivan Astapov (MEPhI)
Dmitry Blau (NRC Kurchatov Institute)
Serge Bondarenko (BLTP JINR)
Fedor Guber (INR RAS)
Vadim Kolesnikov (JINR)

Summary and Outlook

- **Feasibility study for anisotropic flow:**
 - evFlowEP wagon for v_n measurements is implemented in the MpdRoot and already tested
 - Results from reconstructed and generated data are in a good agreement for all methods
 - New PFSimple interface available and tested on MPD-FXT production
 - Flow performance for MPD-FXT: good agreement between reconstructed and generated data in backward rapidity and midrapidity regions
 - MPD-FXT and BM@N can be complementary to each other in terms of flow measurements and noticeably widen available rapidity region
- **Performance of the global Λ polarisation P_Λ :**
 - Results were recently published in EPJA
 - Invariant mass fit method for P_Λ measurements was implemented and tested
 - Good agreement between “reco” and “associated MC” results
 - More statistics needed for differential $P_\Lambda(p_T, y)$ measurements

Thank you for your attention!

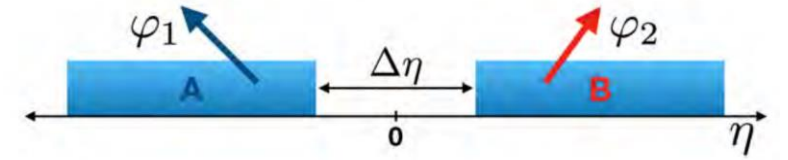
Backup slides

Methods for v_n measurements

- **Sub-event 2-particle Q-cumulants $v_2\{2\}$:**

$\Delta\eta=0.1$ is applied between 2 sub-events A, B to suppress non-flow

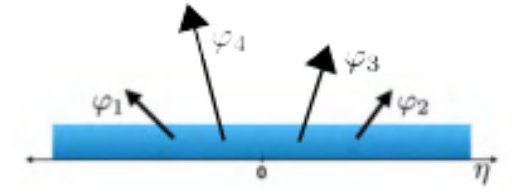
$$Q_n = \sum_{i=1}^M e^{in\phi} \quad \langle 2 \rangle_{a|b} = \frac{Q_{n_a} Q_{n_b}^*}{M_a M_b} \quad v_2\{2\} = \sqrt{\langle \langle 2 \rangle \rangle_{a|b}}$$



- **4-particle Q-cumulants $v_2\{4\}$**

$$\langle 2 \rangle = \frac{|Q_n|^2 - M}{M(M-1)} \quad v_2\{4\} = \sqrt[4]{2 \langle \langle 2 \rangle \rangle^2 - \langle \langle 4 \rangle \rangle}$$

$$\langle 4 \rangle = \frac{|Q_n|^4 + |Q_{2n}|^2 - 2\Re[Q_{2n} Q_n^* Q_n^*] - 4(M-2)|Q_n|^2 - 2M(M-3)}{M(M-1)(M-2)(M-3)}$$



- **Event plane method: $\Delta\eta=0.1$**

$$Q_{n,x} = \sum_i w_i \cos(n\phi_i) \quad \Psi_n^{EP} = \frac{1}{n} \tan^{-1} \left(\frac{Q_{n,y}}{Q_{n,x}} \right)$$

$$Q_{n,y} = \sum_i w_i \sin(n\phi_i)$$

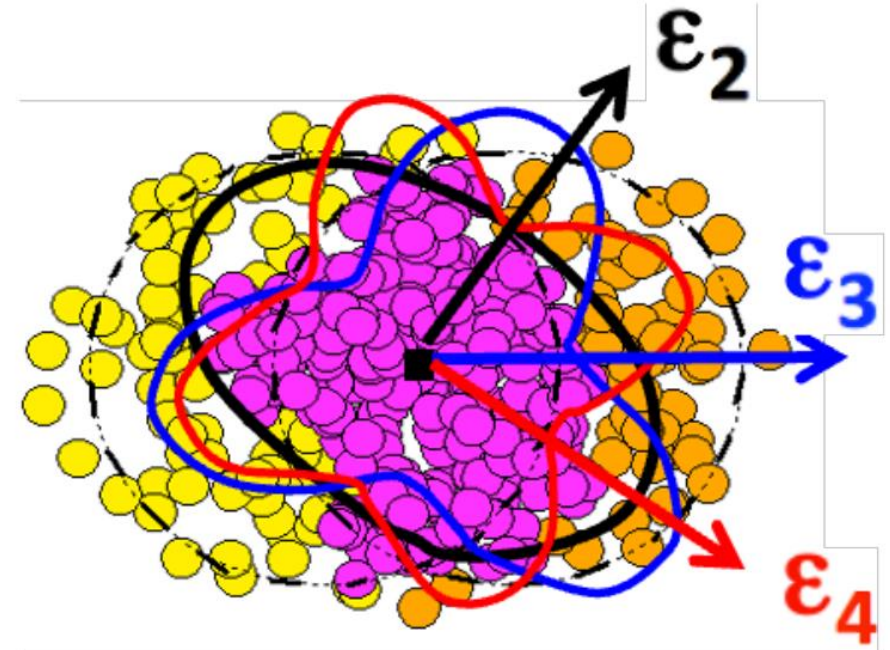
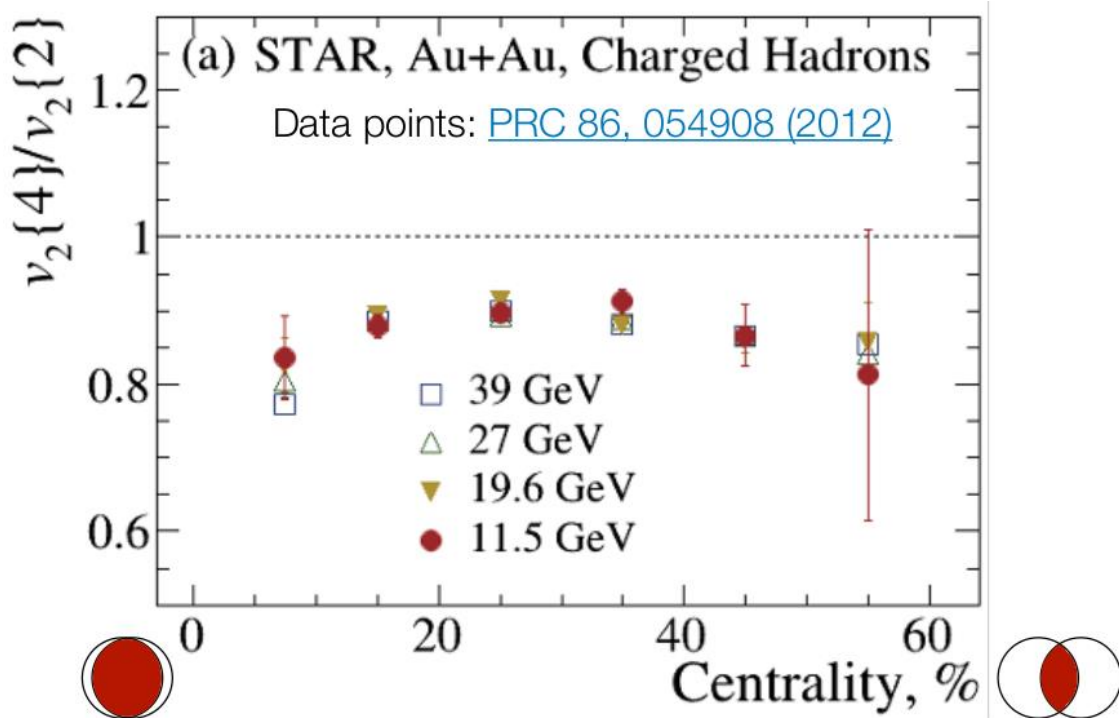
$$v_n = \frac{\langle \cos[n(\phi - \Psi_n^{EP})] \rangle}{\sqrt{\langle \cos[n(\Psi_{n,a} - \Psi_{n,b})] \rangle}}$$

Here: w_i - $p_{T,i}$ transverse momentum of the i-th track in the TPC

ϕ_i - azimuthal angle of the i-th track in the TPC

Ψ_n - event plane angles

Motivation of elliptic flow fluctuation study



v_2 fluctuations at $\sqrt{s_{NN}}=11.5-39$ GeV
observed in STAR:

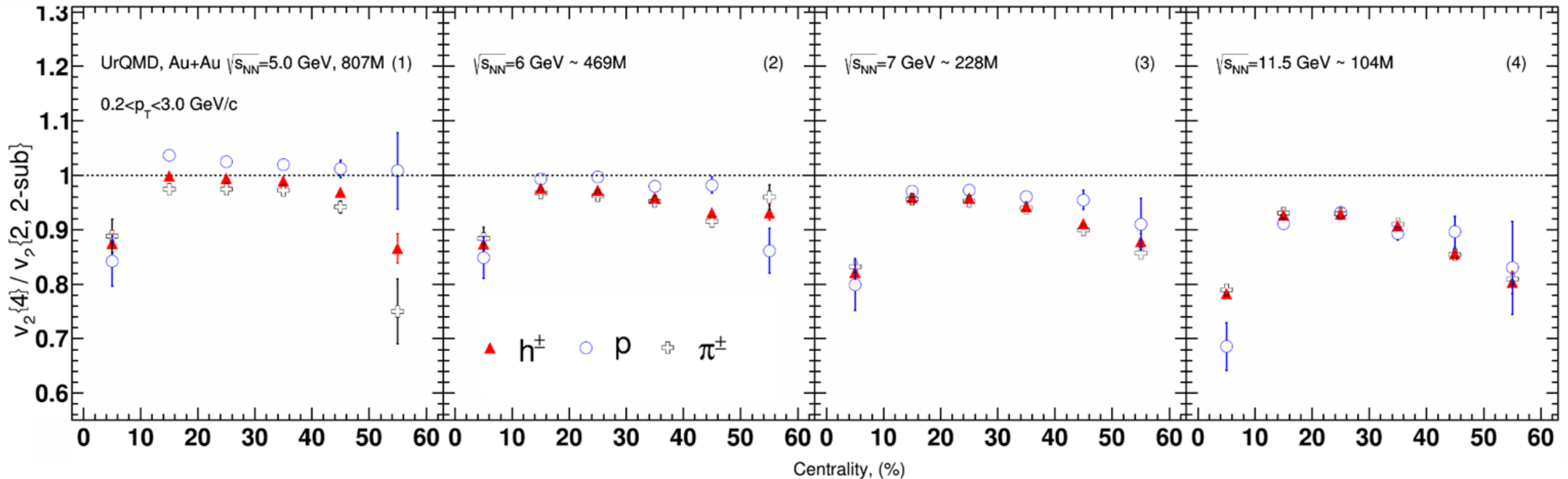
- Weak dependence on collision energy

- Indicate a dominated initial state driven fluctuations σ_{ϵ_2}
- Provide constraints for IS models and shear viscosity $\eta(T/s)$

How about v_2 fluctuations at NICA energies?

Relative v_2 fluctuations of identified hadrons

For more details see A.Demanov's [talk](#) on ISHEP-2023



- Weak dependence between $v_2\{4\}/v_2\{2\}$ of protons and pions at 11.5 GeV
- The difference between $v_2\{4\}/v_2\{2\}$ of protons and pions increases with decreasing energy

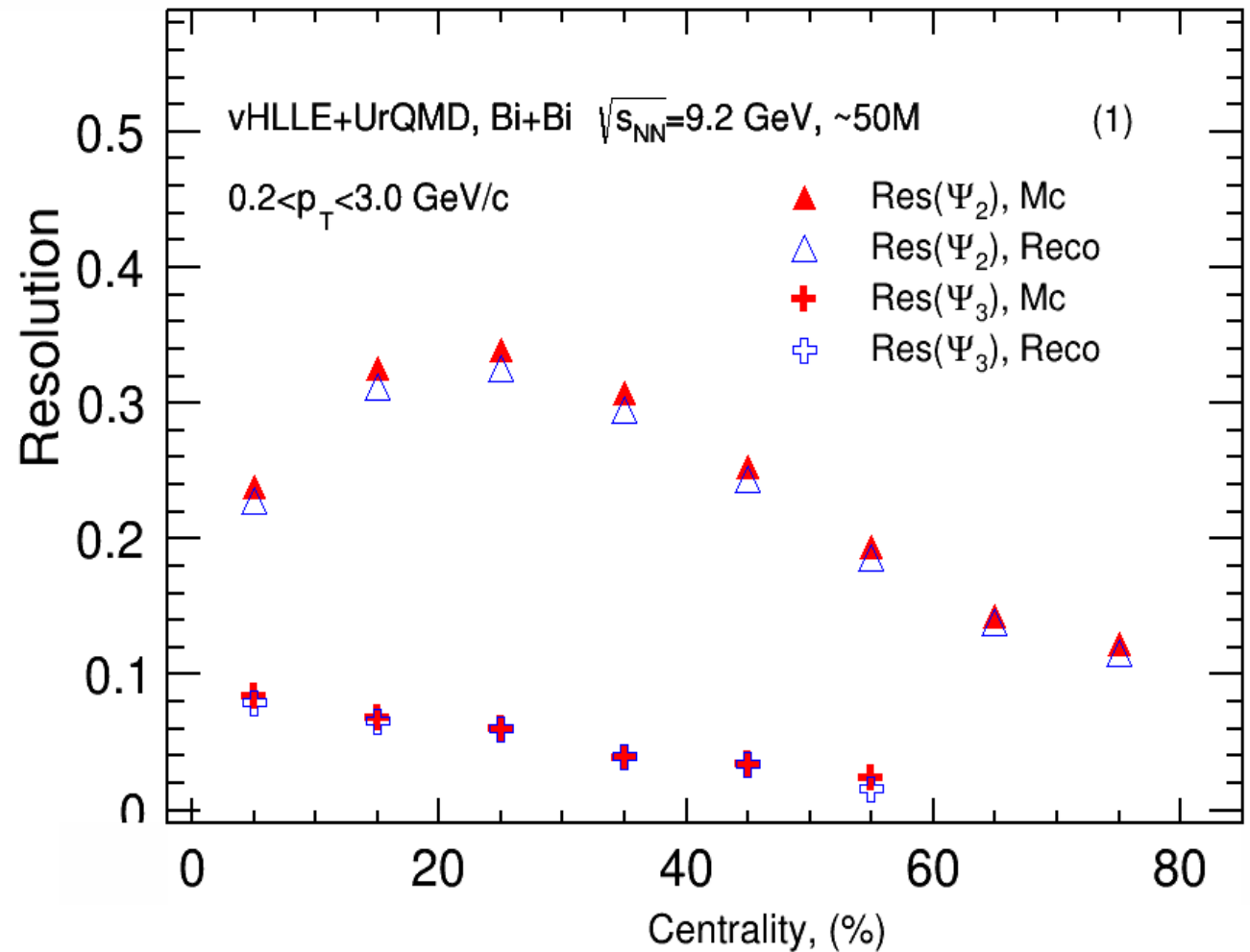
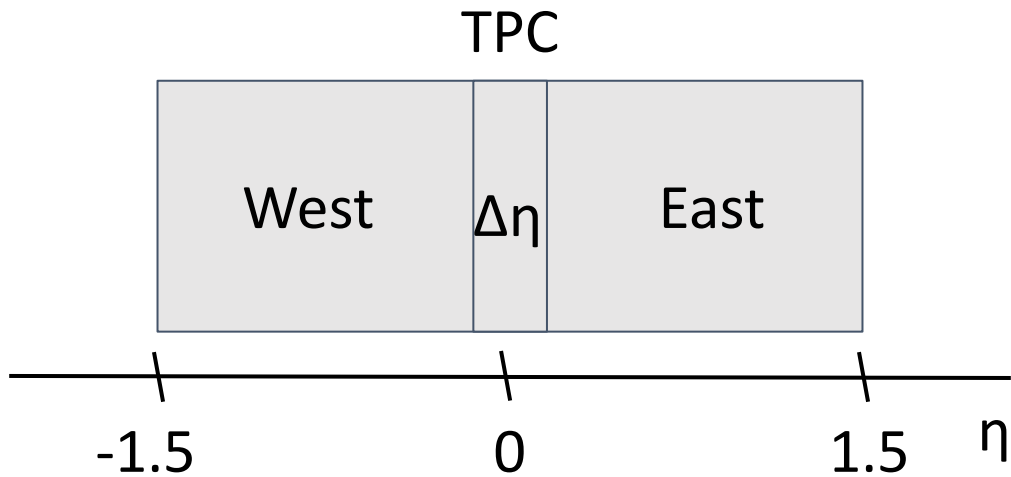
Event plane Resolution

2 sub event: $\Delta\eta=0.1$

$$Res\{\Psi_n^{E(W)}\} = \sqrt{\langle \cos [n(\Psi_n^E - \Psi_n^W)] \rangle}$$

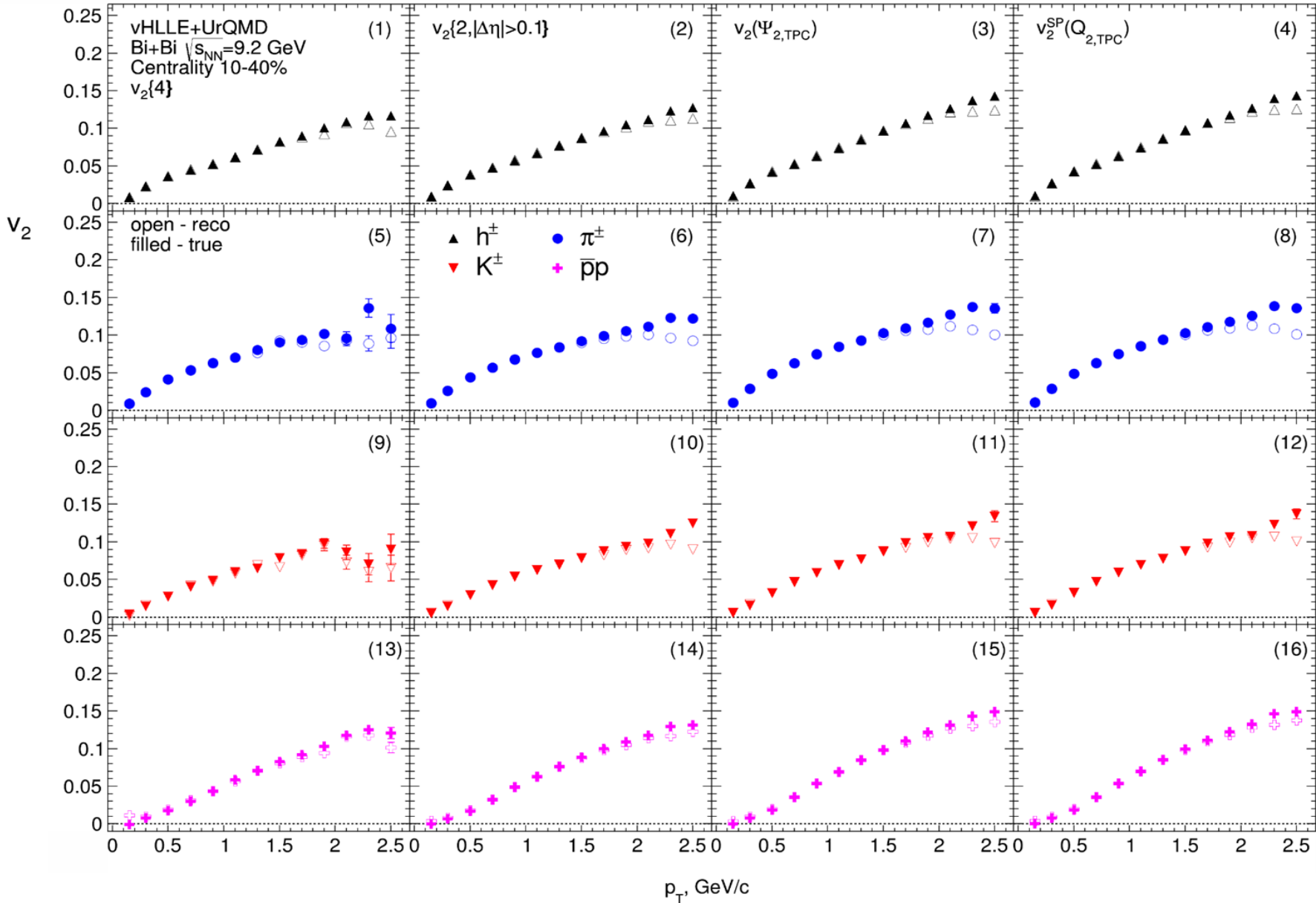
Anisotropic flow is measured as follows:

$$v_n = \frac{\langle \cos [n(\phi - \Psi_n^{EP})] \rangle}{\sqrt{\langle \cos [n(\Psi_{n,a} - \Psi_{n,b})] \rangle}}$$



- We do not measure the Ψ_3 resolution after to 60% centrality
- Ψ_3 resolution are smaller than Ψ_2
- Good agreement between $R_{MC}(\Psi_n)$ and $R_{reco}(\Psi_n)$

Comparison of Reco and MC: v_2 eta-sub EP



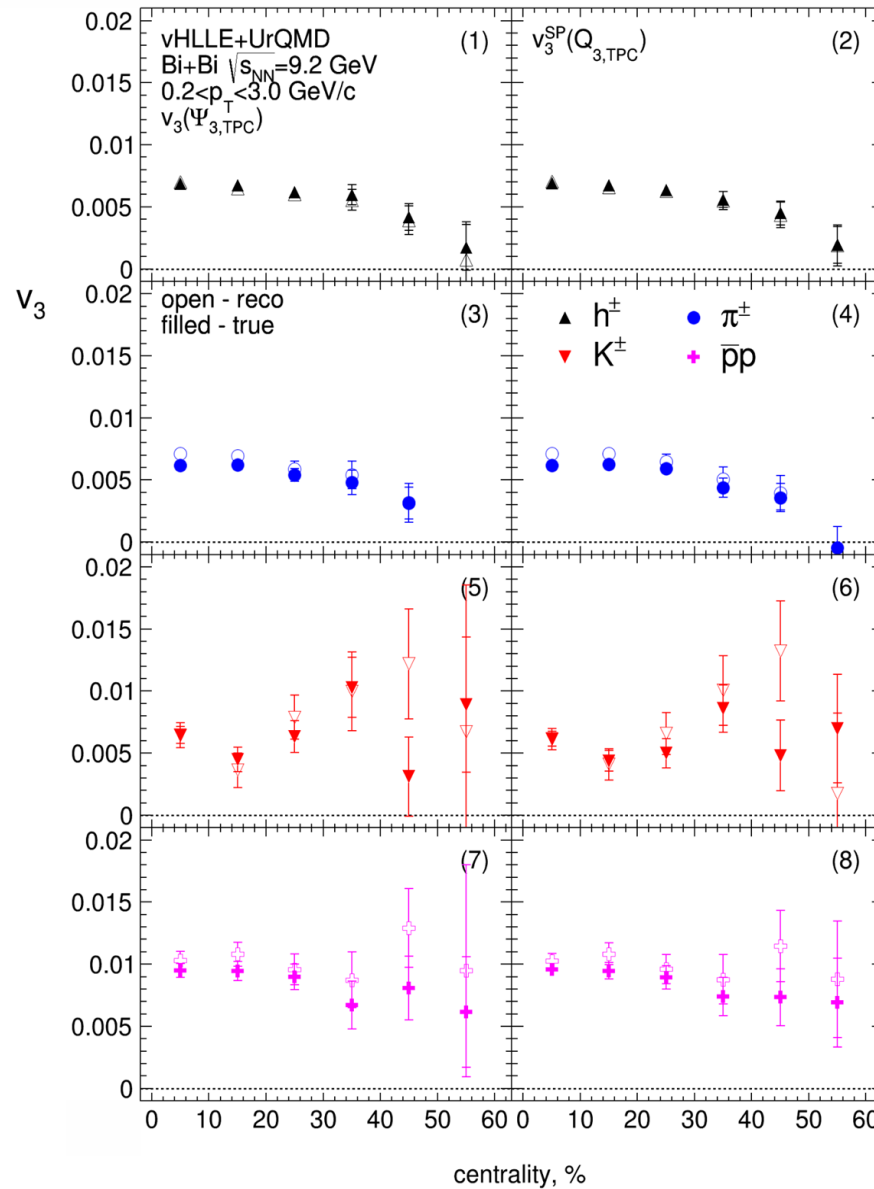
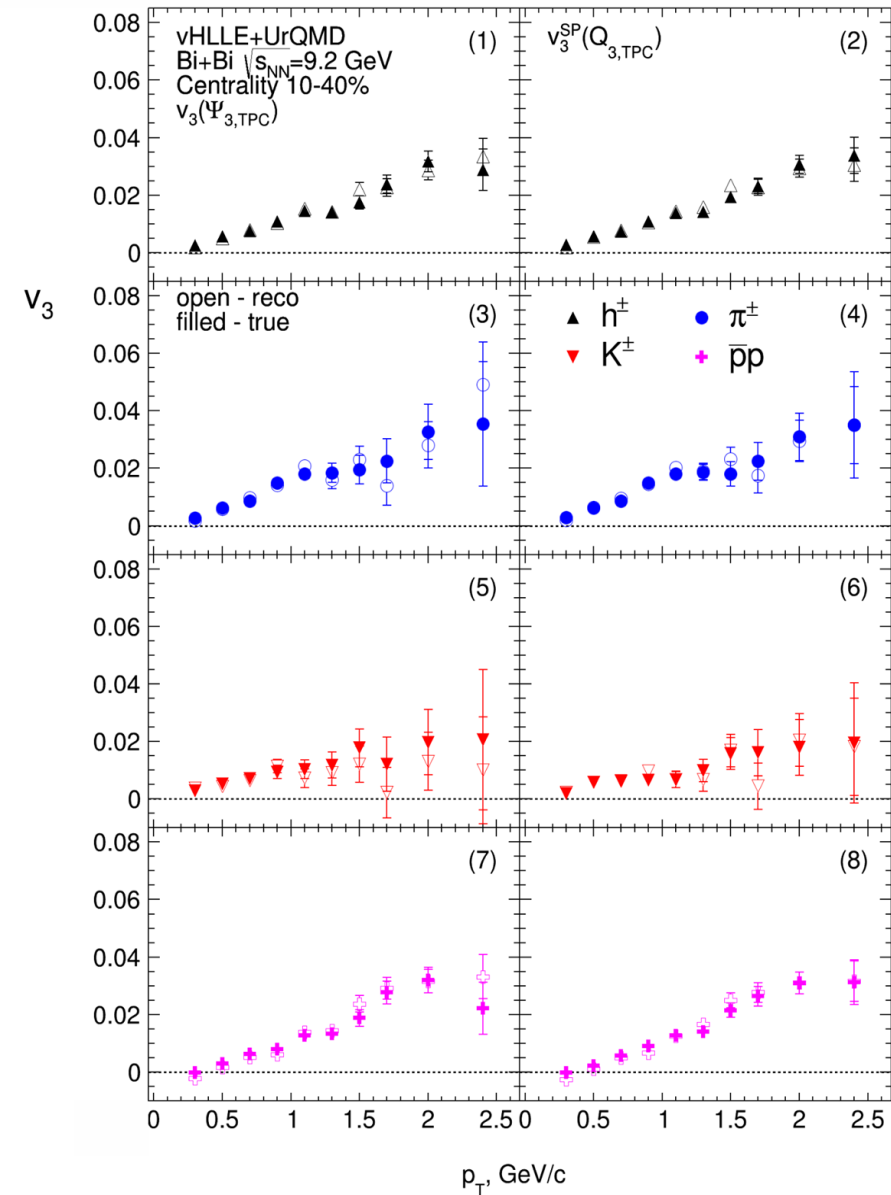
Cuts:

- Charged particles only
- Primary
- $|\eta| < 1.5$
- $\Delta\eta = 0, 1$
- $p_T > 0.2 \text{ GeV}/c$
- $|DCA| < 3\sigma$
- nTPC hits ≥ 16
- PID: PDG code

□ good agreement of the $v_{2,mc}$ with $v_{2,reco}$ data

□ The difference at large p_T between $v_{2,mc}$ and $v_{2,reco}$ (non-flow)

Comparison of Reco and MC: v_3 eta-sub EP

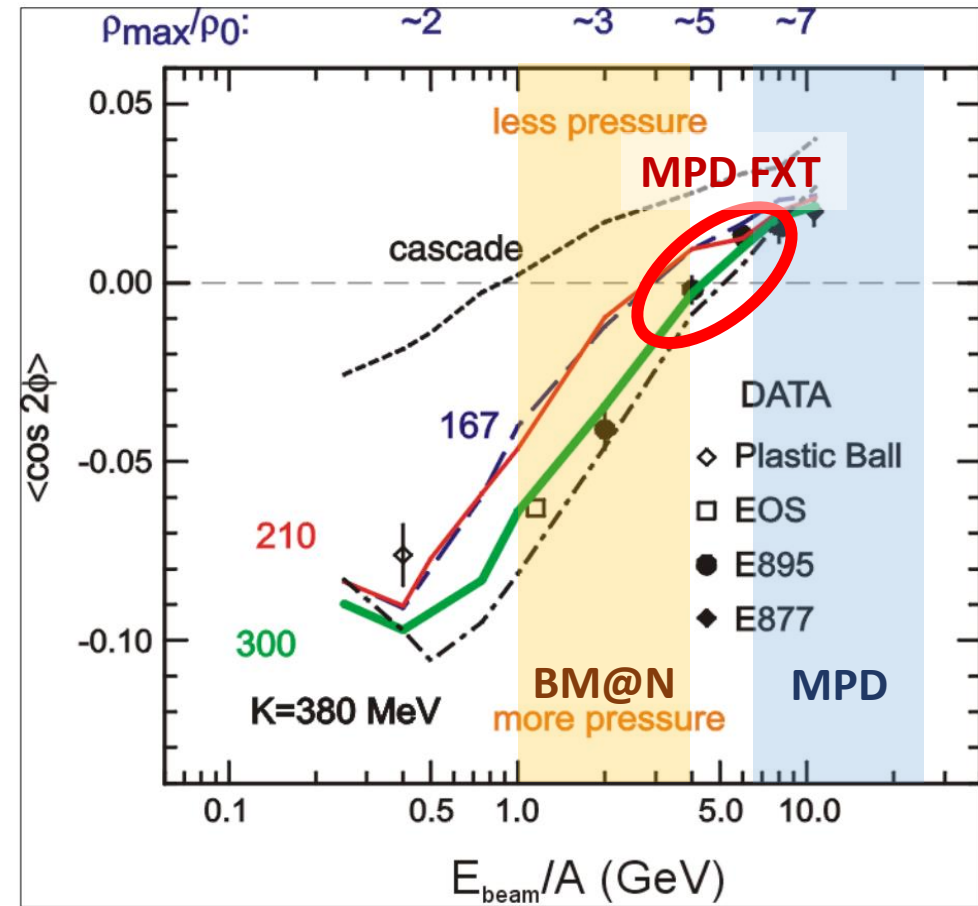
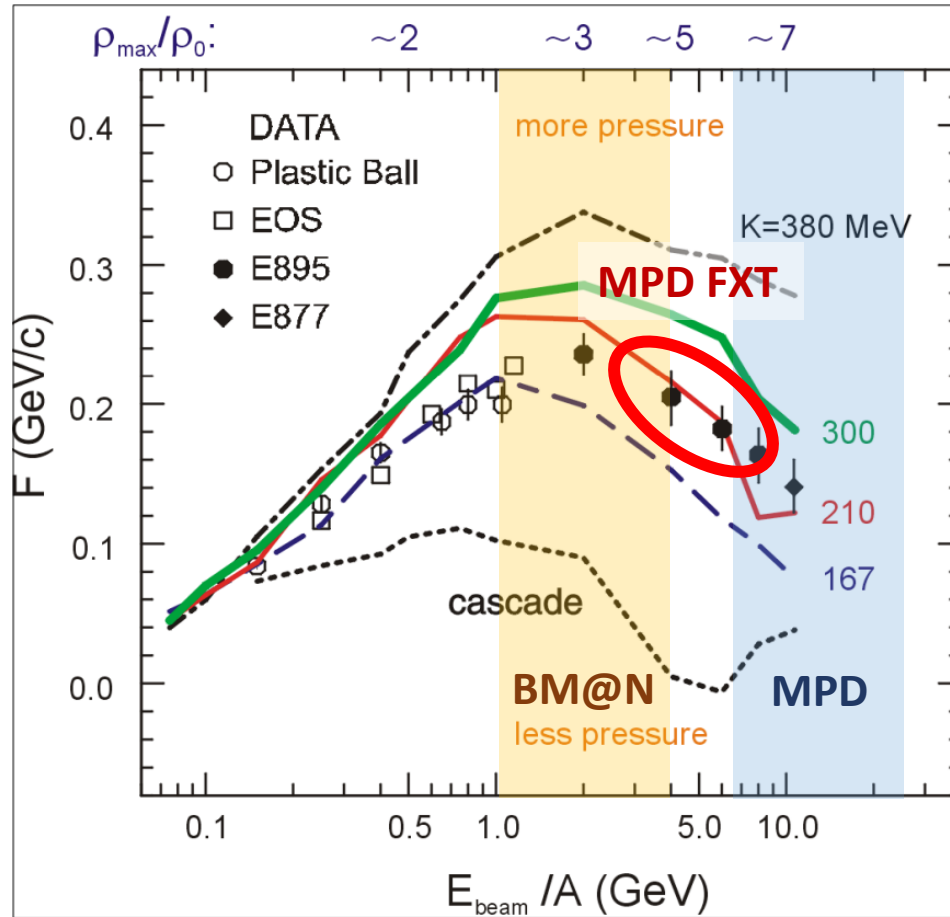


Cuts:

- Charged particles only
- Primary
- $|\eta| < 1.5$
- $\Delta \eta = 0, 1$
- $p_T > 0.2$ GeV/c
- $|DCA| < 3\sigma$
- nTPC hits ≥ 16
- PID: PDG code

- Good performance for v_3 measurements
- Further research is required (need more statistics)

Flow performance study for MPD in fixed-target mode



P. DANIELEWICZ, R. LACEY, W. LYNCH [10.1126/science.1078070](https://doi.org/10.1126/science.1078070)

- **The flow data from E895 experiment have ambiguous interpretation:**
 v_1 suggests soft EOS while v_2 corresponds to hard EOS
- **Additional measurements are essential to clarify the previous measurements**

The Bayesian inversion method (Γ -fit): main assumptions

Relation between multiplicity N_{ch} and impact parameter b is defined by the fluctuation kernel:

$$P(N_{ch}|c_b) = \frac{1}{\Gamma(k(c_b))\theta^k} N_{ch}^{k(c_b)-1} e^{-N_{ch}/\theta} \quad \frac{\sigma^2}{\langle N_{ch} \rangle} = \theta \simeq const, k = \frac{\langle N_{ch} \rangle}{\theta}$$

$$c_b = \int_0^b P(b') db' \text{ – centrality based on impact parameter}$$

Mean multiplicity as a function of c_b can be defined as follows:

$$\langle N_{ch} \rangle = N_{knee} \exp\left(\sum_{j=1}^3 a_j c_b^j\right) \quad N_{knee}, \theta, a_j \text{ – 5 parameters}$$

Fit function for N_{ch} distribution: b -distribution for a given N_{ch} range:

$$P(N_{ch}) = \int_0^1 P(N_{ch}|c_b) dc_b \quad P(b|n_1 < N_{ch} < n_2) = P(b) \frac{\int_{n_1}^{n_2} P(N_{ch}|b) dN_{ch}}{\int_{n_1}^{n_2} P(N_{ch}) dN_{ch}}$$

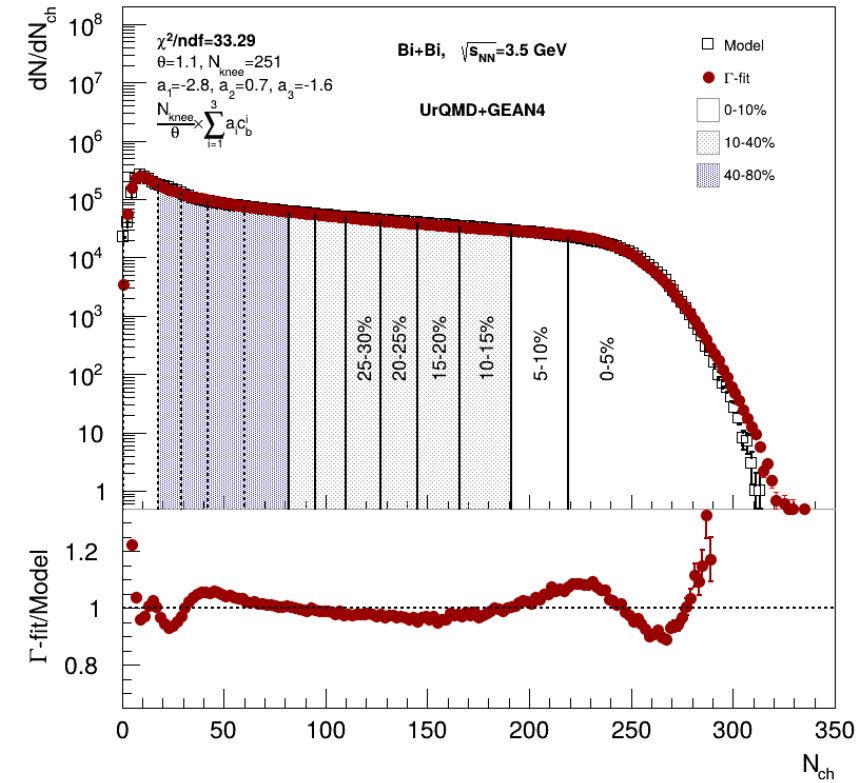
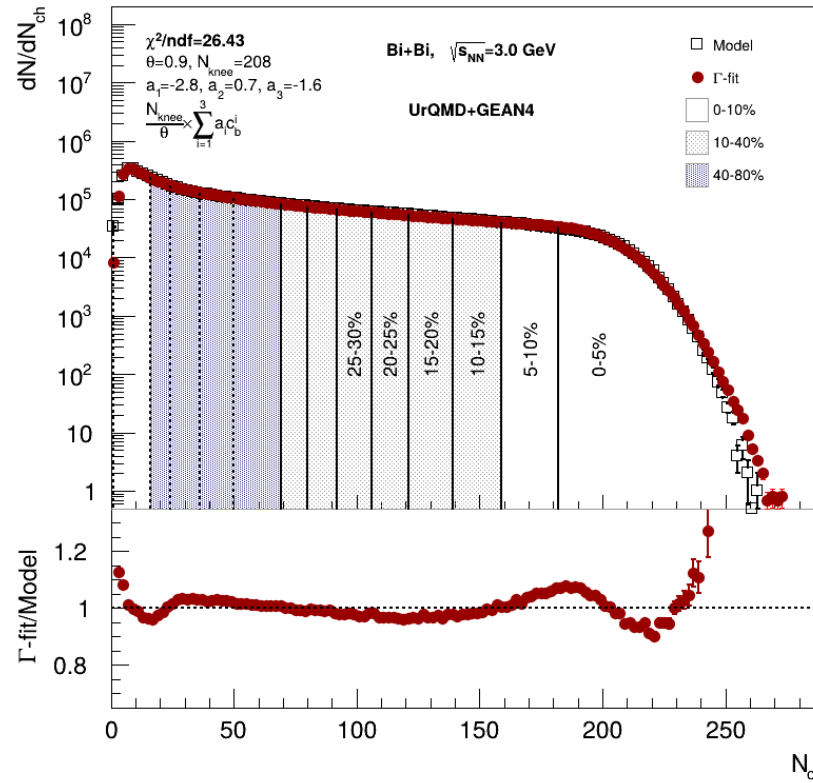
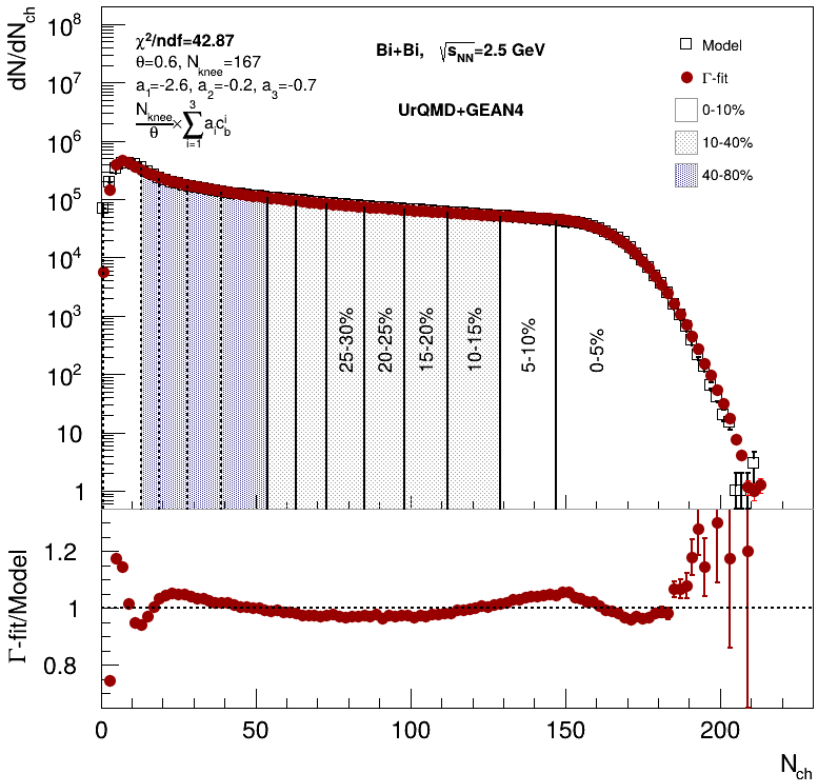
2 main steps of the method:

Fit experimental (model) distribution with $P(N)$



Construct $P(b|E)$ using Bayes' theorem:
 $P(b|N) = P(b)P(N|b)/P(N)$

Centrality determination: multiplicity fit



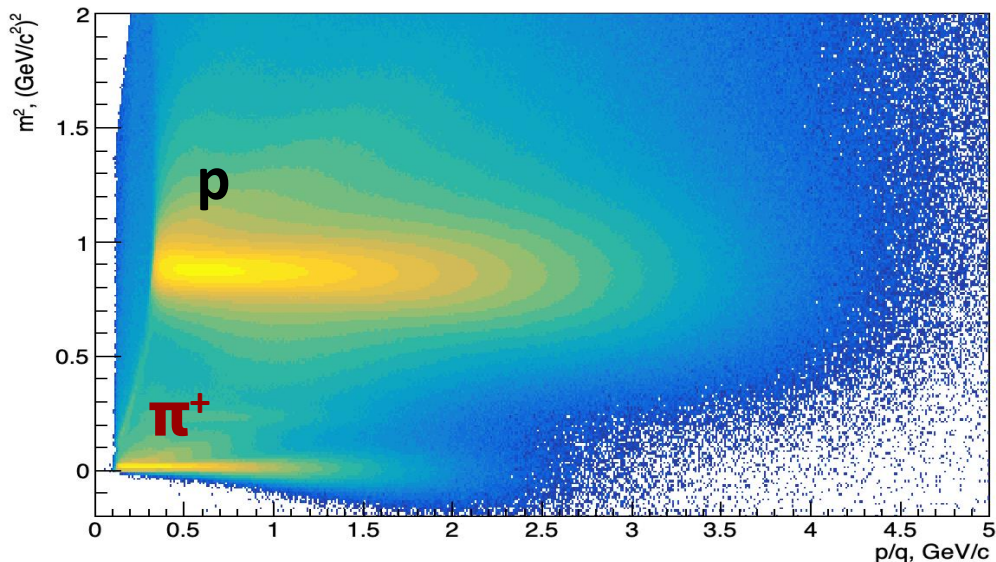
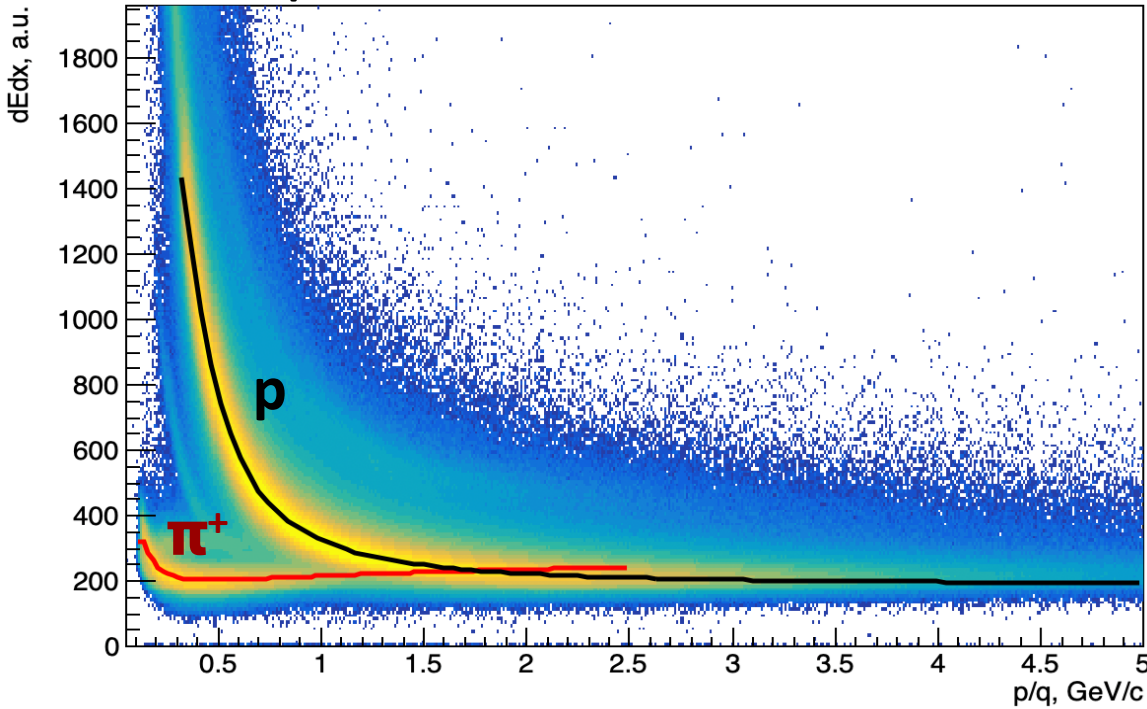
Cuts on tracks:

- $N_{\text{hits}} > 16$
- $0 < \eta < 2$

Good agreement between fit and data

Multiplicity-based centrality determination using inverse Bayes was used

PID procedure



Fit dE/dx distributions with Bethe-Bloch parametrization:

$$f(\beta\gamma) = \frac{p_1}{\beta p^4} \left(p_2 - \beta p^4 - \ln \left(p_3 + \frac{1}{(\beta\gamma)p^5} \right) \right)$$

$$\beta^2 = \frac{p^2}{m^2 + p^2}, \quad \beta\gamma = \frac{p}{m}$$

p_i - fit parameters

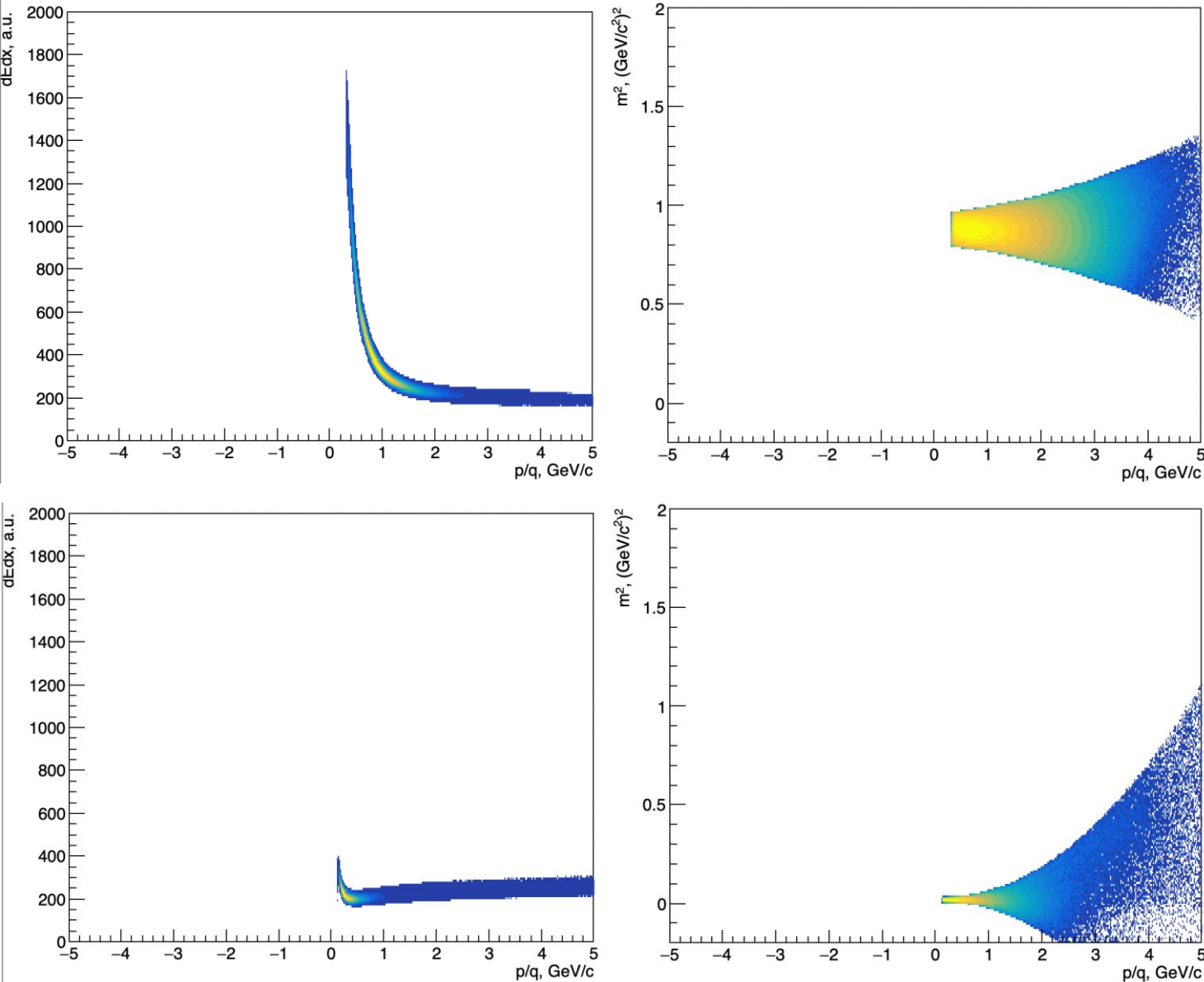
Fit $(dE/dx - f(\beta\gamma))/f(\beta\gamma)$ with gaus in the slices of p/q and get $\sigma_p(dE/dx)$

Fit m^2 with gaus in the slices of p/q and get $\sigma_p(m^2)$

$(dE/dx, m) \rightarrow (x, y)$ coordinates for PID:

$$x_p = \frac{(dE/dx)^{meas} - (dE/dx)_p^{fit}}{(dE/dx)_p^{fit} \sigma_p^{dE/dx}}, \quad y_p = \frac{m^2 - m_p^2}{\sigma_p^{m^2}}$$

PID procedure: Results



$$x_p = \frac{(dE/dx)^{meas} - (dE/dx)_p^{fit}}{(dE/dx)_p^{fit} \sigma_p^{dE/dx}}$$

$$y_p = \frac{m^2 - m_p^2}{\sigma_p^{m^2}}$$

Protons:

$$\sqrt{x_p^2 + y_p^2} < 2, \sqrt{x_\pi^2 + y_\pi^2} > 3$$

Pions (π^+):

$$\sqrt{x_\pi^2 + y_\pi^2} < 2, \sqrt{x_p^2 + y_p^2} > 3$$

Pions (π^-):

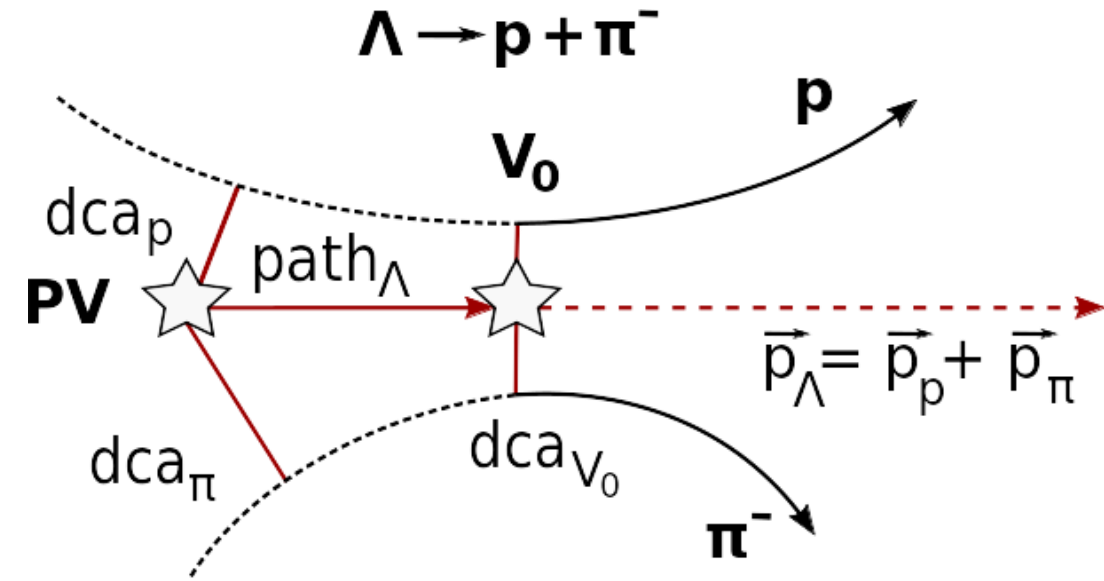
charge < 0

Measurements of global hyperon polarization

- Polarization can be measured using the azimuthal angle of proton in Lambda rest frame ϕ^*

$$\bar{P}_{\Lambda/\bar{\Lambda}} = \frac{8}{\pi\alpha} \frac{1}{R_{EP}^1} \langle \sin(\Psi_{EP}^1 - \phi^*) \rangle$$

- Determine centrality
- Determine event plane (Ψ_{EP}^1, R_{EP}^1)
- Reconstruct Lambda
- Measure global polarization

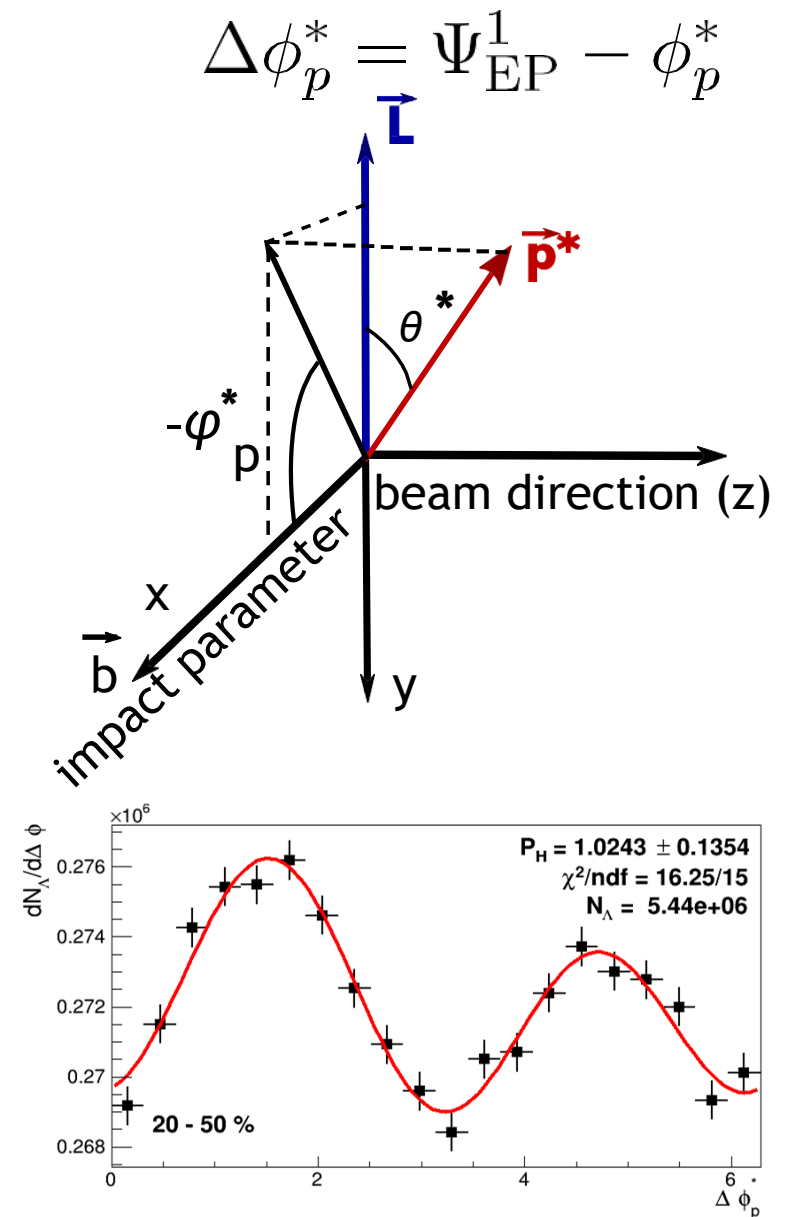


- PV — primary vertex
- V_0 — vertex of hyperon decay
- dca — distance of closest approach
- path — decay length

P_H measurements: $\Delta\phi$ -method

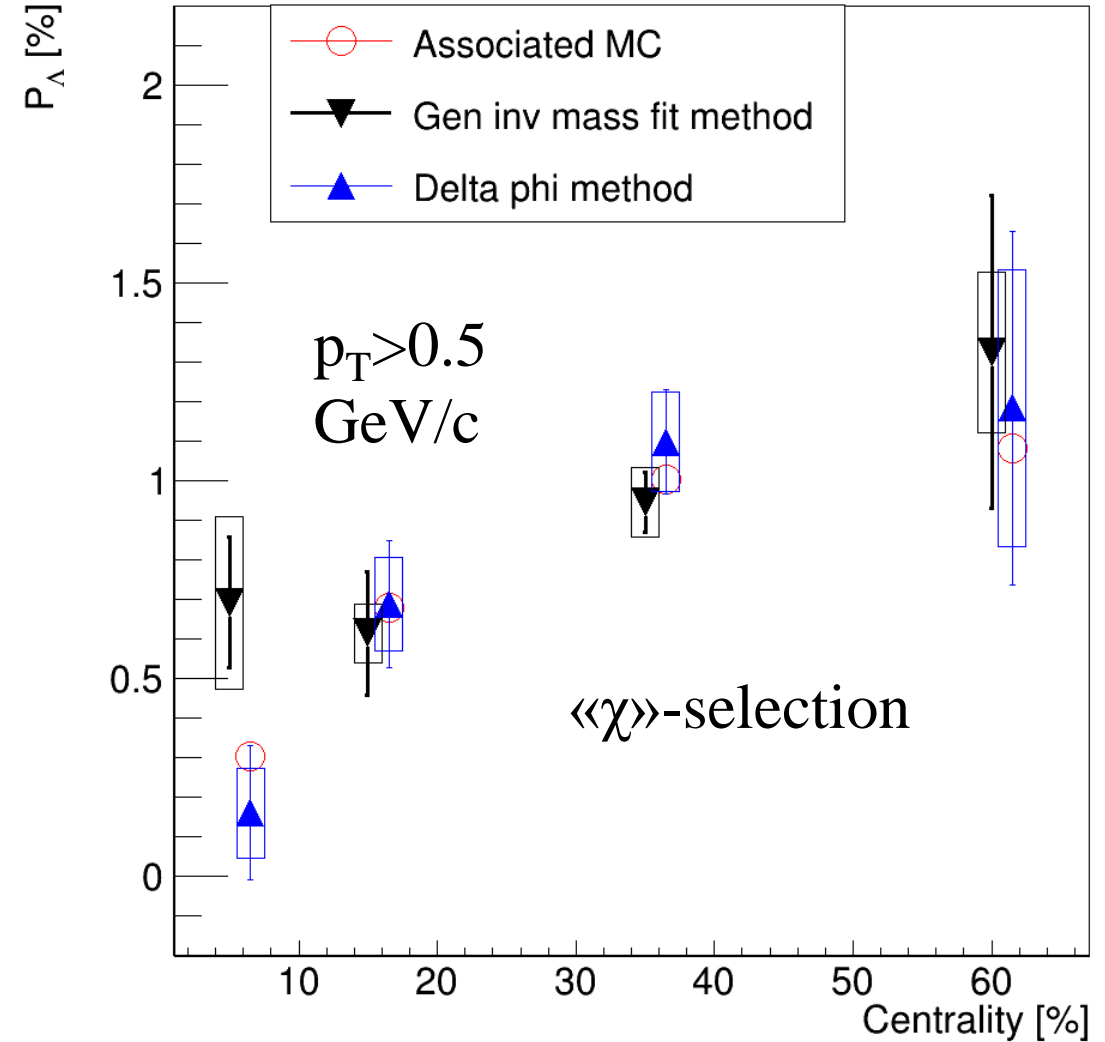
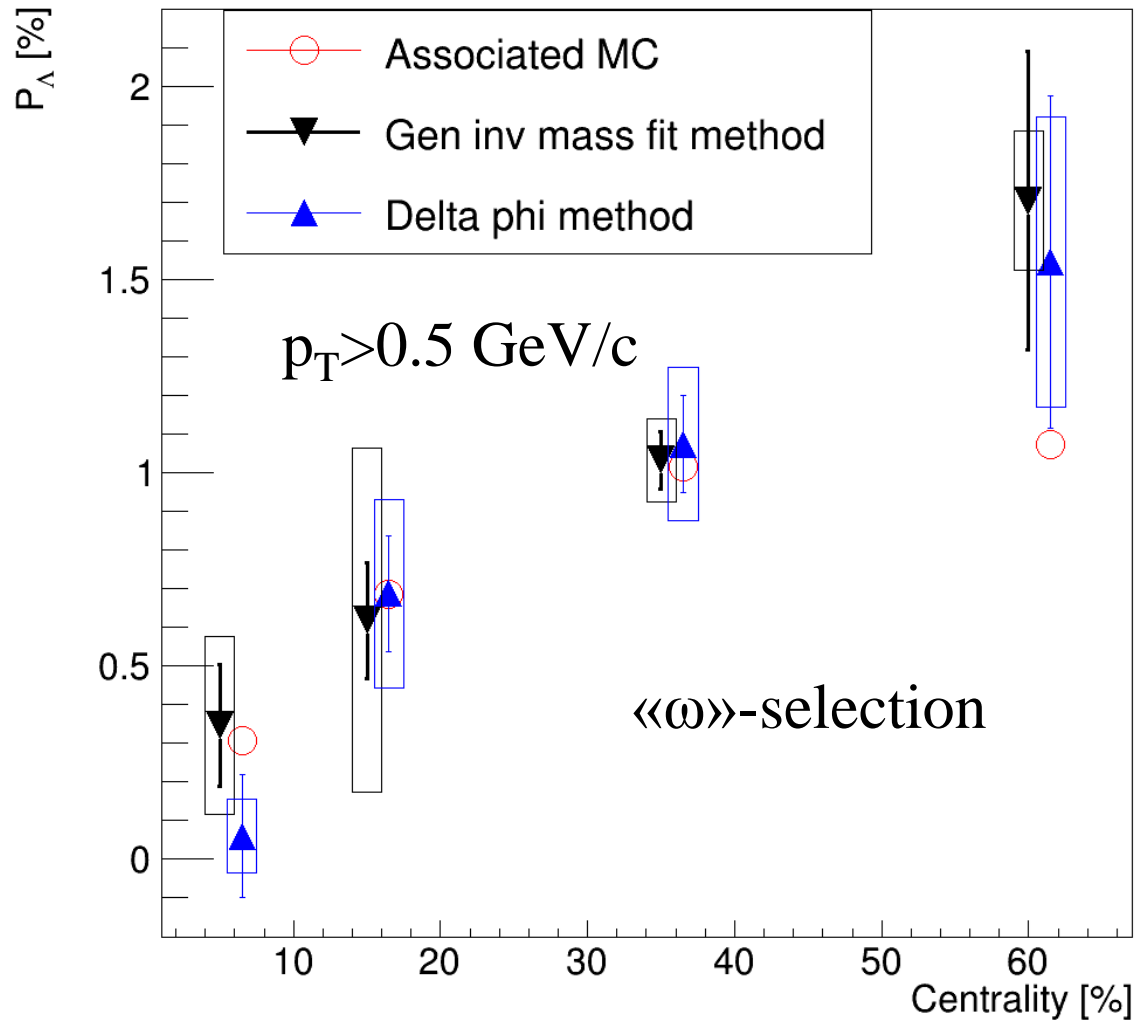
- Obtain invariant mass distribution in bins of
 - Net amount of Λ in each bin
 - Distribution of $N_\Lambda(\Delta\phi_p^*)$
- Fit of the distribution to get $\langle \sin(\Delta\phi_p^*) \rangle \rightarrow P_\Lambda$
 - $dN/d\Delta\phi_P^*$
 - $P_\Lambda = \frac{8}{\pi\alpha_\Lambda} \frac{p_1}{R_{EP}^1}$

$$\bar{P}_{\Lambda/\bar{\Lambda}} = \frac{8}{\pi\alpha} \frac{1}{R_{EP}^1} \langle \sin(\Psi_{EP}^1 - \phi_p^*) \rangle$$



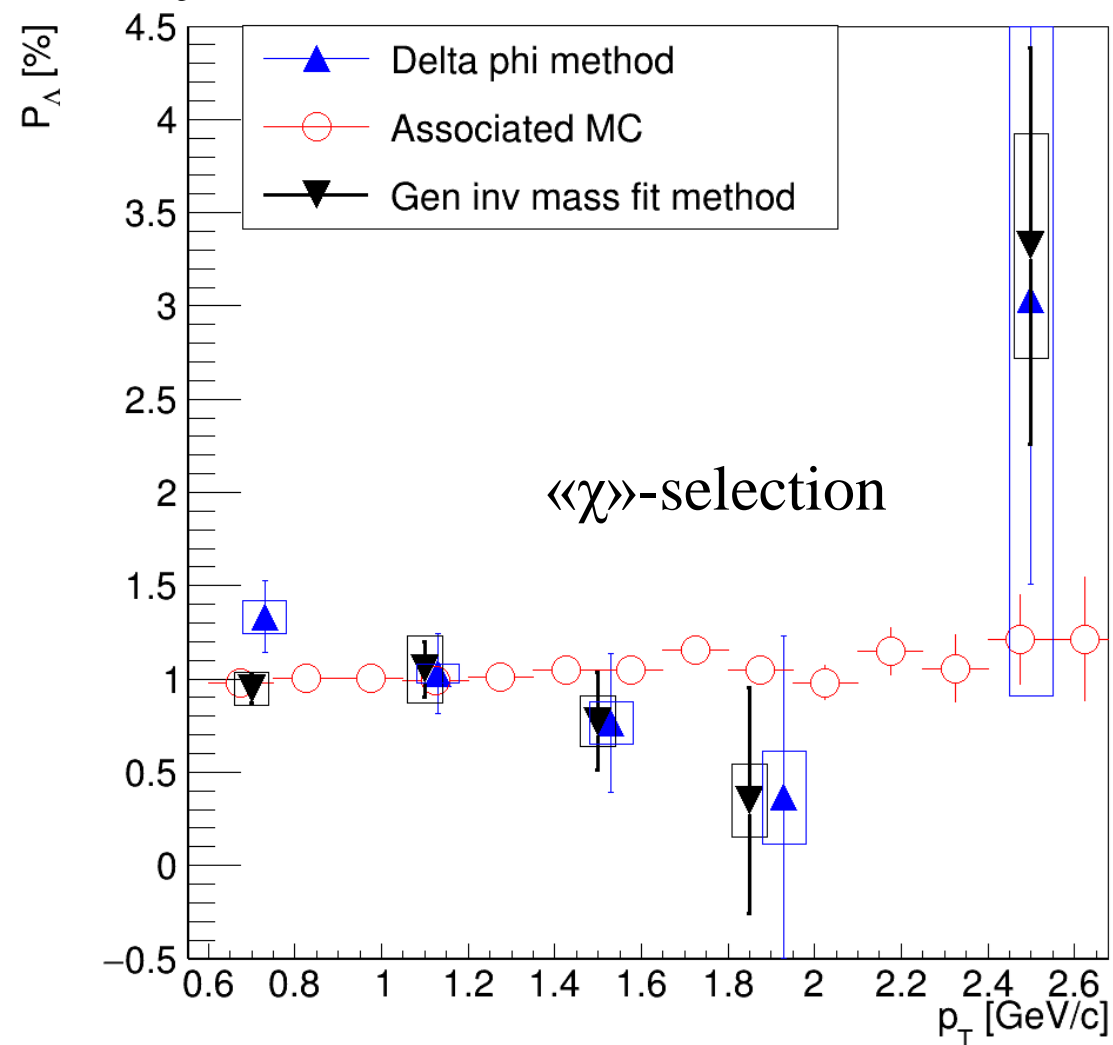
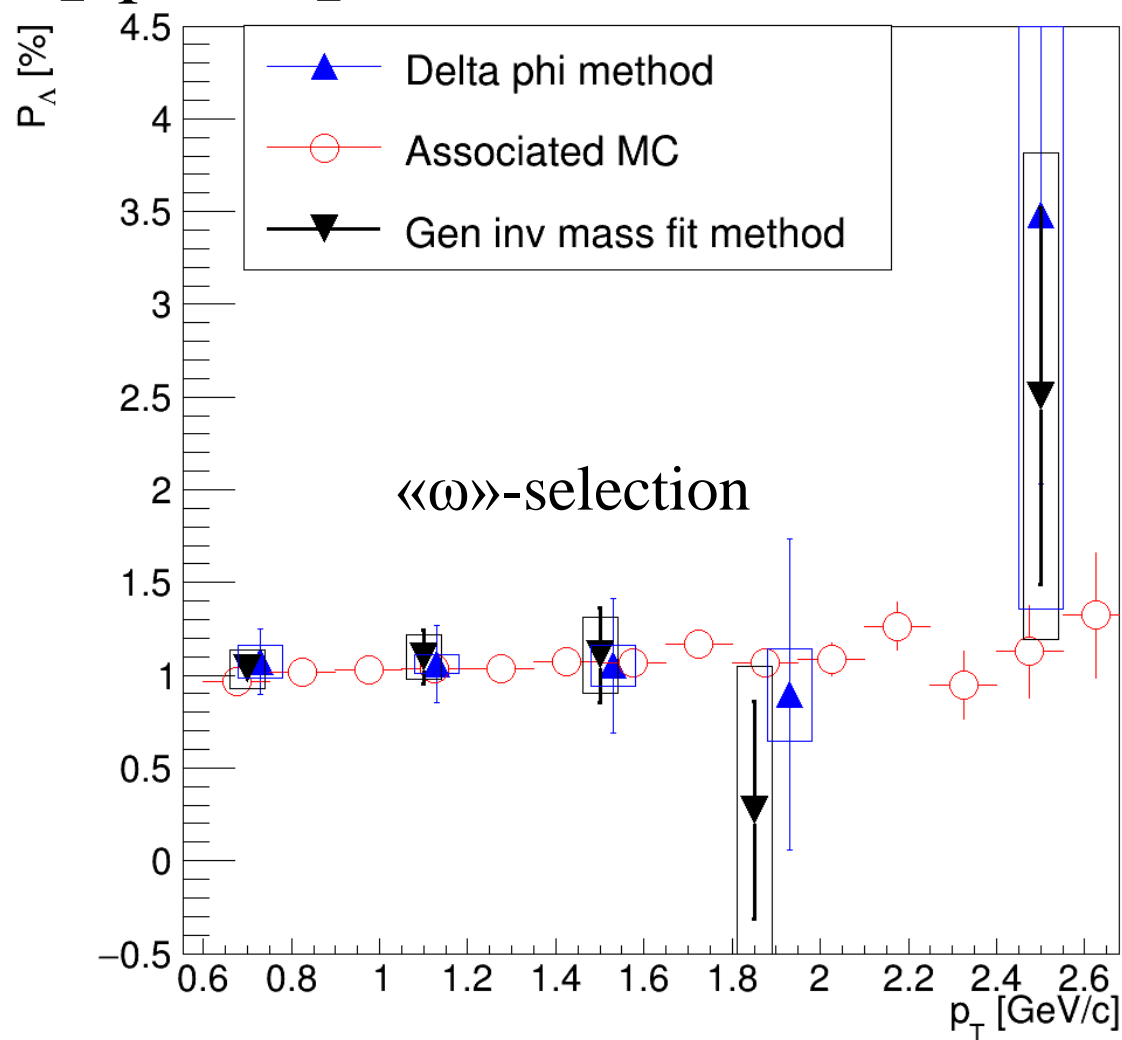
$$\frac{dN}{d\Delta\phi_P^*} = p_0(1 + 2p_1 \sin \Delta\phi_p^* + 2p_2 \cos \Delta\phi_p^* + 2p_3 \sin 2\Delta\phi_p^* + 2p_4 \cos 2\Delta\phi_p^* + \dots)$$

Centrality dependence of P_Λ



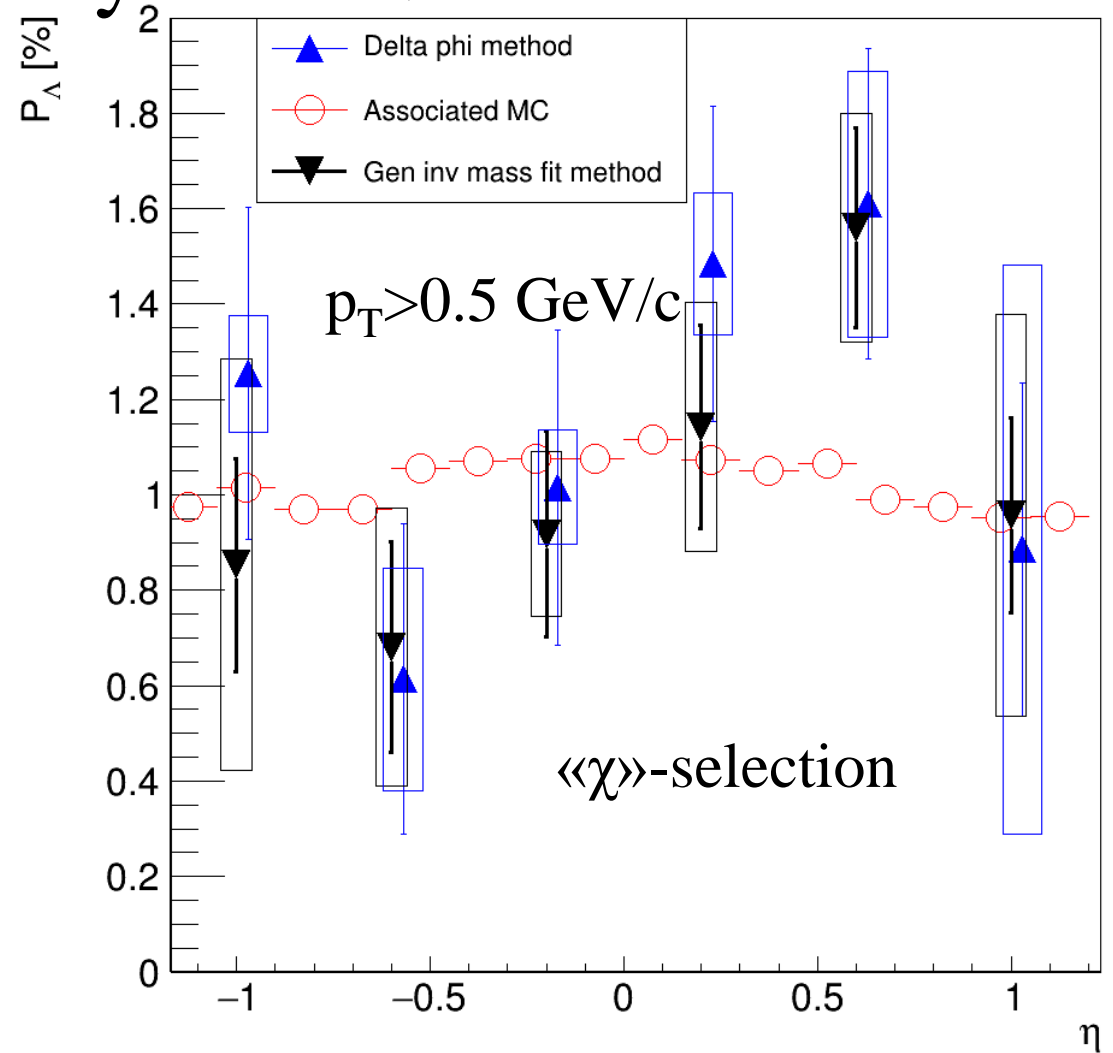
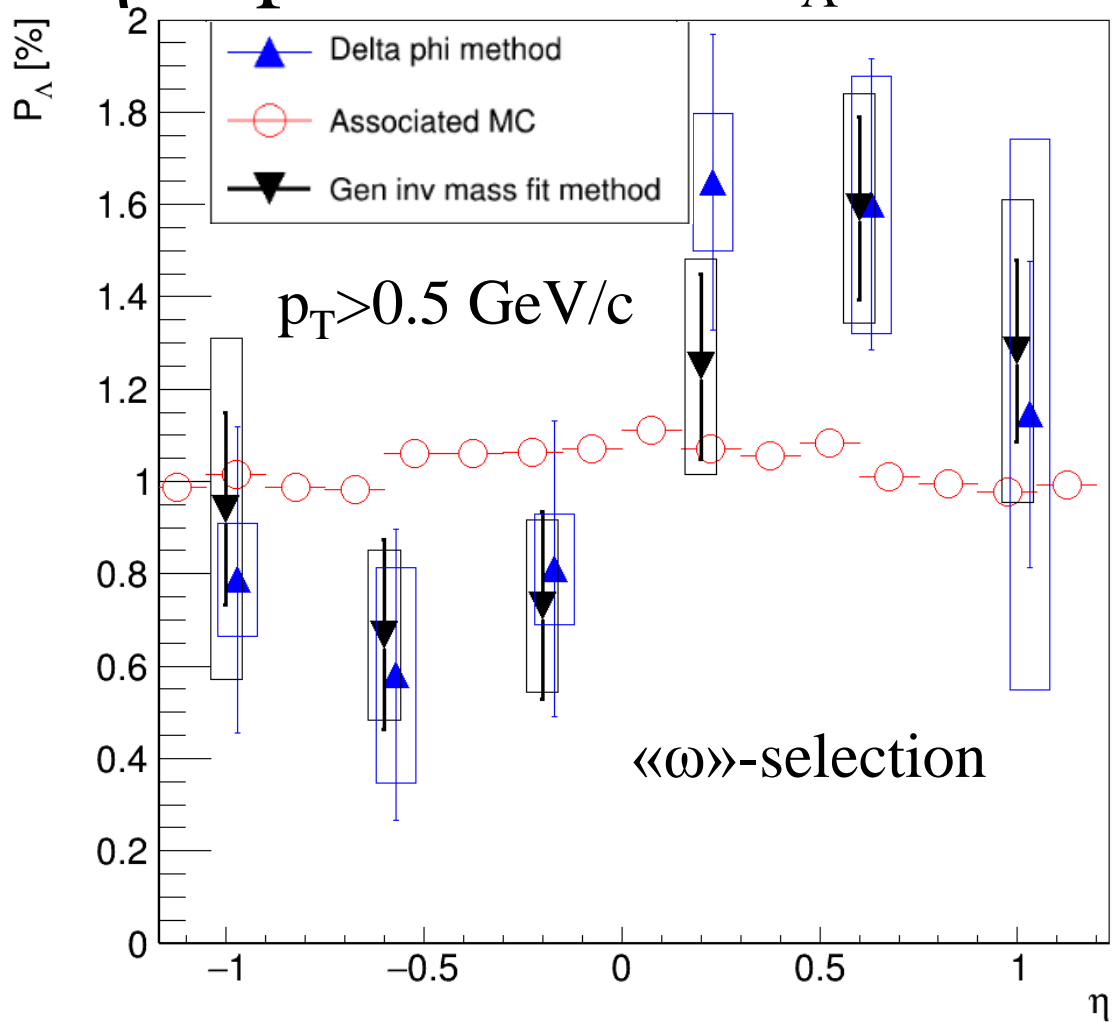
Both methods have a good agreement with Associated MC

p_T - dependence of P_Λ for centrality 20-50%



Both methods have a good agreement with Associated MC
 Need more statistics to study high p_T region

η -dependence of P_{Λ} for centrality 20-50%

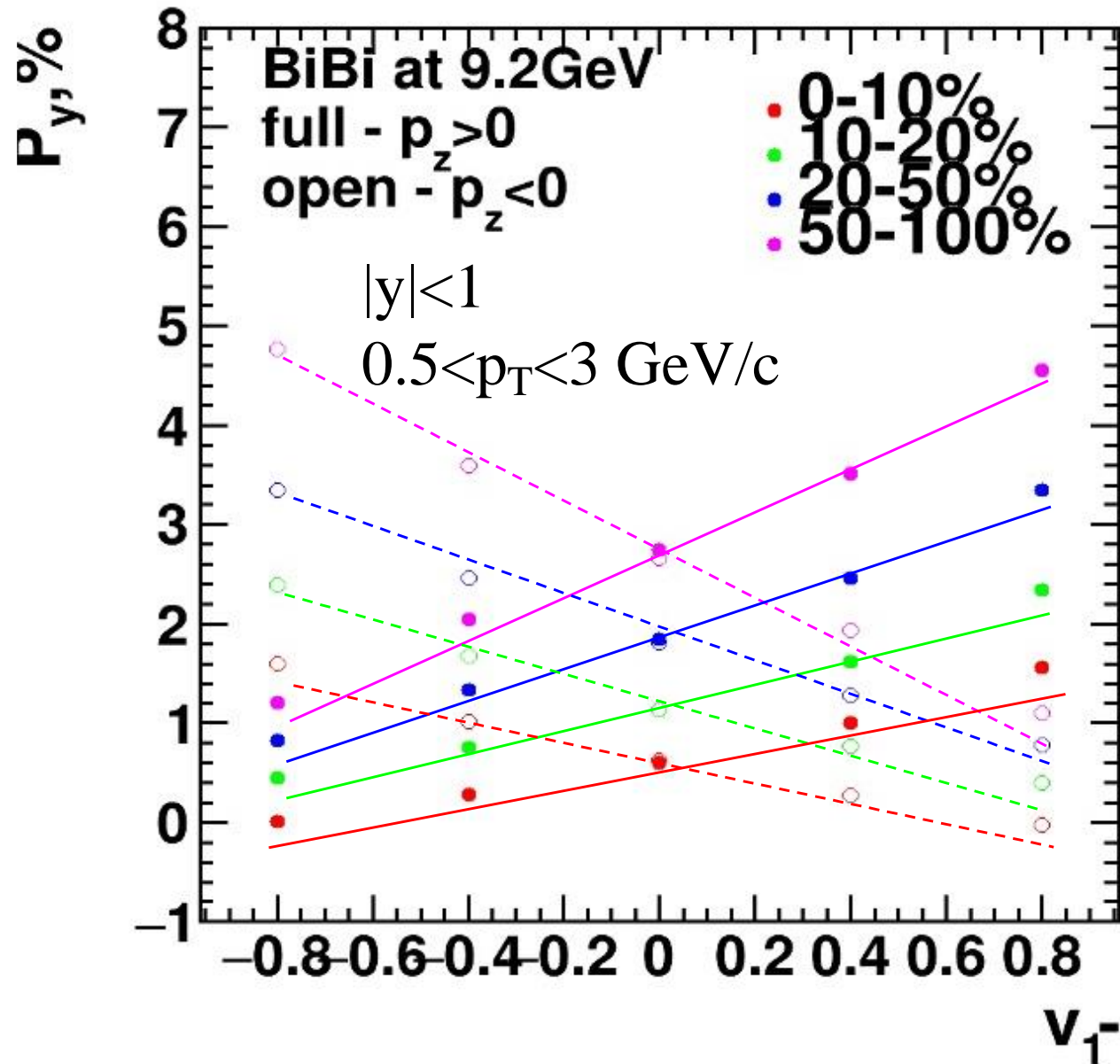


Both methods have an agreement with Associated MC

Need more statistics to study η -dependence

Correlation between P_y and v_1

See O. Terayev's [talk](#) at INFINUM-2023 and V. Voronyuk's [talk](#) at XI MPD CM

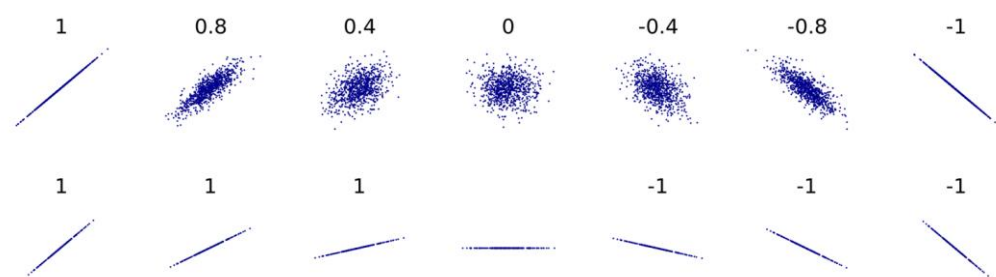


- P_y vs v_1 correlation is not optimal for a differential analysis
- Pearson correlation coefficient represent linear correlation between two sets of data from -1 to 1

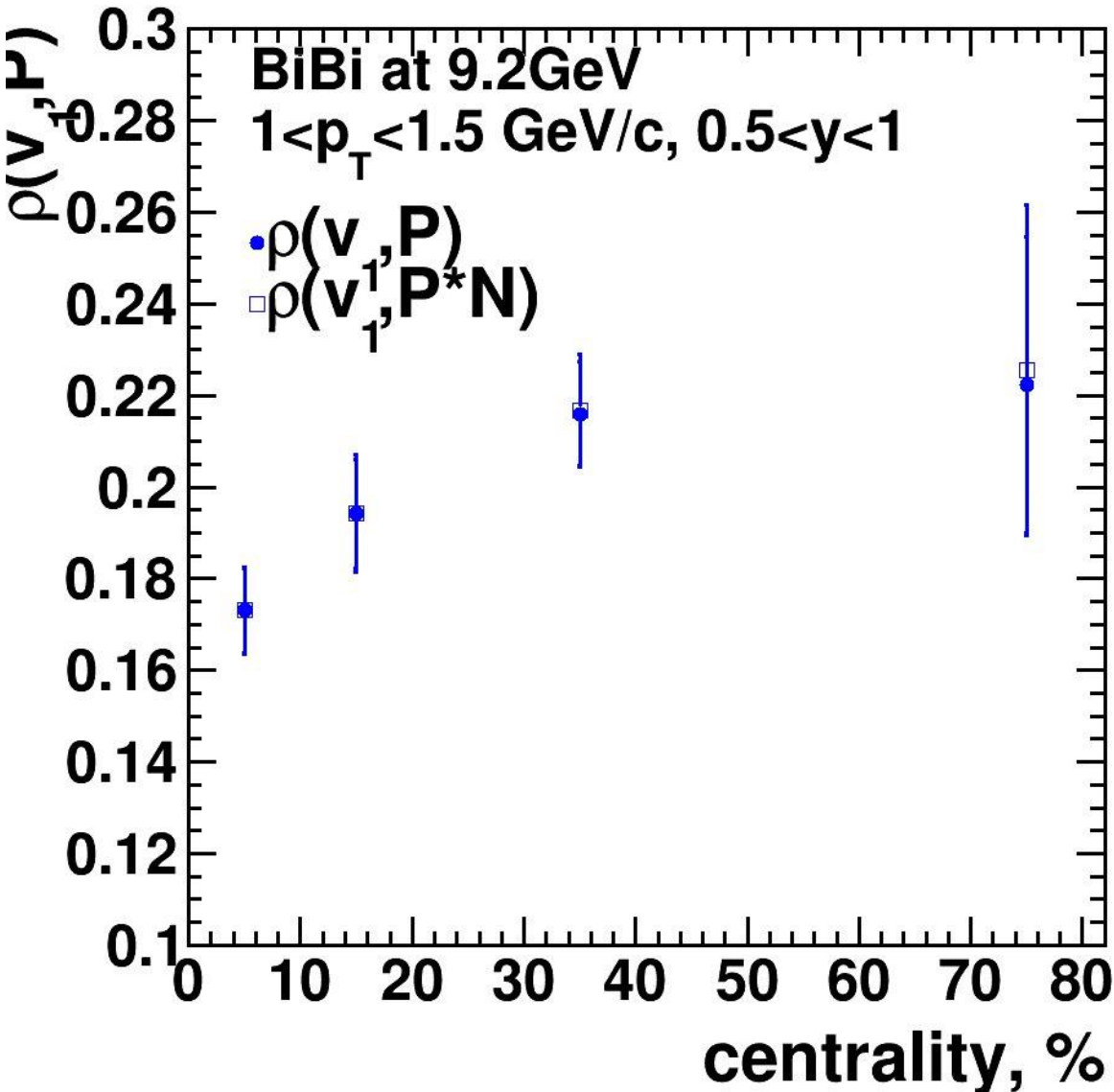
$$\rho(X, Y) = \frac{Cov(X, Y)}{\sqrt{Var(X)Var(Y)}}$$

$$Cov(X, Y) = \langle XY \rangle - \langle X \rangle \langle Y \rangle$$

$$Var(X) = \sqrt{\langle X^2 \rangle - \langle X \rangle^2}$$



Pearson correlation coefficient between P_y , v_1 and N



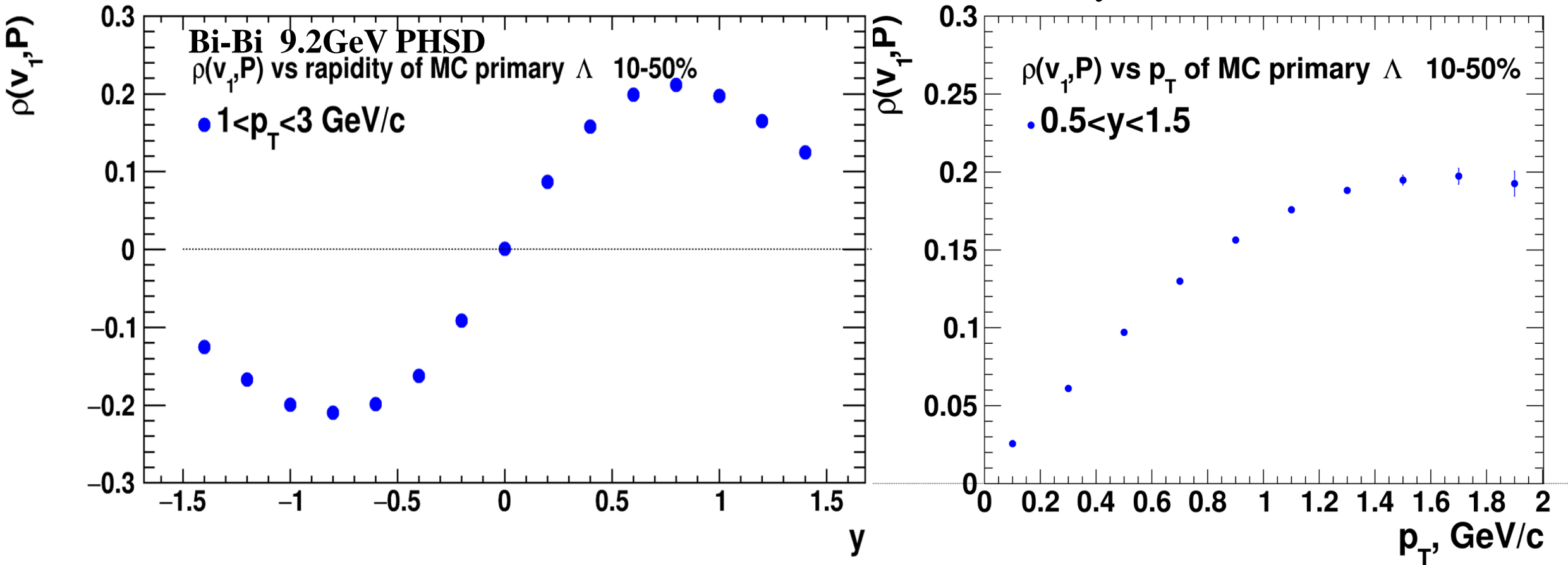
$$\rho(P, v_1) = \frac{\langle P v_1 \rangle - \langle P \rangle \langle v_1 \rangle}{(\sqrt{\langle v_1^2 \rangle - \langle v_1 \rangle^2})(\sqrt{\langle P^2 \rangle - \langle P \rangle^2})}$$

$$\rho(P, v_1 * N) = \frac{\rho(P, v_1) - \rho(P, N)\rho(v_1, N)}{(\sqrt{1 - \rho(P, N)^2})(\sqrt{1 - \rho(v_1, N)^2})}$$

N - multiplicity of Primary Λ

$\rho(P_\Lambda, v_1)$ is insensitive to multiplicity fluctuations of primary Λ

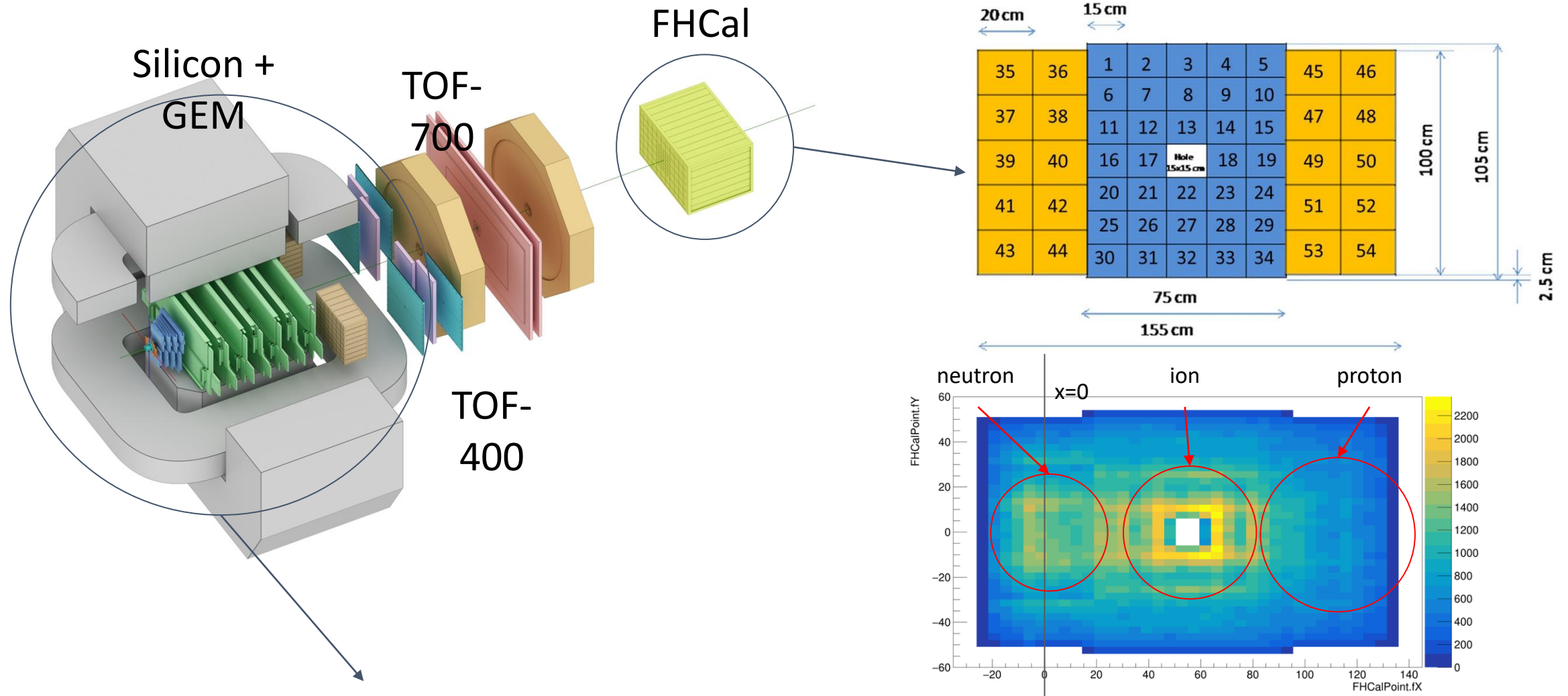
Pearson correlation coefficient between P_y and v_1



$$\rho(P, v_1) = \frac{\langle P v_1 \rangle - \langle P \rangle \langle v_1 \rangle}{(\sqrt{\langle v_1^2 \rangle - \langle v_1 \rangle^2})(\sqrt{\langle P^2 \rangle - \langle P \rangle^2})}$$

- Non-zero linear correlation between P_y and v_1
- increasing with p_T
- highest for $0.5 < y < 1$

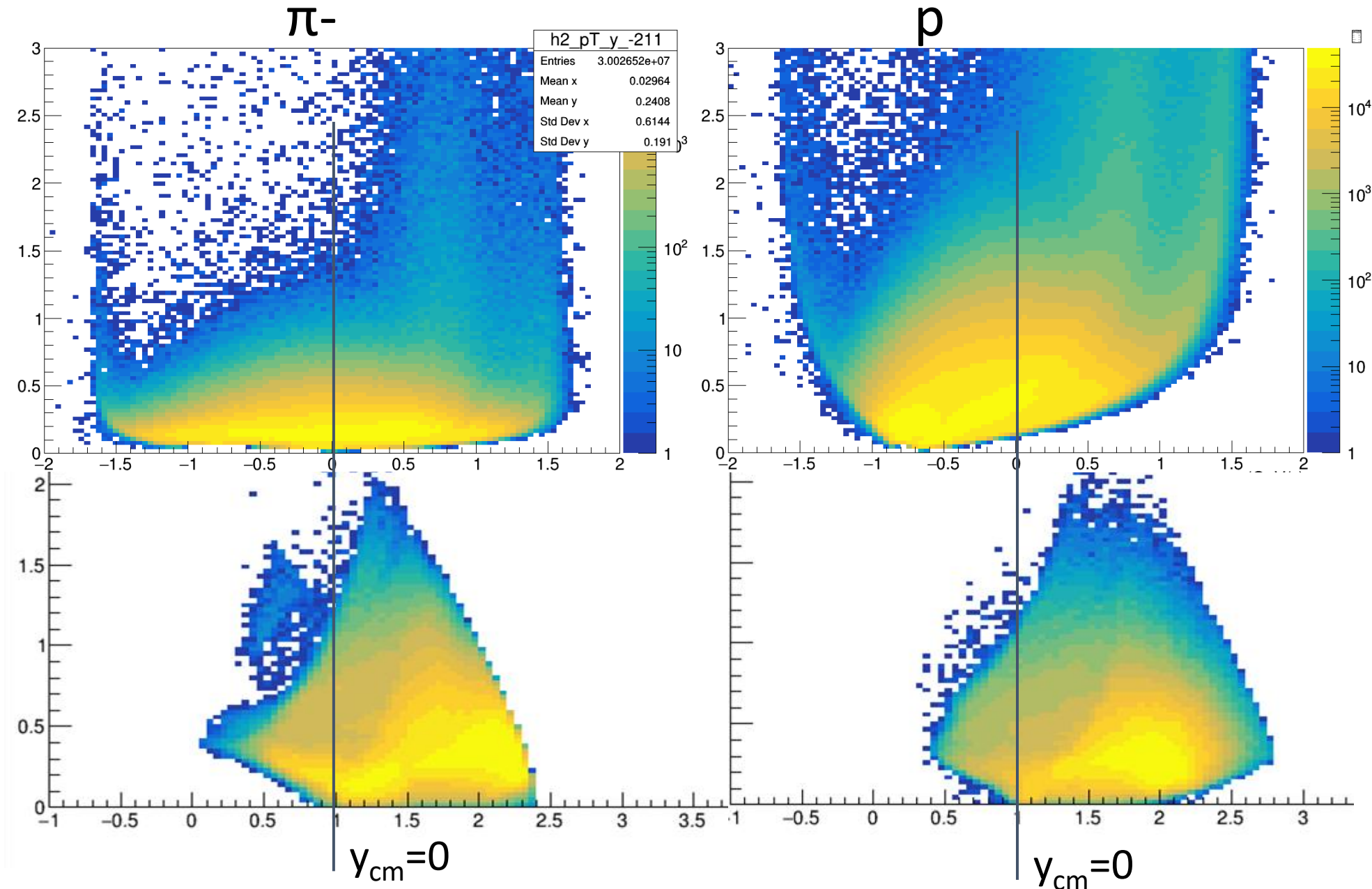
The BM@N experiment (GEANT4 simulation for RUN8)



Square-like tracking system within the magnetic field deflecting particles along X-axis

Charge splitting on the surface of the FHCAL is observed due to magnetic field

BM@N vs MPD: p_T - y acceptance

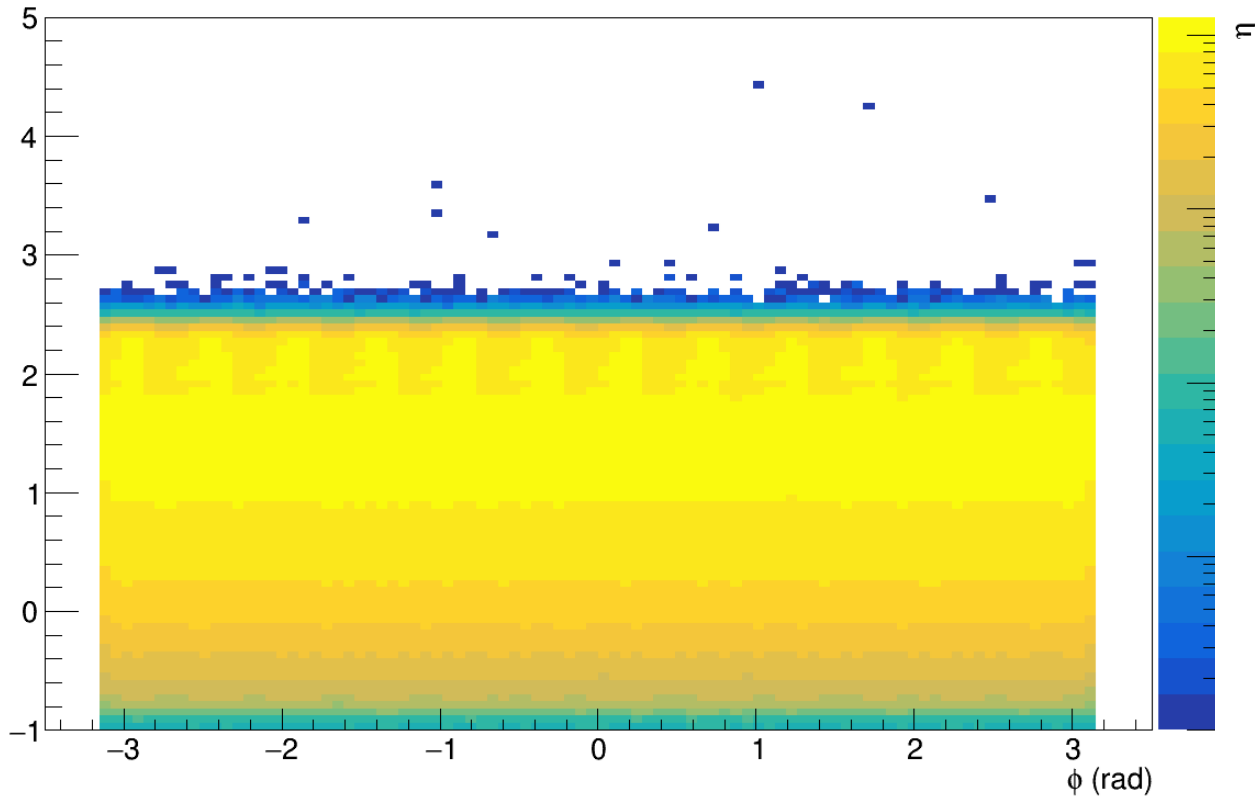


MPD has greater coverage of backward area (even covers projectile spectators) and MPD covers midrapidity region

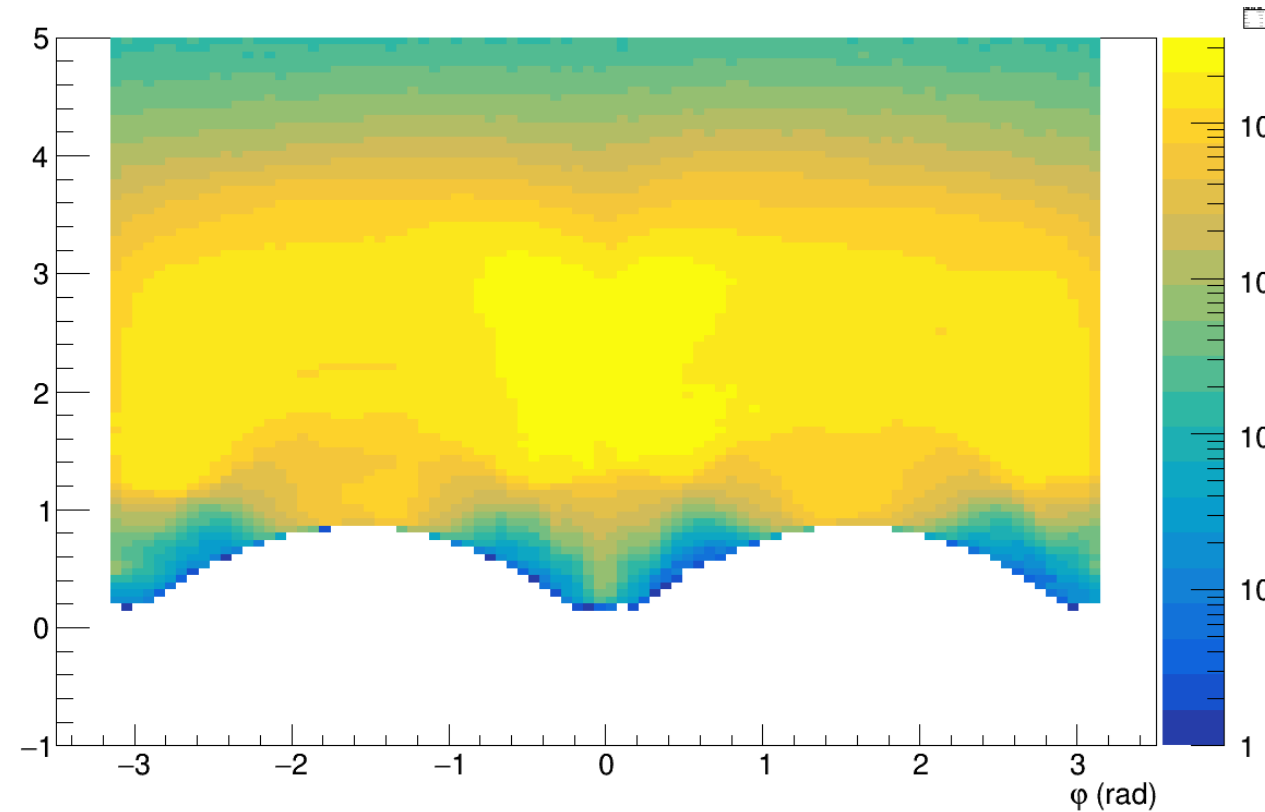
BM@N has greater coverage of forward area

BM@N vs MPD: η - ϕ acceptance

MPD



BM@N



- MPD has more uniform acceptance along ϕ -axis
- BM@N has non-uniform acceptance due to square-like shape of the tracking system

Summary for main topic 1

- Software implementation of MC Glauber and Γ -fit with multiplicity based fitting procedure is used for MPD
- Relation between impact parameter and centrality classes is extracted
- Centrality determination procedures based on MC sampling of spectators energy are developed and tested based on NA61/SHINE data for both MC-Glauber and inverse Bayes approaches
- Results are tuned on the spectator production implemented in the DCM-QGSM-SMM model
- Simplified procedure for hadron calorimeters based on Gauss distribution is also proposed for MC-Glauber approach

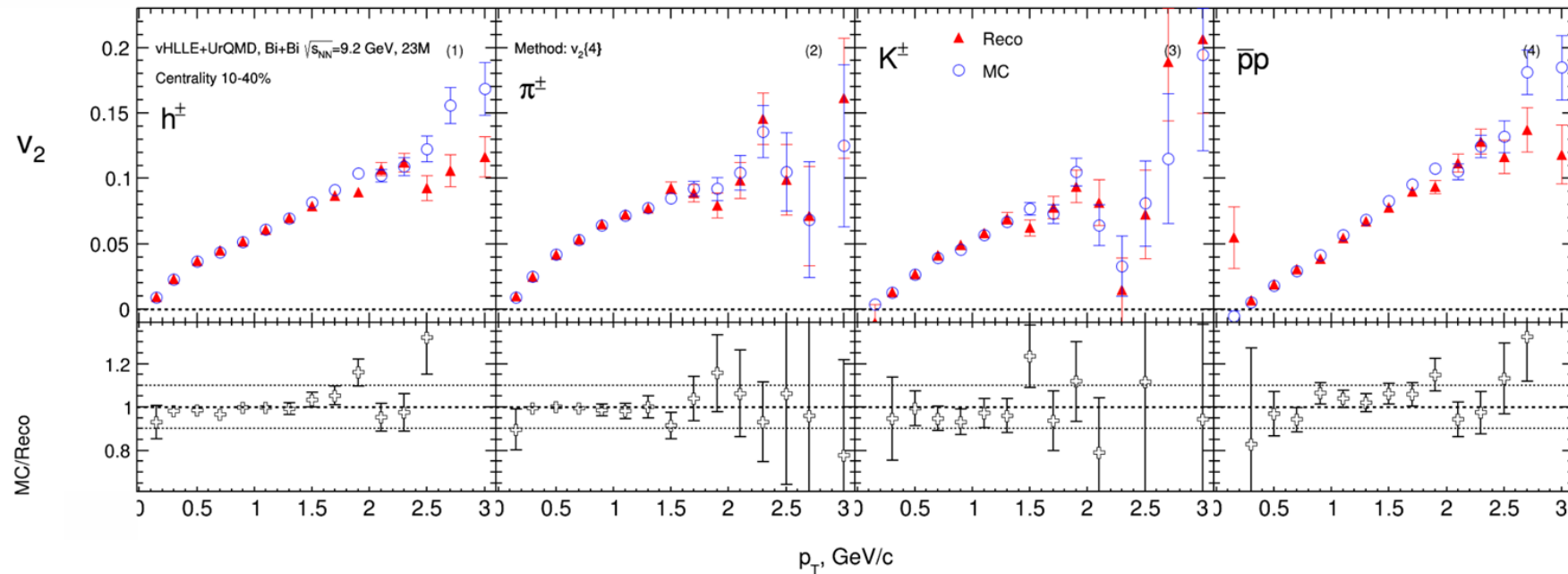
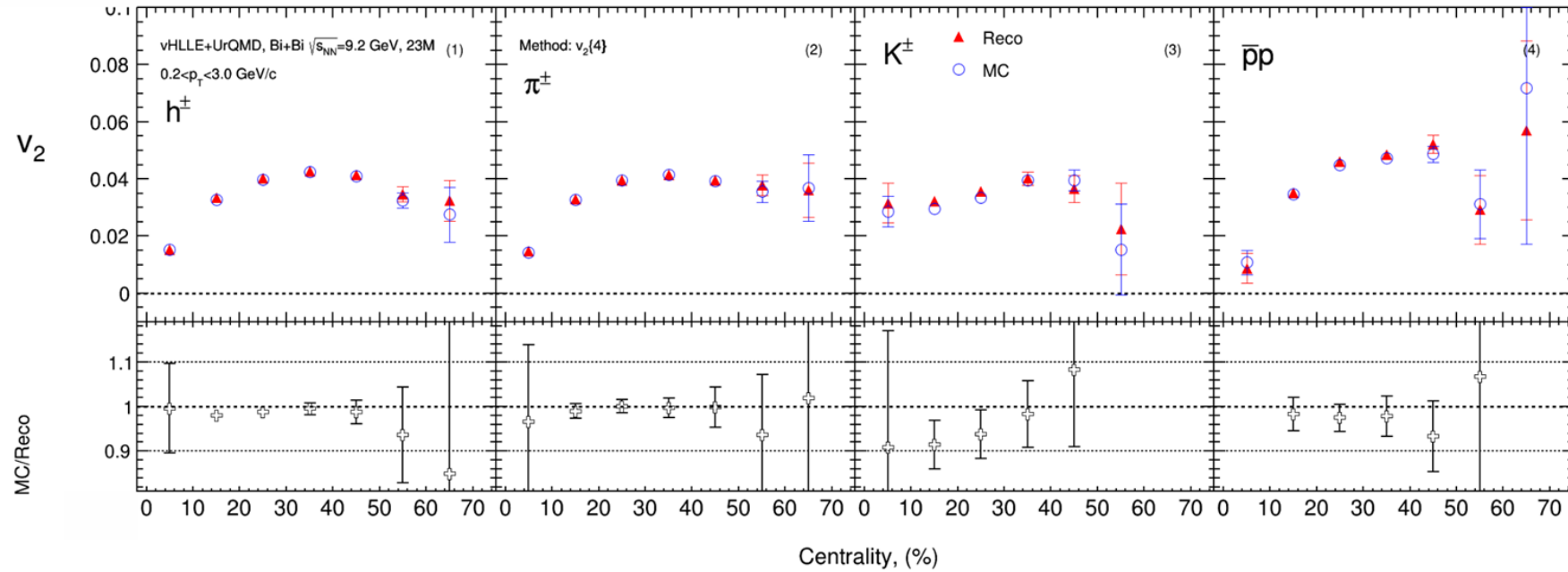
Summary for main topic 2

- **Flow measurements for UrQMD model (req. 25):**
 - Directed and elliptic flow measurements were done using several methods: event plane, scalar product and Q-Cumulant.
 - Results are ready for the second collaboration paper
- **Flow measurements for vHLE+UrQMD model (req. 32):**
 - Observed outlier events in the distribution Mult vs b - typical for this model
 - Centrality classes have been determined using the Inverse Bayes method. For this model, flow measurements (without cut on Mult vs b) are possible up to 50-60%
 - There is a good agreement between $v_{2,mc}$ and $v_{2,reco}$. But there are differences at large p_T region - contribution from non-flow.
 - Current statistics are not enough for v_3 measurements.

Summary for the main topic 3

- **Performance study for v_n measurements using FFD detector:**
 - Event plane Resolution of FFD is much more smaller than FHCAL resolution;
 - Good agreement for 2 and 3 sub event methods
 - FFD has extremely small Resolution for 2-nd harmonic
 - FFD can be used for directed flow measurements
 - FFD needs more statistics than FHCAL for elliptic flow measurements due to low resolution
- **Performance study for v_n measurements in MPD-FXT:**
 - For each particle species v_1 and v_2 are consistent with the model signal mostly in backward rapidities
 - Official production for different beam energies ($\sqrt{s_{NN}}=2.5, 3.0, 3.5$ GeV 10-11 M min bias events each) has been requested for the further studies

Comparison of Reco and MC: $v_2\{4\}$



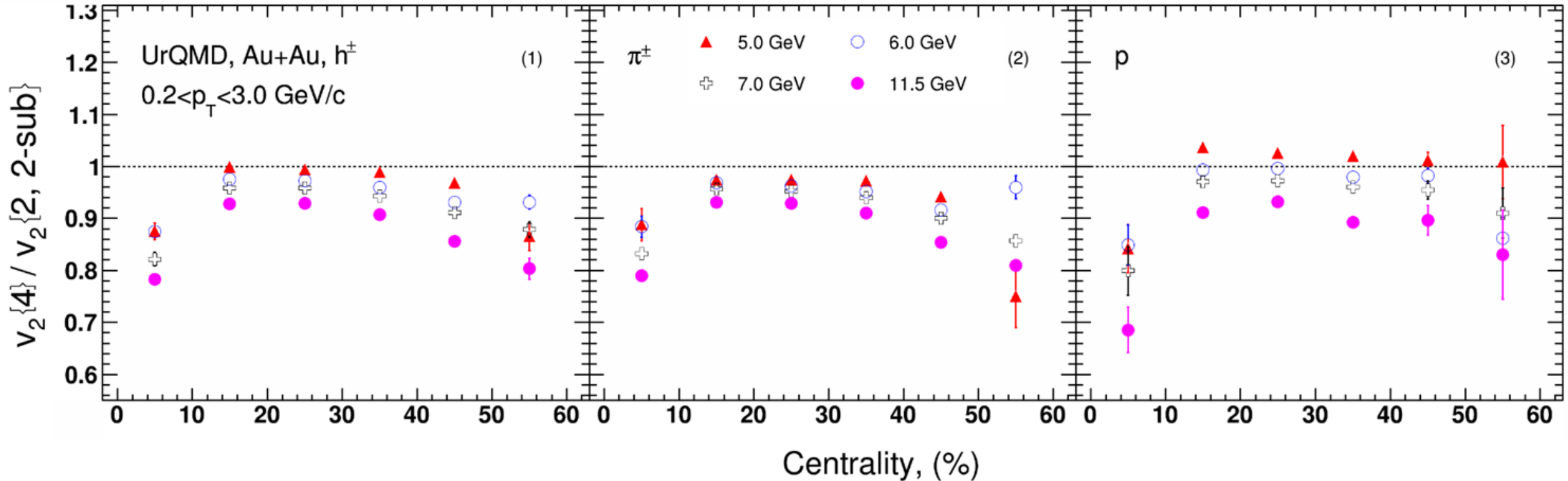
Cuts:

- Charged particles only
- Primary
- $|\eta| < 1.5$
- $\Delta \eta = 0, 1$
- $p_T > 0.2$ GeV/c
- $|DCA| < 3\sigma$
- $n_{TPC\ hits} \geq 16$
- good agreement of the $v_{2,mc}$ with $v_{2, reco}$ data

- The difference at large p_T between $v_{2,mc}$ and $v_{2, reco}$ is less than for other methods -> Not

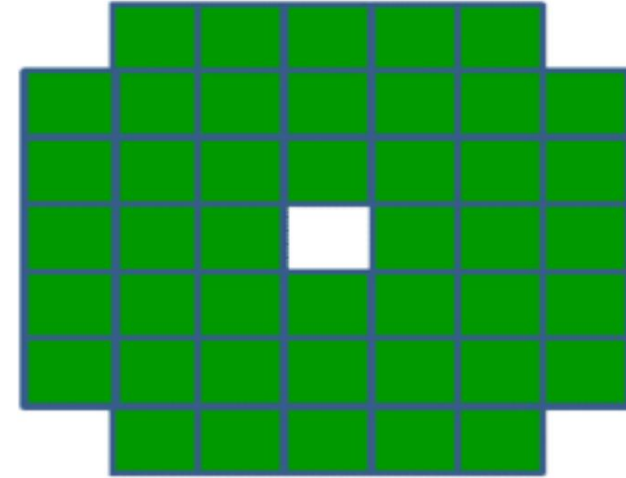
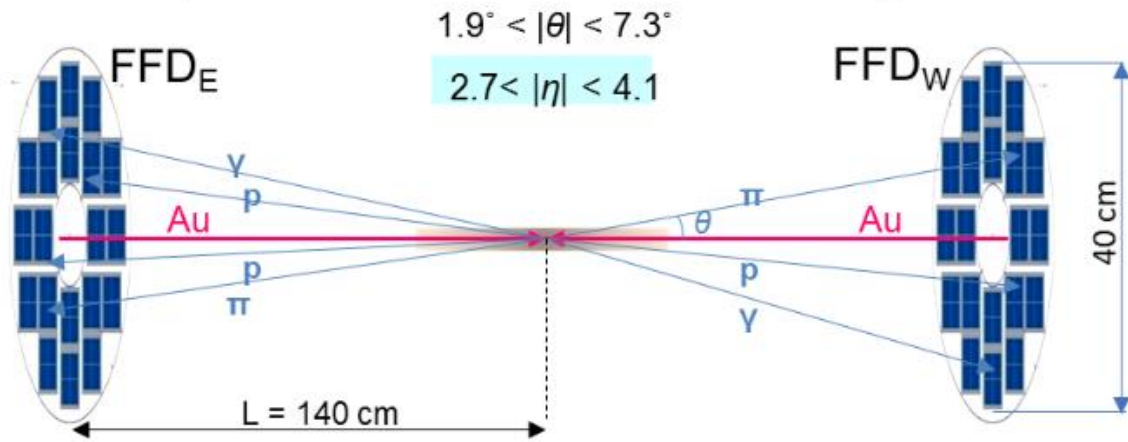
v_2 fluctuations at $\sqrt{s_{NN}} = 5 - 11.5$ GeV

For more details see A.Demanov's [talk](#) on ISHEP-2023



- v_2 fluctuations decrease with decreasing energy more strongly than at $\sqrt{s_{NN}} = 11.5-39$ GeV
- The energy dependence of the $v_2\{4\}/v_2\{2\}$ is stronger for protons than for pions

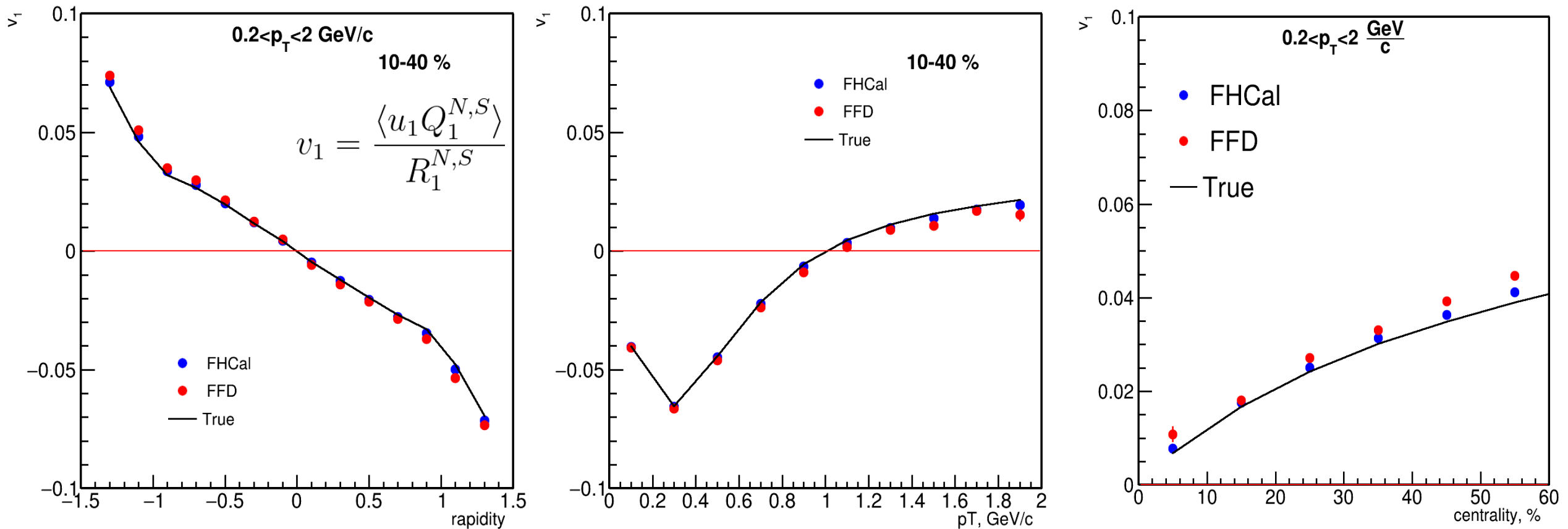
FHCal and FFD detectors



The FFD consists of two sets of Cherenkov counters located at ± 140 cm from the nominal interaction point. Each set has 20 physical detectors with 4 read-out channels each. As a result, the total number of read-out channels is 2 sides 80 channels = 160 channels.

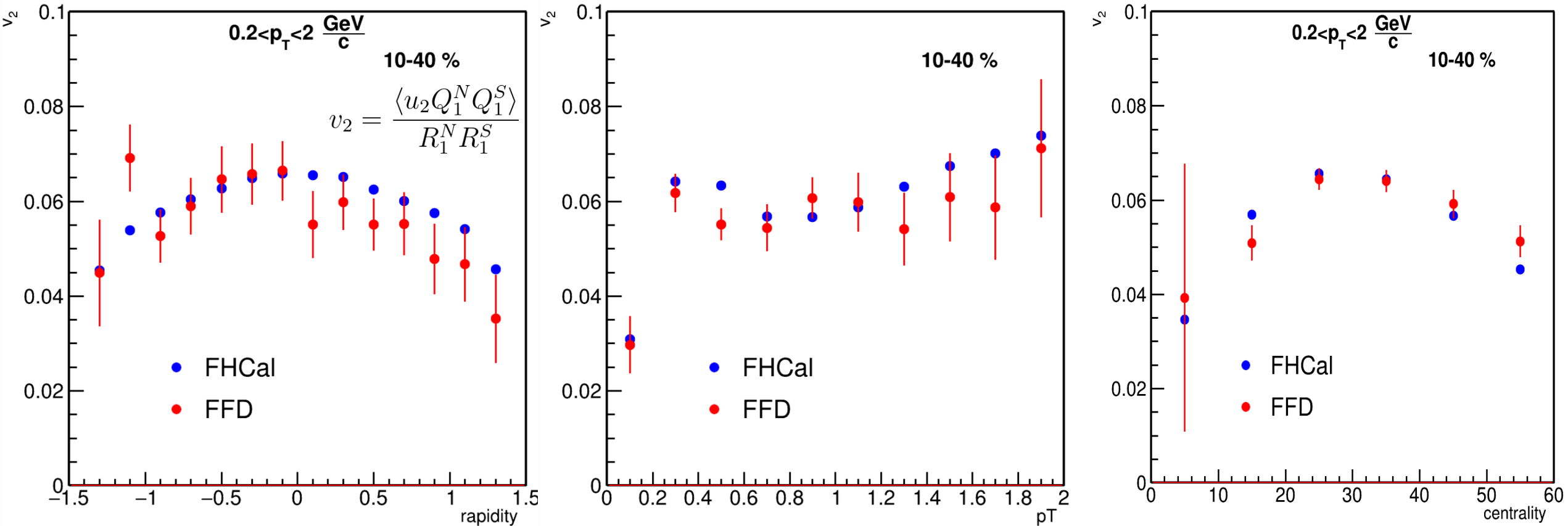
FHCal consists of two sets of hadron calorimeters in pseudorapidity region $2 < |\eta| < 5$. Each set has 44 modules from azimuthal symmetry. Total number of modules 88.

Directed flow of charged hadrons with FHCAL and FFD



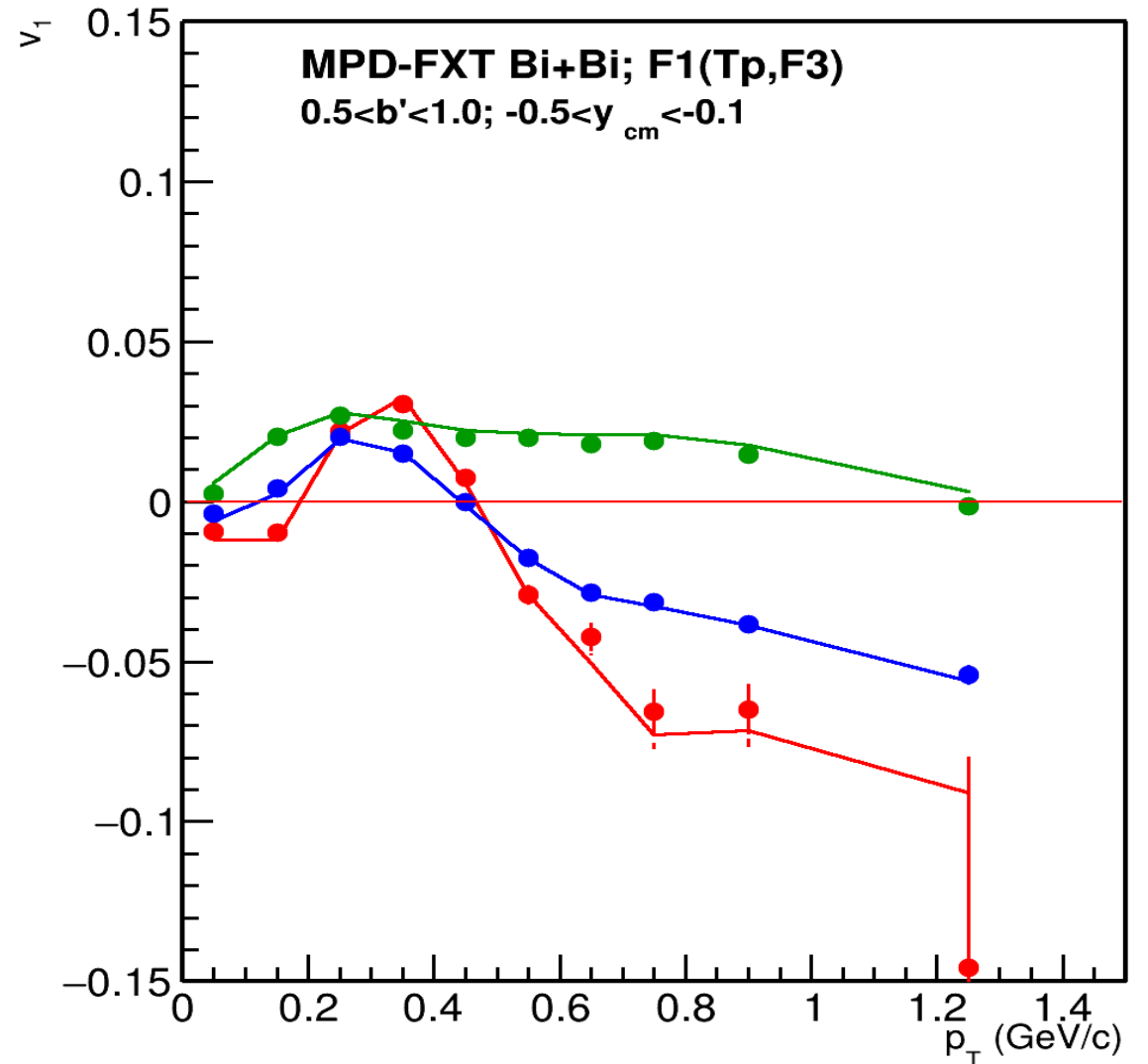
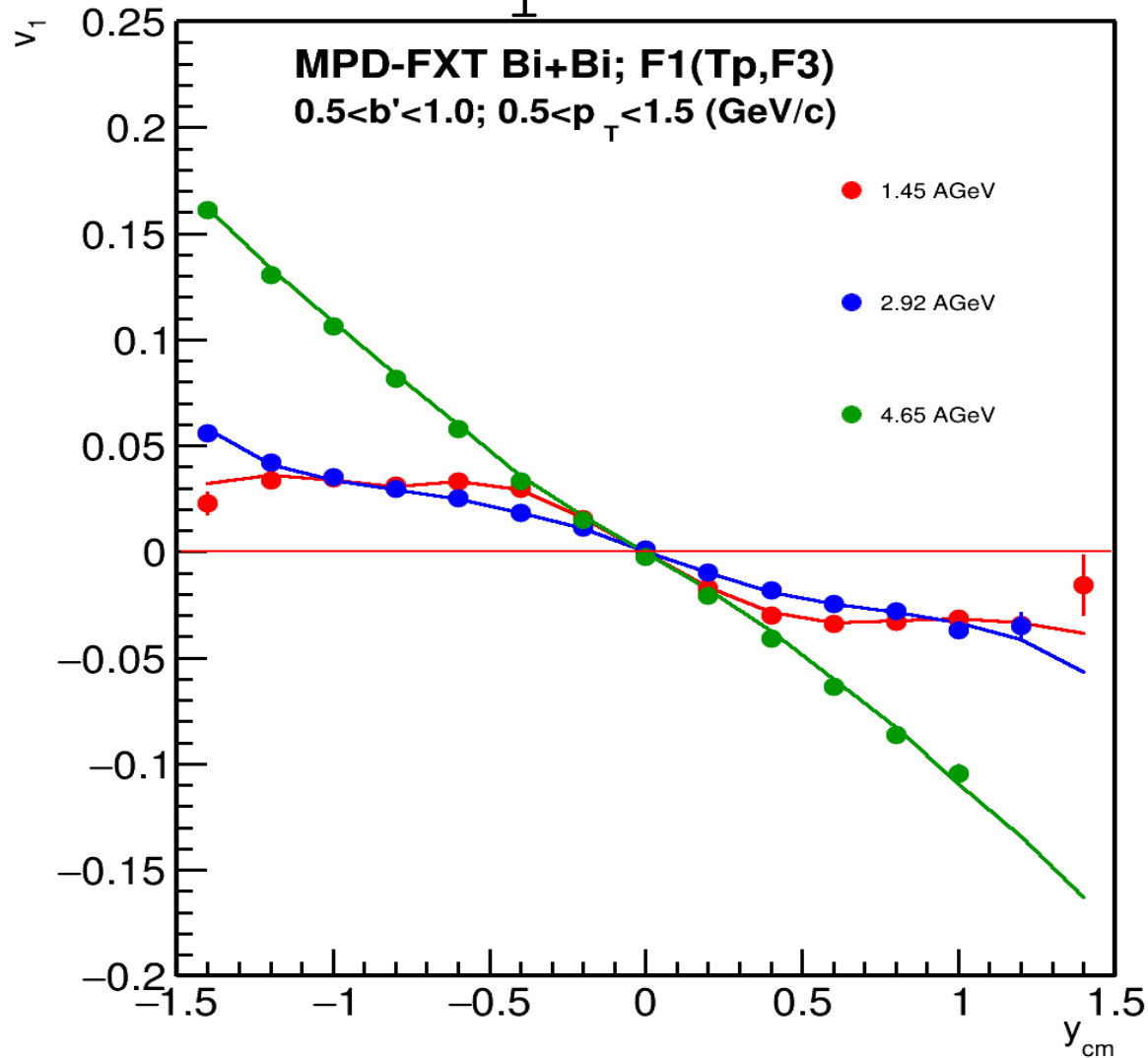
FHCAL and FFD have consistent results; both can be used for directed flow measurements.

Elliptic flow of charged hadrons with FHCAL and FFD



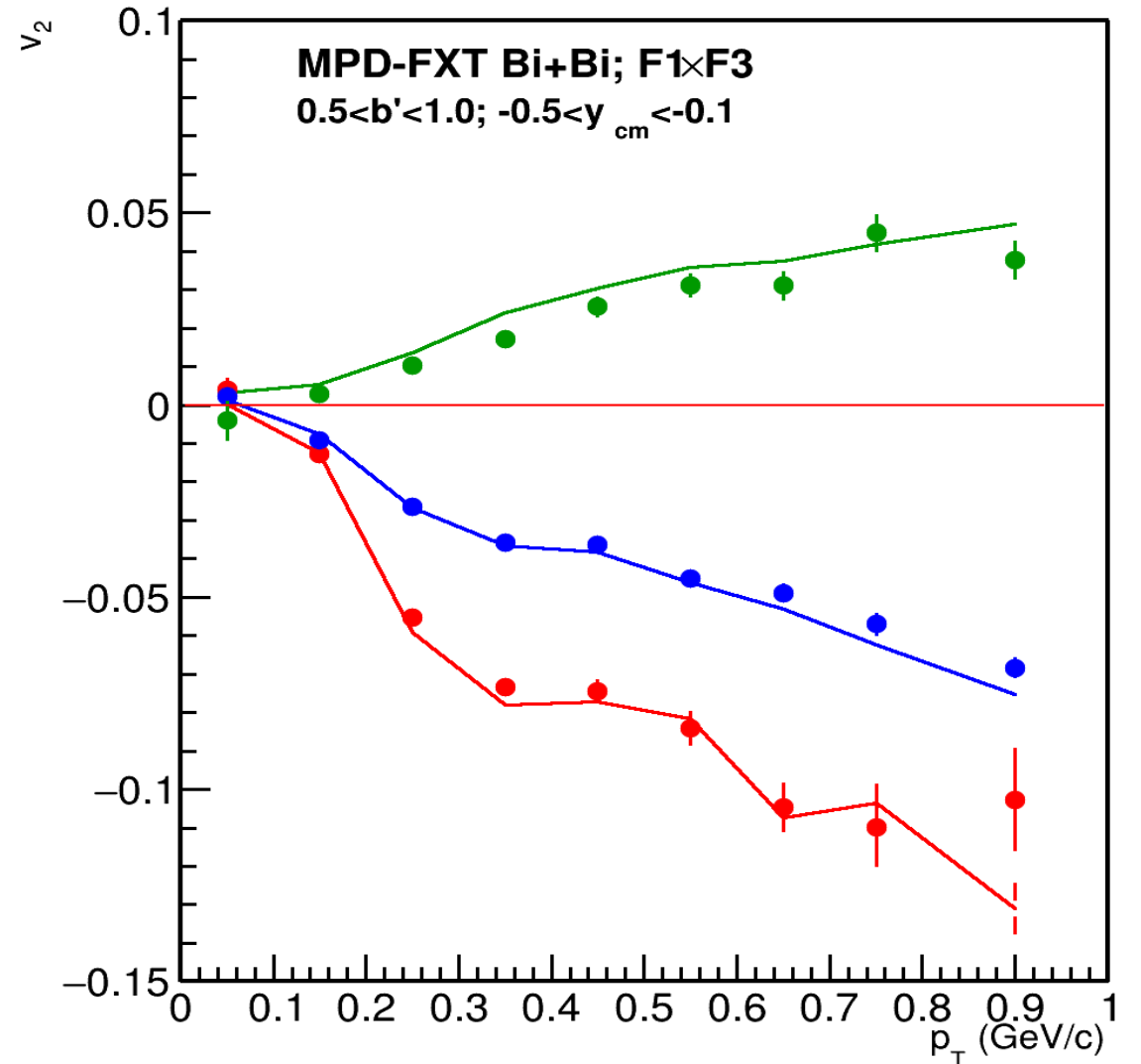
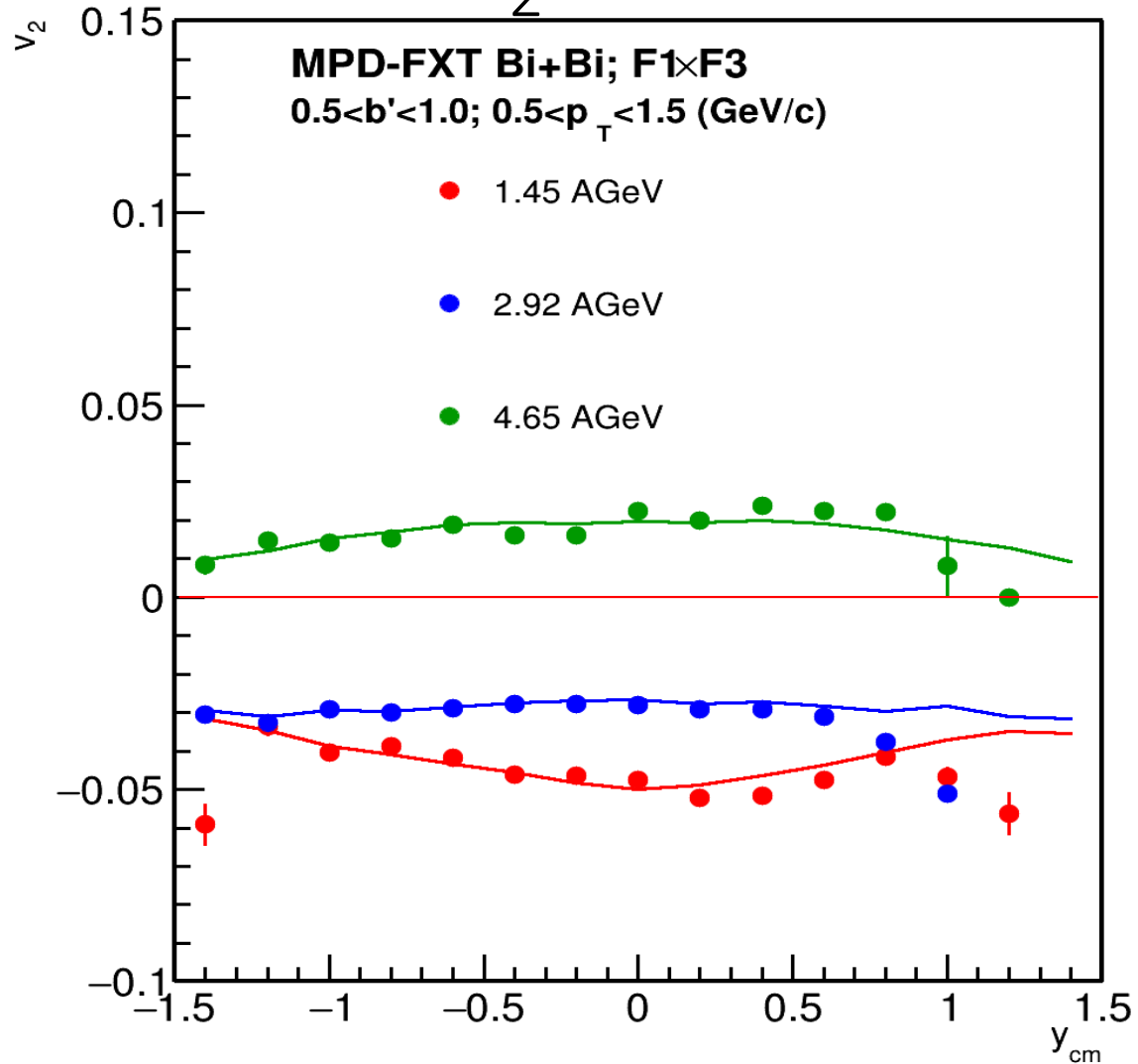
Due to low Resolution FFD need more statistics than FHCAL for elliptic flow measurements.

MPD-FXT: v_1 for π^+



v_1 is consistent with model signal for $y < 1$
No efficiency corrections were applied yet

MPD-FXT: v_2 for π^+



v_2 is consistent with model signal for $y < 0.5$
No efficiency corrections were applied yet